SCALABLE EXPANSION AND ERYTHROCYTE PRODUCTION OF HUMAN INDUCED PLURIPOTENT STEM CELLS

by

Ying Wang

A dissertation submitted to Johns Hopkins University in conformity with the requirements for the degree of Doctor of Philosophy

Baltimore, Maryland

August 2015

Abstract

In vitro production of erythrocytes in physiologic numbers from human induced pluripotent stem cells (hiPSCs) holds great promise for improved transfusion medicine and novel cell therapies. However, large-scale production of hiPSCs and their progeny by robust and economic methods has been one of the major challenges for translational realization of hiPSC technology.

First, this thesis demonstrates a scalable culture system for hiPSC expansion using the E8 chemically defined and xeno-free medium under either adherent or suspension conditions. To optimize suspension conditions guided by a computational simulation, we developed a method to efficiently expand hiPSCs as undifferentiated aggregates in spinner flasks. Serial passaging of two different hiPSC lines in the spinner flasks using the E8 medium for more than 10 passages preserved their normal karyotype and pluripotency. Second, an optimized differentiation medium was developed for robust and consistent production of hematopoietic stem and progenitor cells (HSPCs) and progeny erythrocytes from hiPSCs, minimizing risk and variation due to the animal-derived products in cell cultures. Several crucial reagents were evaluated and replaced with regulatory-approved pharmacological reagents, such as Romiplostium, to establish a feeder-free and xeno-free condition, in which all the animal-derived products were eliminated. Erythrocytes from either the corrected or its parental (uncorrected) iPSC line were generated with similar efficiencies, showing enucleation and hemoglobin expression. Finally, a strategy for scalable generation of HSPCs from hiPSCs and subsequent erythrocytes specification was established, by using stepwise cell culture

conditions and by integrating spinner flasks and rocker platform. This system supported robust and reproducible definitive hematopoietic differentiation of multiple hiPSC lines. An ultra-high yield of up to 4×10^9 $CD235a^+$ erythrocytes at >98% purity was achieved when using a 1-liter spinner flask for suspension culture. Erythrocytes generated from this system can reach a mature stage with red blood cell (RBC) characteristics of enucleation, β-globin protein expression and oxygen-binding ability.

In conclusion, this thesis demonstrates a xeno-free and cGMP-compliant system that provides the opportunity to produce clinical-grade erythrocytes from hiPSCs in a large-scale bioprocess. Therefore, this study is a significant step towards the goal of large-scale generation of RBCs for therapeutic purposes.

Thesis Advisor:

Prof. Sharon Gerecht, Ph.D.

Prof. Linzhao Cheng, Ph.D.

Thesis Committee:

Prof. Konstantinos Konstantopoulos, Ph.D.

Prof. Peter Searson, Ph.D.

Prof., Zack Z. Wang, Ph.D.

Prof. Chao Wang, Ph.D. (internal alternate)

Prof. Warren Grayson, Ph.D. (external alternate)

Acknowledgments

First I would like to express my sincere gratitude to my academic co-advisors, Dr. Sharon Gerecht and Dr. Linzhao Cheng. Without their guidance, support and encouragement throughout the years during graduate studies, I could not make all these progress. I will always be appreciative of my time spent in their labs and the transformation that occurred both for my career and personality. Both of them resemble the perfect example of how to be a great researcher, leader, inspirer and most importantly, a contributor to the scientific society. I have learned a lot from their efficient collaboration and ways of thinking. Their incomparable support to my career development is priceless.

I would like to thank Dr. Zack Z. Wang, Dr. Hai-Quan Mao and Dr. Warren Grayson to serve my graduate review board member to evaluate my research progress during the last three years, and Dr. Kostas Konstantopoulos, Dr. Peter Searson for taking the time from their busy schedule to serve as members of my thesis committee. I would also like to thank Dr. Guokai Chen at National Institute of Health, Dr. Xiuli An at New York Blood Center and Dr. Vincent Chen at Beckman Institute in City of Hope Hospital for their generous help in my research project.

It's a fortune to have so many wonderful lab members with whom I have built friendships. Dr. Zhaohui Ye, Dr. Xiaosong Huang, Dr. Bein-Kuan Chou and Dr. Hasan Erbil Abaci gave me tremendous help in my research. Other lab members always show their warmest supports when hard time came to me. I would like to thank all of them.

Table of Contents

List of Figures & Tables

1 *Introduction*

1.1 *Scalable expansion of human pluripotent stem cells*

Human pluripotent stem cells (hPSCs), including human embryonic stem cells (hESCs) and human induced pluripotent stem cells (hiPSCs), are capable of not only indefinitely self-renewing but also differentiating into any mature cell type of the body. Thus, hPSCs hold great promise for revolutionizing regenerative medicine, disease modeling, and drug discovery. In the past several years, researchers have been inspired by the development of techniques for the derivation, expansion, and differentiation of hPSCs, as well as by the ever-increasing knowledge about their genetic, epigenetic, and functional properties. In spite of unsolved problems, these developments have moved us significantly closer to the ultimate goal of hPSC-based cell therapies. Manufacturing an hPSC-based product will comprise a number of complex steps, including cell isolation, initial purification and expansion, derivation of hPSC lines, creation of master and working cell banks, large-scale expansion, differentiation, purification, storage, distribution, and transportation of the final product, in addition to intensive quality control and testing for each step. This chapter focuses on one crucial hurdle impeding the realization of late-stage clinical trials and commercialization of hPSC regenerative medicine — the efficient and scalable expansion of hPSCs under clinically compliant conditions. We cover primarily the essential aspects of the commitment to clinical

requirements, the development of culture media and substrates for expanding hPSCs, the demands and current situation of large-scale production.

1.2 *Human pluripotent stem cells*

First derived from the inner cell mass of the human blastocyst by James Thomson and colleagues in 1998 [1], hundreds of hESC lines have been generated and thoroughly studied. According to the NIH Human Embryonic Stem Cell Registry, the NIH has approved the registration of a total of 210 hESC lines, 49 of which contain disease-specific mutations. These hESC lines offer precious opportunities for the study of early human development, stem-cell biology, *in vitro* differentiation, and tissue formation. However, the derivation of hESCs requires the destruction of human embryos, which has raised an ethical controversy and led to stringent legal restrictions in the United States [2]. The limited sources of federal funding and the paucity of hESC lines representative of specific diseases, especially for somatic or aging-dependent diseases, have narrowed down the potential applications of hESCs in disease modeling, pathology, and cell therapy. Moreover, the allogeneic nature of hESC therapies requires that the donor and the patient have matching human leukocyte antigen (HLA) types to reduce immune rejections, further increasing the limitations.

Scientists have actively sought to use somatic-cell nuclear transfer (SCNT) technology to generate personalized hPSCs for patient-specific research, especially after the report of cloning of Dolly the sheep in 1997 [3]. Noggle et al. generated a blastocyst by transferring the genome of an adult somatic cell into an oocyte with an intact nucleus, and then derived hESC lines from the blastocyst [4]. The resultant triploid cell line and,

more generally, the limited availability of human oocytes have kept this technology from practical and widespread implementation. Very recently, Tachibana et al. reported rapid derivation of hESC lines from blastocysts they generated by optimized SCNT protocol that allowed to remove oocyte nucleus and to develop normal diploid blastocysts [5]. In addition to ethic controversy and practical difficulty to obtain sufficient eggs from female donors, the complexity and low efficiency of current SCNT technique will unlikely become a steady technology to generate autologous hPSCs in the near future.

After the momentous 2006 announcement that induced pluripotent stem cells (iPSCs) had been derived from mouse fibroblasts [6], Yamanaka and colleagues reported altering human cell fates to generate hiPSCs from human fibroblasts by expression with only four transcription factor genes [7]. Thomson and colleagues achieved the same marvel by using slightly different 4 factors at the same time [8]. This revolutionary finding stimulated many follow-up studies and opened up a completely new field — the generation and use of hiPSCs in a wide variety of human biology and disease research [9]. In addition to skin fibroblasts, mononuclear cells in the peripheral blood of human adults were also successfully used to generate integration-free hiPSCs, offering an easier way to avoid skin biopsy operations to get donor samples from probably the most commonly accessible cell sources in clinic [10-13].

Research showed that human iPSCs share equivalent phenotypical and functional properties with hESCs. They have identical morphologies; they grow indefinitely and exhibit telomerase activities; they can be positively stained for alkaline phosphatase activity; they express comparable levels of such pluripotency genes as *OCT4*, *SOX2,* and *NANOG*, as well as of such embryonic cell surface antigens as TRA-1-60, TRA-1-81,

SSEA3, and SSEA4; and they can differentiate into cells from all three embryonic germ layers *in vitro* after induction. Their developmental pluripotency is also validated by their ability to form teratoma (in immune-deficient mice), a benign tumor consisting of cells of all the 3 embryonic germ layers that was uniquely formed by pluripotent cells. Recent studies of genome-wide gene expression and DNA methylation have revealed subtle but detectable differences between hiPSCs and hESCs (although variations between hESC or iPSC lines also exist) [14] Gene expression and DNA methylation revealed the epigenetic markers present in the parental somatic cells were not completed erased in derived iPSCs and remaining ones (i.e., the so-called epigenetic memory) do exist although diminish with serial passages. Evidence that hiPSC lines differentiated more efficiently into the cell types from which they were derived, or less to another cell type also existed [15, 16]; this, from a positive point of view, could prove beneficial for providing more efficient differentiation on demand even than from hESCs.

Although many unknowns remain in the emerging field of hPSC research, pioneers have already cautiously started to explore potential clinical applications using hPSCs. One booming field is hPSC-based tissue engineering. Using hPSC-derived cells, researchers have generated fully or partially functional human tissues like those from liver, bone, neuron, blood vessel, heart, eye, etc [17-23]. These studies provided proof-of-concept for potential cellular therapies, and yet were still at the starting line of the long journey towards realistic clinical implement.

1.3 ***Clinically compliant settings***

In order to examine the clinically compliant settings for hPSC expansion, we can learn more from approved clinical trials. In 2009, the U.S. Food and Drug Administration (FDA) approved the world's first human clinical trial of hESC-based therapy by Geron Corporation for treating spinal cord injuries. In this study, hESCs were differentiated into oligodendrocyte progenitor cells (OPCs). The patients, all of whom had severe spinal cord injuries, each received an injection of approximately 1.5 million hESC-derived OPCs in order to repair the myelin insulation around their nerve cells and restore spinal cord functions [24]. However, the company stopped this trial abruptly in 2012 [25]. Although the exact reason(s) unclear, there were at least two possibilities: first, the cell dosage used in the study might not have been large enough to affect the patients' injured spinal cords; second, the process of expansion and differentiation of hESCs under clinical compliant settings was complex, causing dosage or unacceptable pricing problems. Currently, only three ongoing clinical trials of hPSC therapy have gained approval by FDA. All three of these phase I/II trials led by Advanced Cell Technology (ACT) Inc. are based on transplanting hESC-derived retinal pigment epithelial (RPE) cells for an eye disease.

1.3.1 **Ongoing clinical trials of hESC therapies**

RPE cells are critical for supporting photoreceptors in the human retina. Diseases such as advanced dry age-related macular degeneration (AMD) and Stargardt's macular dystrophy (SMD) can destroy RPE cells, causing vision impairment and even blindness. The researchers attempted to replace degenerate RPE cells and restore visual function by establishing an efficient method for differentiating hESCs into RPE cells followed by

their retinal injection [26]. The phase I trials sought to study the efficacy, safety, and tolerability of this therapeutic approach to treating AMD and SMD. In their studies, the transplantation of 50,000 to 200,000 hESC-derived RPE cells constituted one dosage. Data gathered halfway through the clinical trials showed that patients having either of these two diseases experienced improved vision [27]. Because this treatment would work with small dosage sizes and because the final RPE cell product for implantation did not require the use of additional materials, such as scaffolds or nanoparticles, which may lead to complicated categories (combinations of Tissue, Device, and Biologic) that usually trigger slow regulatory process [28, 29], the FDA found it suitable to approve this hESC-based therapy ahead of other potential hPSC therapies. More recently, an institutional review board in Japan granted conditional approval of a planed clinical trial using RPE cells derived from hiPSCs, which is awaiting final approval from the Japanese government [30].

1.3.2 **Current applications of hiPSCs**

With concern about safety issues, research exploiting the unique clinical properties of hiPSCs has focused mainly on establishing disease models for the study of pathology, toxicology, diagnosis, and drug screening [31], giving an advantage to broad patient-specific cell sources [32-34]. Another potential clinical application of hiPSCs, gene-correction based stem cell therapy [35], would use the strategy of deriving an iPSC line from a patient with a disease caused by a genetic defect such as sickle cell disease [36]. Such diseases could then be treated by gene correction using zinc finger nuclease (ZFN) [37], transcription activator-like effector nuclease (TALENs) [38], or the newly

reported CRISPR/Cas9 system [39] to repair the endogenic pathogenic mutations, after which they repaired genes would be expanded and differentiated into desired cell types for pathology study or transplantation purpose. For additional reading, please refer to thorough reviews about the use of hiPSCs in disease modeling and gene therapies [9, 40] by Robinton et al. and Merkle et al. To keep its focus on the expansion of hPSCs, this review will consider several prominent aspects for developing bioprocess of hPSC expansion.

1.3.3 **Xeno-free conditions and chemically defined reagents**

According to the *Guidelines for the Clinical Translation of Stem Cells* (available at http://www.isscr.org/home/publications/ClinTransGuide) developed by the International Society for Stem Cell Research (ISSCR) [41], although the inclusion of animal materials in the hPSC manufacturing process does not prohibit using the cells in humans, the processes and products must undergo additional tests to exclude the transmission of animal pathogens, antigens, and mycoplasma into the products. This will increase the cost and time for clinical grade manufacture. One option is to find alternative components of human origin to avoid xenogeneic contamination. In any case, whether the products come from animal or human sources, they remain undefined because they contain a complex mixture of growth factors, hormones, extracellular matrix proteins, and many other functional and nonfunctional molecules that cannot be completely determined and excluded. They also have a high risk of exposure to viral contaminants, which will necessitate complex virus detection screening of the products [42, 43]. Moreover, due to the instability of the source tissue, these products tend to exhibit batch-

to-batch variations, reducing the reproducibility and reliability of therapeutic cell products [44]. The preparation of feeder cells is also time-consuming and requires irradiation equipment and qualified personnel. All of these factors make it more practical and economical to use, where possible, chemically defined components that can reduce the variance and the uncertainty of generating cell-based products with consistent quality.

1.3.4 **Current good manufacturing practices (cGMP)**

The term cGMP is a "quality management system" for manufacturing and testing products intended for human use, assuring that they are "safe, pure, and effective" (http://www.fda.gov/Drugs/GuidanceComplianceRegulatoryInformation/Guidances/ucm 064971.htm, FDA cGMP guidelines). All clinical trials in the U.S. must manufacture any cell products under FDA cGMP guidelines (Code 21 CFR 210–211, 312, 600, and 1271). Especially, human cells, tissues, and cellular- and tissue-based products (HCT/Ps) must comply with the current good tissue practices (cGTP) rules (Code 21 CFR 1271). Equivalent regulatory rules have also been established in Europe (EU Directive 2003/94/EC) and many other countries and regions internationally (ICHQ7). Thus, cGMP compatibility must receive specific consideration during the development of hPSC culture systems for clinical use. The manufacturing processes and analytical methods should be carefully developed, fully controlled, and exhaustively documented. This comprises many elements, such as valid protocols, control of work flow and cross-contamination, clean room operation, monitoring and control of critical environmental parameters (including temperature, O_2, and CO_2), and so on. The cGMP also requires the rigorous validation of facilities, critical utilities, and equipment, along with extensive

training of staff and technicians. Meticulous documentation management is extremely important for a cGMP process. All of these rules aim to avoid any possible contaminations and operational errors throughout the process and to retain the ability, for any problem that might occur, to trace its origin, correct the problem, and identify all possible impacts.

Many companies and research institutes have established cGMP-compliant hPSC culture facilities and relevant protocols, mainly for the purpose of cell banking, including the WiCell Research Institute (http://www.wicell.org), Cellular Dynamics International (http://www.cellulardynamics.com), the City of Hope National Medical Center [45], Upstate Stem Cell cGMP Facilities at the University of Rochester Medical Center (http://www.urmc.rochester.edu/upstate-stem-cell-facility), etc. These facilities provide cGMP-compliant services for all hPSC derivation, expansion, and differentiation for cell banking and clinical trials.

1.3.5 **Demand of robust and scalable cultivation of hPSCs**

Thus far, clinical trials with hPSCs have been limited to therapies that need only small dosages of cells. Apparently, the size of hPSC dosage required to treat a certain disease is a critical considerations for decision-makers choosing which disease to investigate using stem cell therapy. Although the desired scale of hPSC expansion in autologous therapies may be much smaller than in allogeneic therapies, autologous treatments for many other diseases and injuries still demand what are estimated to be large quantities of hPSCs and/or their progenies to replace cells that do not regenerate. For example, research has suggested that it would take at least 1×10^9 hPSCs to obtain

enough islets for the transplantation treatment of type I diabetes [46]; an optimized dose for performing hematopoietic stem cell (HSC) transplantation for a 70-kg adult patient contains from 4.2×10^8 to 5.6×10^8 $CD34^+$ cells [47]; an engineered myocardial tissue should contain at least 1 to 2 $\times10^9$ to repair the damaged heart from a typical myocardial infarction [48]; a minimum number of 10^6 surviving tyrosine hydroxylase-immunopositive neurons per side of the brain were necessary to have a positive clinic response for Parkinson's disease treatment [49], which may require 10^9 to 10^{10} hPSCs considering the low differentiation and survival rate [50].

Moreover, even for the small-dosage therapies, such as the clinical trials mentioned above for treating AMD, moving to phase II/III clinical trials can require the participation of hundreds to thousands of patients in multiple clinical sites, necessitating the development of batch cultures with the capacity to produce several hundred dosages, not to mention the requirements for the bulk manufacture of final commercial products. Clinical trials for these applications can only receive approval once the difficult problems in efficient (timely and economical) and scalable expansion and differentiation of hPSCs and their progenies for therapeutic purposes.

An optimal culture system would support the self-renewal of undifferentiated hPSCs with minimal selective pressure. Culturing cells under stressful conditions or for long periods may cause DNA deletions, rearrangements, and other genetic or epigenetic abnormalities that can lead to pathogenic disasters like cancer. Thus, hPSCs should be expanded vigorously for a minimized period and finally reached the desired quantity in one batch of production with high capacity. For a rough estimation as an example, a good culture system for clinical applications should be able to expand 10^6 frozen hPSCs to a

clinically relevant quantity of 10^{12} cells within 20 to 30 days in approximately 5-10 passages, considering the current status of development in this field.

1.4 *The evolution of feeder cells and substrates*

One intrinsic feature of hPSCs is that the cells require tight cell-to-cell contact for survival and proliferation [51, 52]. To provide the necessary signals and a substrate for cells to attach to, researchers have developed various feeder cells or substrate materials. Conventionally, mouse embryonic fibroblast (MEF) feeder cells were used to support the derivation and self-renewal of hPSCs in a two-dimensional (2-D) adhesion culture. For example, the hESCs used in the current RPE clinical trials were cultured on MEF feeder cells [26]. To eliminate xenogeneic contaminations, various types of human feeder cells from allogeneic muscle, skin, marrow, and endometrial cells, etc. [53-56], as well as from autogenic hESC-derived fibroblasts [57, 58], were developed in the early 2000s. Some of these new feeder cells also proved capable of supporting the derivation of new hPSC lines [54, 55, 58].

Since the first study, published more than a decade ago in 2001 [59], Matrigel (BD Biosciences) has been widely used as a substrate for the feeder-free adhesion culture of hPSCs. Matrigel -- a mixture of extracellular matrix materials extracted from Engelbreth-Holm-Swarm (EHS) mouse sarcoma cells, contain (approximately) 60% laminin, 30% collagen IV, 8% entactin, growth factors and indeterminate components (http://www.bdbiosciences.com/documents/BD_CellCulture_Matrigel_FAQ.pdf). It was established in the 1980s [60] and originally used for promoting differentiation and the outgrowth of differentiated cells from tissue explants [61]. It remains the most broadly

used feeder-free substrate for 2-D and 3-D cell cultures. A similar product, Geltrex (Invitrogen) is also commercially available. However, beyond being xenogeneic, both of these materials suffer from lot-to-lot inconsistency, uncertainty of stable composition, risk of viral contamination, and inconvenient temperature sensitivity; all of these factors make them problematic for clinical grade manufacturing.

To address these concerns, many researchers have focused their efforts on developing defined, xeno-free substrates that support the derivation and expansion of hPSCs. The primary candidates were individual or simple mixtures of purified extracellular matrix (ECM) proteins from Matrigel. Initial studies showed that purified laminin could support the growth of undifferentiated hESCs, while culturing hESCs on fibronectin- or collagen IV-coated surfaces was not promising [59]. Thomson et al. made a breakthrough, finding that a combination of collagen IV, fibronectin, laminin, and vitronectin can replace Matrigel to derive and expand hESCs in defined conditions [62]. Purified laminin from human placentas was proved sufficient for long-term maintenance of hESCs in media containing activin A [63]. Recently, further studies have reported on the improvements to laminin-based substrates and the related mechanisms [64-66]. Miyazaki and colleagues demonstrated that recombinant human laminin -- specifically the isoforms laminin-511, laminin-332, and laminin-111 -- support the attachment and long-term self-renewal of hPSCs in an undifferentiated state [64, 66]. These studies found the binding and signaling activity of the ECM through the major cell surface integrin receptor, $\alpha 6\beta 1$, critical to interactions between the cell and the ECM. By keeping the essential binding sites of integrin $\alpha 6\beta 1$, the truncated laminin fragments LM511-E8 and LM332-E8 were shown to be sufficient to support long-term expansion of hPSCs [65].

Recombinant human E-cadherin, which is recognized by integrin αEβ7 [67] and α2β1 [68], has also exhibited the ability to act as an equivalent alternative to Matrigel.[69] Human fibronectin, which binds to integrin α5β1 and αVβ3 [70], was shown to support hESC expansion in a serum-free medium [71]. Another ECM component, vitronectin, was used to replace Matrigel, supporting the attachment and proliferation of hPSCs by mainly binding to integrin αVβ5 [72]. Chen et al. enhanced the attachment and survival of hPSCs on vitronectin-coated surfaces by cutting off the N-terminal and/or C-terminal fragments from full-length vitronectin [73]. These recombinant human ECM-based substrates offered significant improvements in establishing defined and xeno-free culture conditions for adhesion cultures of hPSCs under clinically compliant settings. Most of them were successfully transferred into commercially available products, such as CELLstart (Invitrogen), Laminin-511, and Laminin-521 (BioLamina); and Vitronectin XF (STEMCELL Technologies). Furthermore, the development of truncated protein substrates can not only offers improvements of the supportive effects in culture, but also enhances the yield and simplifies the procedure of production and purification of large recombinant proteins, providing the sort of economical benefit that has become one of the major concerns in the production of therapeutic applications [65, 73].

An extreme condition for truncated ECM substrates is to cut off most of the protein, keeping only a small peptide sequence of the active domain. Polymers, such as acrylate [74], or self-assembled molecules, such as alkanethiol [75], were arranged on the tissue culture surface to form a monolayer. Such peptides can be easily conjugated on a synthesized acrylate or alkanethiol surface during manufacturing to avoid the coating process. By following this strategy, researchers found that several laminin peptides

supported the growth of hESCs using an alkanethiol array [76]. Peptides originated from bone sialoprotein [74], vitronectin [74, 75], and laminin (such as Synthemax from Corning) [74] also proved capable of maintaining long-term undifferentiated cultures of hESCs. These peptides allow cells to attach and spread by binding to the glycosaminoglycans or integrins on the cell surface. However, the high price of peptide synthesis and the difficulty of bulk sterilization by gamma radiation due to degradation of the peptide remain the major hurdles to broad application of this technology. To make economical and ready-to-use culture surface, fully synthetic plastic surfaces without peptide fragments were recently studied [77-81]. Among all reported synthetic surfaces, poly[2-(methacryloyloxy)ethyl dimethyl-(3-sulfopropyl)ammonium hydroxide] (PMEDSAH) [79] and aminopropylmethacrylamide (APMAAm) [81] exhibited the best results, supporting robust and long-term expansion of multiple hPSC lines without compromising pluripotency or inducing abnormal karyotypes. Although how they do so remains not fully understood, both mechanical (including stiffness, wettability, and rigidity) and chemical properties of synthetic surfaces influenced cell attachment and proliferation by mimicking the biological microenvironment as other ECM substrates. For additional reading, please see an updated review [82] by Villa-Diaz et al. Appropriately treating the polystyrene surface with ultraviolet light and then coating with serum or vitronectin was also showed to improve hPSC compatibility [83].

Synthetic surfaces are suitable for large-scale robotic adhesion cultures because they eliminate the need for the coating procedure and allow storage and handling at room temperature. Furthermore, the compatibility with sterilization techniques used in bulk manufacture, such as electron beam- and γ-radiation [82], is also a critical factor for

making ready-to-use products. Generally, substrates or surfaces containing protein or peptide components are not suitable for large-scale sterilization by γ-radiation due to the possible denaturation or degradation of these components [84]. The radiation may also affect the physical and chemical properties of the synthetic or the plastic surface. Therefore, the surfaces that have been proven to be capable for bulk sterilization, such as PMEDSAH, facilitate using cGMP in the production of commercial disposable vessels for large-scale expansion of clinical grade hPSCs.

1.5 *The evolution of culture media for hPSC expansion*

Strictly speaking, a discussion of feeder cells and substrates should also consider the corresponding culture medium as a system. The culture media for hPSCs have also evolved rapidly in recent years. Initially, hESCs were derived and cultured in a basal medium substituted with a serum or serum replacement, such as KnockOut Serum Replacement (Invitrogen), N2 supplement, or B-27 supplement (Invitrogen), which mainly contain human or animal serum albumin combined with various cytokines and growth factors either on feeder cells or on Matrigel [1, 7, 59]. At the same time, researches using feeder-free cultures often used media conditioned with feeder cells (i.e., conditioned media, or CM), which typically had serum replacement added to it before its incubation with feeder cells and the many undefined factors that they secreted. For a long time, MEF-CM was considered the gold standard for feeder-free expansion of hPSCs and was usually used as a baseline for comparison during the development of hPSC culture media.

Over the past decade, to develop fully defined media without any unknown components or additives, researchers have systematically screened and optimized a

variety of formulas [62, 71, 73, 85-93]. In these studies, both fibroblast growth factor 2 (FGF2) and the TGF/Activin/Nodal pathways appeared to be indispensable for the stable self-renewal of undifferentiated hPSCs. Some other cytokines could also help to maintain the pluripotency of hPSCs by activating similar pathways, such as Smad2/3, AKT and ERK1/2 [94]. Oh's review comprehensively summarizes the mainstream evolution of serum-free medium [94]. Table 1-1 provides an updated summary of the media and culture conditions with regard to clinically compliant settings. Among these formulations, mTeSR1 (STEMCELL Technologies) and StemPro (Invitrogen) -- based on two publications in 2006 [62] and 2007 [89], respectively -- constituted significant milestones in the exploration of defined media. In 2010, the International Stem Cell Initiative Consortium performed an exhaustive study that documented the side-by-side validation of eight defined media [95]. Surprisingly, only mTeSR1 and StemPro media supported the attachment and undifferentiated expansion of most of the twelve different hESC lines tested during the ten-week test period in four different labs internationally. In other media tested, the cells either died due to low attachment or underwent progressive differentiation on Geltex or Matrigel [95]. Another side-by-side evaluation reported in 2010 introduced a comparison of the three most popular feeder-free culture systems: mTeSR1-Matrigel, StemPro-CELLStart and mTeSR1-vitronectin [96]. Many other individual studies also used mTeSR1 and StemPro as standard serum-free media on different xeno-free substrates (Table 1-1). However, both of these media contain bovine serum albumin (BSA) fragment V, an animal product that contains complex albumin and

Table 1-1. Serum-free and feeder-free adhesion culture systems and their clinical compliant features

								Clinical compliance					
								Media			Substrate		
Ref.	Media	Substrate	Cell line tested (#)[1]	Pass -age	Folds (days)	Charact-rization[2]	New cell line derivation	XF	CD	Eco	XF	RTU[3]	Eco
[85]	X-VIVO 10[4]	hLM	ES (1)	40	4.5-6.8 (5-7)	Full	No	●	●	○	○	○	○
[87]	N2B27[5]	Matrigel	ES (2)	22	6 (4-5)	Full	No	○	●	○	○	○	○
[62]	mTeSR1	Matrigel	ES (4)	25	7-15 (7)	Full	Yes	○	○	○	○	○	○
[89]	StemPro	Matrigel	ES (5)	25	3 (~5)	Full	No	○	○	○	○	○	○
[64]	MEF-CM +FGF2	rh LM511	ES (3)	10	4-5 (4-5)	Partial	No	○	○	○	●	○	○
[72]	mTeSR1	rh VNT	ES (3)	5	3-4 (7)	Partial	No	○	○	○	●	○	○
[69]	mTeSR1	rh E-cadherin	ES (2) iPS (3)	37	~10 (7)	Full	No	○	○	○	●	○	○
[96]	StemPro	CELLStart	ES (2)	30	ND (5)	Partial	No	○	○	○	●	○	○
[83]	mTeSR1	VNT-UVPS	ES (3)	27	3 (6)	Full	No	○	○	○	●	○	●
[73]	E8	Truncated rh VTN	ES (1) iPS (5)	20	~10 (3-4)	Full	Yes	●	●	●	●	○	●

[1] Cell line tested (#): the number of cell line tested and the type of the cell line, ES or iPS.

[2] Characterization: including expression of pluripotency markers, *in vitro* and *in vivo* differentiation assay and karyotyping.

[3] RTU: ready-to-use, indicating capability to be fabricated on culture vessel and sterilized as a single product, with no need for coating before use.

[4] X-VIVO10: X-VIVO10 medium supplemented with nonessential amino acid (NEAA), L-glutamine, b-mercaptoethanol, rh FGF2, rh stem cell factor (SCF), rh Flt3 ligand, and rh leukemia inhibitory factor (LIF).

[5] N2B27: DMEM/F12 medium supplemented with B2 supplement, B27 supplement, NEAA, L-glutamine, b-mercaptoethanol, BSA, and rh FGF2.

Abbreviations: XF, xeno-free; CD, chemically defined; Eco, economically efficient; RTU, ready-to-use; rh, recombinant human; hLM, human laminin; VNT, vitronectin; ND, not determined; UVPS, UV/ozone-treated polystyrene.

Table 1-1. (Continue)

								Clinical compliance					
								Media			Substrate		
Ref.	**Media**	**Substrate**	**Cell line tested (#)[a]**	**Pass -age**	**Folds (days)**	**Charact-rization[d]**	**New cell lines**	**XF**	**CD**	**Eco**	**XF**	**RTU**	**Eco**
[73]	E8	Truncated rh VTN	ES (1) iPS (5)	20	~10 (3-4)	Full	Yes	●	●	●	●	○	●
[65]	mTeSR1 StemPro	LM511-E8 LM332-E8	ES (3) iPS (2)	30	~10 (4-6)	Full	No	○	○	○	●	○	○
	TeSR2	LM511-E8 LM332-E8	ES (1)	30	~10 (4-6)	Partial	No	●	○	○	●	○	○
[75]	mTeSR1	Heparin-binding peptide	ES (6) iPS (2)	20	10-12 (5-7)	Full	No	○	○	○	●	●	○
[80]	mTeSR1	Hit 9 polymer	ES (2)	10	3 (5-7)	Full	No	○	○	○	●	○	●
[74]	X-VIVO10 mTeSR1	Synthemax	ES (2)	10	30-94 hours[*]	Full	No	● ○	● ○	○ ○	●	●	○
[81]	mTeSR1	APMAAm	ES (2)	20	3-6 (3-5)	Partial	No	○	○	○	●	ND	●
[77]	mTeSR1	PMEDSAH	iPS (1)	20	~38 hours[*]	Full	Yes	○	○	○	●	●	●

liquid components that are not fully defined. A xeno-free alternative for mTeSR1, which replaces BSA with human serum albumin, is also commercially available (TeSR2, STEMCELL Technologies), but its undefined nature and high price are still major drawbacks for clinical applications. Some studies have also used NutriStem XF/FF medium (Stemgent) as a xeno-free and feeder-free culture medium for hPSCs on Matrigel to remove MEF before other experiments, such as gene targeting [37, 97]. These studies observed the preservation of marker expression and differentiation potential, but no systematic comparative study has reported an examination of the long-term culture of hPSCs with this media.

Impressively, Chen et al. recently reported a further refinement that finally eliminated BSA from their previous TeSR formula [73]. When reconsidering the necessity of the medium components in TeSR by double knockout, they found that BSA was not necessary in the absence of β-mercaptoethanol, a biological antioxidant. After further filtration, they simplified the formula to just eight essential components, including DMEM/F12 basal medium; the result, called E8 medium, is xeno-free and chemically defined. Combined with this group's separate finding that truncated vitronectin substrate supported the expansion of hPSCs, this system was shown to support the derivation and continuous culture of multiple hPSC lines with improved reprogramming efficiency, robust expansion (6 to 14 folds every 3 to 4 days), and well-kept pluripotency [73]. This low-protein medium (now commercially available as Essential 8 from Invitrogen and as TeSR-E8 from STEMCELL Technologies) has demonstrated reproducible and promising results when used with either Vitronectin XF or Matrigel in a number of studies [98]. The simplified formula lowered the list price of the medium by 25 to 30 percent compared to

StemPro or mTeSR1, and even more dramatically by 50% compared to the xeno-free alternative TeSR2.

Compared to CM-MEF conditions, hPSC cultures in many feeder-free systems showed significantly higher expansion rates, lower differentiation rates, and homogenous populations -- but with a simpler process. Normally by using these systems, about 5 to 15 folds of expansion can be achieved from one passage period within 3 to 7 days, and the culture can keep more than 80 to 90 percent of the hPSCs with positive expression of markers for undifferentiated state and normal karyotype for more than 20 passages. More importantly, combining many of these media with xeno-free substrates produced efficient systems for deriving hESC and hiPSC lines, showing promise as initial steps towards the clinical grade production of hPSCs in adhesion cultures.

1.6 *Expanding hPSCs in suspension*

The strategy of rapidly expanding hPSCs in adhesion was criticized for its intrinsic lack of scalability. Although the capacity of an adhesion culture can increase linearly to a certain level by adding more flasks in an automated system, a suspension culture system using conventional stirred-tank bioreactors is still preferred for its well-established geometric scalability and its compatibility with the online monitoring/control of temperature, O_2, CO_2, pH, glucose, lactate and biomass [99], especially at the pilot scale or larger. Along with the evolution of culture media and substrates, the past decade has seen significant progress in the culturing of hPSCs in suspension. Generally, researchers have developed two distinct types of suspension cultures: one based on microcarriers, and the other based on cell aggregates.

1.6.1 **Microcarrier-based suspension culture**

In making the transition from adhesion to suspension cultures, initial studies focused on growing hPSCs on microcarriers in a "pseudo-suspension" culture condition. Coating the microcarriers with feeder cells or the other substrates mentioned above, the studies demonstrated that microcarriers provided large surface areas that hPSCs could attach to for expansion in agitating vessels such as spinner flasks. The microcarriers examined so far are spherical or cylindrical particles ranging in size from 60 to 800 μm and made of polystyrene, dextran, cellulose, or glass with similar density as the media [100-109]. A conclusive review covering microcarrier-based hPSC cultures was recently published [25] by Chen et al. In most studies, hPSCs were cultured in media conditioned with MEF or human feeder cells. Thus, in Table 1-2, we highlight only the two studies that were targeting clinical use, avoiding conditioned media and feeder-coated microcarriers. Importantly, Oh et al. showed that microcarrier-based suspension cultures could offer high-yield expansion of hESCs, reaching a maximum cell density of 3.5×10^6 cells ml^{-1} in a seven-day culture [104], as compared to 0.8 to 1.5×10^6 cells ml^{-1} in side-by-side adhesion cultures on Matrigel. Such high-yield cultures are preferable to the large-scale production of cells, because of the high conversion efficiency of media and labor. The authors hypothesized that, in a stirred bioreactor, microcarriers provide a larger surface area and better O_2 and nutrient transfer than adhesion cultures [104]. Heng et al. demonstrated the use of human laminin to coat microcarriers, followed by culturing hESCs for 20 passages for average yields of approximately 1.5×10^6 cells ml^{-1} without

Table 1-2. Microcarrier-based suspension culture systems for hPSCs

									Media			MC + coating		
Ref.	**Media**	**Micro-carriers**	**Coating**	**Stirring**	**Cell line tested (#)**	**Pass-age**	**Folds (days)**	**Charact-rization**	**XF**	**CD**	**Eco**	**XF**	**RTU**	**Eco**
[104]	mTeSR1 StemPro	DE-53	Matrigel	Spinner flask	ES (2)	25	5.8-10 (4-7)	Full	○	○	○	○	○	○
[109]	StemPro	Poly-styrene	hLM mVNT	Shaker	ES (2)	20	8.5 (7)	Full	○	○	○	● ○	○	○

Table 1-3. hPSC aggregate-based suspension culture systems in spinner flasks

Ref.	**Media**	**Volume (ml)**	**Cell line tested (#)**	**Passage**	**Folds (days)**	**Max yield (cells ml^{-1})**	**Characteri-zation**	**Undifferen-tiated (%)**	**XF**	**CD**	**Eco**
[110]	mTeSR1	100	ES (1)	4	5 (5-6)	1.6×10^6	Full	76 - 98	○	○	○
[111]	mTeSR1	50	ES (3)	5	2 (7)	$2\text{-}2.4 \times 10^6$	Full	85 - 98	○	○	○
[112]	mTeSR1	50	ES (3) iPS (2)	10	2-3 (4-7)	$2\text{-}3 \times 10^6$	Full	> 85	○	○	○
[113]	IL6RIL6[a]	50	ES (7) iPS (6)	20	17.7 (6)	1.89×10^6	Full	ND	○	○	○
[114]	HFF-CM[b]	100	ES (2) iPS (2)	20*	8 (7-10)	2.8×10^6	Partial	95 - 98	●	○	○
[115]	mTeSR1	100	iPS (1)	2*	5.5 (7)	2×10^6	Partial	69 - 97	○	○	○
[116]	StemPro	60-250	ES (3)	21	3.2-4.3 (3-4)	1.1×10^6	Full	> 90	○	○	○

[a] IL6RIL6: DMEM/F12 medium supplemented with KO-serum replacement, nonessential amino acid (NEAA), L-glutamine, β-mercaptoethanol, rh FGF2, and rh full-length interleukin-6 and interleukin-6 receptor (IL6RIL6) chimera.

[b] HFF-CM: Human foreskin fibroblasts conditioned DMEM/F12, GlutaMAX, rh FGF2.

* Karyotype was not determined.

losing pluripotency and normal karyotype [109]. This remains the only reported study that has successfully cultured hPSCs on microcarriers coated with xeno-free substrate in a nonconditioned medium. Although the microcarrier-based suspension culture has been scaled up to working volumes of 150 ml in spinner flasks, the experiments revealed several shortcomings. Because hPSCs tended to stick together rather than evenly distribute on the microcarrier surface [25], heterogeneous clustering might occur during the culture process, which could induce unexpected differentiation and selection of genetically abnormal populations due to the stress created by insufficient transfer of nutrients and O_2. Moreover, removing microcarriers at harvest required additional filtration that would be a cumbersome step for cGMP manufacturing.

1.6.2 **Aggregate-based suspension culture**

Inspired by the self-aggregation observed in the embryoid body (EB) differentiation of hESCs in suspension [117-120], researchers sought to establish carrier-free suspension culture systems for expanding hPSCs (Table 1-3). Initially, they inoculated cells into suspension cultures as cell clumps, using mechanical or mild enzymatic passaging methods [121, 122], which resulted in relatively heterogeneous formations of cell aggregates and a reduced reproducibility. After the discovery of Rho-associated coiled-coil kinase (ROCK) inhibitors (Y27632, HA-100, etc.) and their function of diminishing apoptosis and permitting the survival of dissociated hPSCs [51, 123], several groups established suspension culture systems that, with the addition of ROCK inhibitors to the culture media, supported single-cell inoculation, uniform aggregation, and long-term proliferation in an undifferentiated state [110-116, 124].

Zweigerdt et al. and Amit et al. reported detailed protocols for the adaptation and expansion of hPSCs in both static and dynamic suspension in a variety of vessel types [112, 113]. Recently, Olmer et al. reported a high-yield culture in a fully controlled bioreactor system. Up to 2×10^8 of hiPSCs were obtained from a working volume of 100 ml in a single run of seven days [115]. Chen et al. moved one step forward to clinically compliant process showing long-term culture of hESCs in suspension with a calculated cumulative expansion of more than 1×10^{13}-fold within 21 passages (about three months). That paper also demonstrated a complete strategy for hESC banking under cGMP conditions using 500 ml disposable spinner flasks to expand cells [116]. Furthermore, Steiner et al. also claimed a complete strategy to derive, expand, and differentiate hESC lines all in suspension conditions [125], making it possible to avoid any effects from feeder cells and substrates.

The key to efficient expansion in aggregate-based suspension cultures is to keep homogeneous aggregate formation to an appropriate size that allows the effective diffusion of nutrients. This can be accomplished by improving media formulation and passaging methods to enhance cell viability, as well as by designing bioreactors with optimized hydrodynamic properties that generate mild but sufficient shear stress in an evenly distributed velocity field. Different hPSC lines have varying adaptability to shear stress [112], which may also constitute a limitation for universal applications. Furthermore, well-controlled one-direction shear flow showed enhancive effect on the hematopoietic and endothelial differentiation of PSCs in adhesion [126, 127]. However, the shear force on the cell surface in the suspension culture system is uncontrolled and ever changing due to the locally unsteady flow and the rotating of the microcarrier or the

cell aggregate. The effect of this inconstant shear stress to *in vitro* cell differentiation has not been clearly understood. Thus, optimization of the operation, including agitating speed, seeding density, media change, and split interval, is a necessary step for each particular hPSC line.

1.7 *Culture scales and equipment*

The scale of hPSC expansion for clinical use should be determined by the demands and specifications of individual therapies. The decision should consider the potential market, cells/dose, doses/year, lots/year, doses/lot and, eventually, determination of the total manufacturing requirement [128].

Potential allogeneic therapies using hPSCs usually aim to provide cell products derived from a single donor to many other patients. Accordingly, the culture scale for this type of therapy could run from tens to hundreds of liters in order to be cost-effective. For hPSC cultures at this level, only a large-scale stirred-tank bioreactor system combined with aggregate-based suspension cultures might meet the requirement, although its development would remain very challenging.

In contrast, the strategy of autogenic therapies relies on providing cell products to treat only the patient who donated the parental cells, which adheres more closely to the principle of hiPSC therapies. Since the cultured products are for a single patient, a relatively small-scale hPSC culture should be adequate, as long as efficient differentiation and downstream processes are well established. For this purpose, the current level of development of highly efficient adhesion cultures might suffice, when combined with such multilayer vessels as CellCube and CellSTACK (Corning) and Cell Factory

(Thermo Scientific Nunc), to obtain the needed cell dosages. A fully controlled, compact and closed planar culture system (Integrity Xpansion, ATMI) has also become commercially available. Achieving productions of hPSCs in large lot-size using adhesion cultures could also occur with the assistance of robotics technology to facilitate the handling of many culture flasks [129]. Successful studies have reported automated hESC adhesion cultures using the CompacT SelecT (TAP Biosystems) and the 3D Cellhost (Hamilton) systems [130, 131]. The CompacT SelecT system can handle an estimated 90 T175 flasks per run, providing 15,750 cm^2 of surface area that can yield approximately 3 $\times 10^9$ hPSCs in a single three-day culture in feeder-free conditions. For comparison, the largest volume used in current studies on suspension cultures of hPSCs was 250 ml. A three- to six-day culture can harvest approximately 2×10^6 cells ml^{-1}, making a total yield of 2×10^9 for four parallel vessels in one regular size CO_2 incubator. It should not be difficult to scale up to 500 ml in a 1-liter spinner flask, due to the compatible platform and bioreactor design. Comprehensive reviews by dos Santos et al. [132] and Want et al. [99] include useful information about bioreactor design and case studies of scale determination for clinical-grade expansion of hPSCs.

1.8 *Hematopoietic differentiation and erythrocyte production from hiPSCs*

As an irreplaceable clinical practice in modern medicine, red blood cell (RBC) transfusion saves lives of patients suffering from severe blood lose or chronic anemia. For example, transfusion-dependent patients often receive two or more units of donated whole blood or isolated RBC concentrates (each unit contains ~2×10^{12} RBCs) every two weeks. Despite of extensive efforts in making synthetic blood replacements in the past

several decades, accessibility and dependence on blood donation remain critical around the world. This is a particularly important issue for the patients who need RBCs of rare blood types, because of severe complications caused by mismatching transfusion or allo-sensitized responses among chronically transfusion-dependent patients [133].

1.8.1 **Erythrocyte generation from primary CD34$^+$ cells**

A potential solution is to manufacture RBCs from hematopoietic stem and progenitor cells (HSPCs) that are isolated from patients themselves or donors with desirable blood types. As the main source of *in vitro* RBC generation, human HSPCs were harvested from mobilized peripheral blood [134], bone marrow [135, 136], cord blood (CB), and fetal liver [137]. CB CD34$^+$ cells were intensively studied as a primary candidate due to their high content of HSPCs, easy accessibility, and the nature as an otherwise discarded medical waste [138-144]. Recently, mature RBCs that were generated *ex vivo* from CD34$^+$ HSPCs were transfused into a volunteer to demonstrate *in vivo* safety [143], albeit at limited quantity (~4×10^{10} RBCs or ~2% of one transfusion unit). One major challenge for clinical applications has been how to expand HSPCs extensively because committed erythroid progenitors have limited proliferative potential before differentiating into mature RBCs [145].

1.8.2 **Erythrocyte generation from hPSCs**

In spite of worldwide study for over 20 years, CB CD34$^+$ cells showed limited life span *in vitro* under current expansion conditions [145]. Instead, hPSCs provide realistic alternative choices for the ability of indefinite expansion and directed differentiation *in vitro*. Early studies achieved enucleation, hemoglobin switch (from embryonic to fetal

and to adult), and functional oxygen carrying ability in hESC-derived RBCs [146-148]. Compared to the ethic and technical challenges of the generation of hESC lines, hiPSCs can be easily derived from donor somatic cells [149], providing a potentially unlimited source of any RBC type, especially universal donor type O Rhesus D-negative (O Rh-) and rare-phenotype matching RBCs, as well as pathogenic gene-corrected RBC for autologous transfusion therapies [150]. Convinced by the prove-of-concept to use hiPSCs as an alternative source of HSPCs and RBCs for their indefinite *in vitro* expansion and ease of genetic modification using rapidly evolving gene editing technologies, governments in UK (Medicines & Healthcare Products Regulatory Agency, https://www.gov.uk/government/organisations/medicines-and-healthcare-products-regulatory-agency) and US (The American Recovery and Reinvestment Act, http://www.recovery.gov/arra/) are investing the generation of pathogen-free iPSCs from O Rh- donors for potential manufacture of universal donor RBCs. However, the efficiency of erythroid expansion was usually reported as 20 to 200-fold lower in hiPSC-derived HSPCs than those from CB $CD34^+$ [151].

1.9 *Scalability of the differentiation system*

Considering a manufacturing process required for clinical purposes, one has to implement a culture procedure with vessels that are suitable for large-scale cell culture and expansion. Most EB differentiation strategies involve separation of individual EBs using multi-well plates. They can only accommodate a pilot scale production in a scale-out process by linearly increasing the number of culture vessels, which requires investment of advanced automation equipment if technically feasible. In contrast, the

methods of forming EBs in suspension showed the capacity to adapt to vessels that were compliant with scale-up bioprocess and generate matured cells, such as cardiomyocytes, myeloid cells, and hepatocytes [152-156]. In these studies, spinner flasks and flat tissue culture flasks placed on a rocker were commonly used due to the scalability of directly transferring to well-established stirred tank bioreactors (up to 2000 L) and wave bag bioreactors (up to 1000 L), respectively. These bioreactor systems are widely utilized in industrial biotechnology for multi-parametric monitoring/control. However, this kind of a scalable system has not yet been established for the generation of human erythrocytes from hiPSCs.

1.10 *Clinical consideration for postexpansion downstream process*

After the differentiation process, the complete removal of undifferentiated hPSCs from the resultant product is strictly required to reduce the risk of tumor generation. For example, the clinical trial of RPE cells claimed that the product RPE dosage contained only 0.00008% parental hESCs. The cryopreservation method should also comply with the cGMP regulations, the expansion system, and the shipping and handling protocols. Hunt and Li et al. provided detailed reviews covering the development of cryopreservation for hPSCs under cGMP settings [157, 158].

Part of this section has been published in Ref. 233.

1.11 *Thesis Overview*

The *ex vivo* production of RBCs from hiPSCs holds great promise to potential clinical applications. However, it requires process that is compliant to large-scale manufacturing. The overall hypothesis of this thesis is that by applying principles of

chemical engineering, such as hydrodynamic analysis, mass transfer, bioreactor design and process optimization of physical cues, combined with optimization of biological cues, such as medium formulation and cytokine/growth factor studies, we can establish scalable systems for the expansion and erythrocyte production of hiPSCs. This thesis can be divided into three specific aims:

Specific Aim 1: Establishing a scalable system for the long-term expansion of undifferentiated hiPSCs in suspension.

Comparing to the reported systems for the expansion of hPSCs in suspension which used undefined media, here we utilized newly development E8 medium in glass-ball type spinner flask to achieve long-term expansion of undifferentiated hiPSCs in xeno-free and chemically defined conditions. The study for this specific aim will be presented in Chapter 3.

Specific Aim 2: Establishing an efficient and reproducible process for HSPC differentiation and erythrocyte production.

We re-formulated the differentiation media using FDA-approved pharmacological reagents enhance the efficiency and reproducibility of the current hematopoietic differentiation process for the HSPC generation from hiPSCs. We also used human plasma to induce terminal maturation towards enucleated and β-hemoglobin expressing erythrocytes. The study for this specific aim will be presented in Chapter 4.

Specific Aim 3: Improving the scalability of the differentiation system for erythrocyte production.

The scalability limitation of the current EB differentiation system using 96-well plates presents a big hurdle in the scale-up process of HSPC generation. Here we

improved the scalability using the combination of spinner flask and platform rocker. The study for this specific aim will be presented in Chapter 5.

2 *Overview of Experimental Methods*

2.1 *Approval of using hiPSCs and primary cells from anonymous donors*

The experiments using hiPSCs were approved by the Institutional Stem Cell Research Oversight (ISCRO) committee in the Johns Hopkins University. Use of anonymous human samples for laboratory research was approved by the Institutional Review Board of the Johns Hopkins University.

2.2 *Maintenance of hiPSCs in adhesion*

Human iPSC lines BC1, TNC1 and E2 were initially maintained on MEF feeders in standard ESC medium as previously described [11]. At passage 30-32, BC1 cells were dissociated using 0.5mM EDTA in calcium- and magnesium-free PBS [159], and directly adapted onto tissue culture plates coated with Matrigel (1.67 μg/cm^2, BD) or truncated recombinant human vitronectin (VNT-N, 5 μg/cm^2, Invitrogen) in E8 medium (home-made as described by Chen *et al*. [73], or Essential 8 from Invitrogen) supplemented with 10 μM ROCK inhibitor Y27632 (Stemgent) for 24 hours. Medium was changed daily. Cells were routinely passaged as small clumps using EDTA method [159] or as single cells using Accutase (Sigma-Aldrich) with the split ratio of 1:8 to 1:12 every 2 to 3 days after reaching 60% to 80% confluent. Cells were stained with 0.4% Trypan Blue, and the cell number was counted by and counted by Countess automated cell counter (Life technologies).

2.3 *Flow cytometry analysis*

Single cell samples were prepared in 3×10^5 cells per aliquot. Undifferentiated iPSCs were stained with anti-TRA-1-60 (mouse IgM, 1:200, Millipore MAB4360), anti-SSEA4 (mouse IgG3κ, 1:200, DSHB MC-813-70), anti-Oct4 (rabbit IgG, 1:100, Santa Cruz C-10), and anti- Nanog (rabbit IgG, 1:100, Peprotech P236) as primary antibodies, and Alexa Flour 488 (goat- anti-mouse IgM, goat-anti-mouse IgG3κ, or goat-anti-rabbit IgG, 1:400, Invitrogen) as secondary antibodies. The cells were fixed and penetrated by following the instruction of FIX & PERM® cell fixation & cell permeabilization kit (Invitrogen) for the staining of nuclear markers. For hematopoietic differentiation, conjugated anti-human CD34-APC, CD45-Alexa Flour 488 (1:20, BD), CD45-APC (Thermo Fisher Scientific), CD235a-FITC (Thermo Fisher Scientific), CD36-APC (BD Biosciences), Band3-FITC or Band3-APC (kindly provided by Dr. Xiuli An at New York Blood Center), CD49d-FITC (Miltenyi Biotec), CD71-PE (Thermo Fisher Scientific), CD14-FITC (Thermo Fisher Scientific), CD41-APC (Thermo Fisher Scientific), CD42a-PE (Thermo Fisher Scientific), CD15-FITC (Thermo Fisher Scientific), CD33-PE (Thermo Fisher Scientific) were used. To analyze hemoglobin expression, cell stained with anti-β-globin-PE (Santa Cruz Biotechnology) and anti-fetal hemoglobin-FITC (Thermo Fisher Scientific) after fixation and permeabilization. To analyze enucleation, cells were co-stained with DRAQ5 (a cell permeable dye for DNA staining, Cell Signaling Technology). Isotype controls were set according to the antibodies. Before analysis by fluorescence-activated cell sorter, dead cells were stained by Via-Probe cell viability solution (BD Bioscience) and gated out in analysis to avoid unspecific staining. Terminal deoxynucleotidyl transferase dUTP nick end labelling (TUNEL) assay (In situ

cell death detection kit fluorescein, Roche) was performed according to the manufacturer's instructions. Negative and positive controls for TUNEL were set following the instructions of the kit. All samples were analyzed with FACSCalibur flow cytometer (BD Bioscience). At least 15,000 gated events were collected and analyzed using FlowJo X software.

2.4 *Immunofluorescent staining and fluorescent microscopy analysis*

Undifferentiated hiPSCs on Matrigel- or VNT-N-coated plates or spontaneously differentiated cells on gelatin-coated plates were prepared for immunofluorescence microscopy as described before [11]. For undifferentiated hiPSCs, anti-TRA-1-60 (1:100), anti-SSEA4 (1:100), anti-Oct4 (1:50), and anti-Nanog (1:50) were used as primary antibodies. The corresponding secondary antibodies were Alexa Flour 555 (goat-anti-mouse IgM, or goat-anti-mouse IgG,1:200, Invitrogen) and Alexa Flour 488 (goat-anti-rabbit IgG, 1:200, Invitrogen), respectively. For spontaneous differentiation, anti-α-fetoprotein (rabbit IgG, 1:500, DAKO), anti-CD31-PE (conjugated, 1:5, BD), anti-β-3-tubulin (mouse IgG, 1:1000, Sigma T8660) were used, and Alexa Flour 555 (1:200) was stained for visualization. After wash, cells were stained for nucleus and mounted with ProLong Gold antifade reagent with DAPI (Invitrogen).

Cells from terminal maturation day 6 (TM6) were incubated in terminal maturation medium with 5 μM Calcein AM (Thermo Fisher Scientific) for 1 hour in 37 °C. After wash once with PBS, 1×10^4 cells were re-suspended in 100 μl PBS+1% FBS with CD235a-PE (1:20, Thermo Fisher Scientific) and DRAQ5 (1:300), and incubated in

room temperature for 20 min. All fluorescent images were acquired using Eclipse TE2000-U microscope (Nikon).

2.5 *Cytospin and histological staining*

All single cells (6×10^4 - 9×10^4 cells per slide depend on cell size) were mounted on slides using Cytospin (Thermo Fisher Scientific) as per manufacturer's instructions. Hema 3 kit (Thermo Fisher Scientific) was used as a Wright-Giemsa-like staining for cell morphology analysis.

2.6 *Colony-forming unit (CFU) assay*

Methylcellulose-based MethoCult Kit (STEMCELL Technologies) was used for hematopoietic CFU assay as per manufacturer's instructions. Suspended cells (5,000 cells) on EB day 13 to 14 were seeded into 35-mm dishes supplemented with 3U/ml erythropoietin (EPO). After 14 days of semi-liquid culture, colonies were scored according to the standards provided in the MethoCult protocol.

2.7 *Statistics*

All analysis of cell number, cell viability, EB size, and flow cytometry were collected from at least three independent experiments ($n \geq 3$), and all measurements were done in duplicates or triplicates to avoid sampling error, if possible. Quantitative real-time polymer chain reaction (qRT-PCR) analysis was performed in two independent experiments with triplicate readings each. The unpaired two-tailed Student's t-test or two-way analysis of variance (two-way ANOVA) followed by Bonferroni's posttest was done using GraphPad Prism 5 for the comparison between two groups or multiple groups,

respectively. Data are presented as mean ± SD if not specified. Significance level was assigned as not significant (n.s.) $P > 0.05$, * $P < 0.05$, ** $P < 0.01$, and *** $P < 0.001$.

3 *Scalable expansion of hiPSCs in the defined xeno-free E8 medium under adherent and suspension culture conditions*

Large-scale production of hiPSCs by robust and economic methods has been one of the major challenges for translational realization of hiPSC technology. Here we demonstrate a scalable culture system for hiPSC expansion using the E8 chemically defined and xeno-free medium under either adherent or suspension conditions. To optimize suspension conditions guided by a computational simulation, we developed a method to efficiently expand hiPSCs as undifferentiated aggregates in spinner flasks. Serial passaging of two different hiPSC lines in the spinner flasks using the E8 medium preserved their normal karyotype and expression of undifferentiated state markers of TRA-1-60, SSEA4, OCT4, and NANOG. The hiPSCs cultured in spinner flasks for more than 10 passages not only remained pluripotent as indicated by *in vitro* and *in vivo* assays, but also could be efficiently induced towards mesodermal and hematopoietic differentiation. Furthermore, we established a xeno-free protocol of single-cell cryopreservation and recovery for the scalable production of hiPSCs in spinner flasks. This system is the first to enable an efficient scale-up bioprocess in completely xeno-free condition for the expansion and cryopreservation of hiPSCs with the quantity and quality compliant for clinical applications.

3.1 *Introduction*

Human pluripotent stem cells (hPSCs), including human induce pluripotent stem cells (hiPSC) and human embryonic stem cells (hESCs) that can differentiate into any mature cell type of the body, hold great promise for revolutionizing regenerative medicine. Specifically, the integration-free reprogramming technologies, such as ones using plasmids, provide a feasible method to generate autologous and clinical-grade hiPSC lines for therapeutic applications under current good manufacture practice (cGMP) conditions. Patient-specific hiPSC lines derived from postnatal somatic cells [11-13], can not only be used to establish disease-specific models for pathological studies, but also exhibit vast potential in practical cellular therapies. These clinical applications require a large number of hiPSCs or their progenies. For example, an optimized dose was suggested to contain 4.2×10^8 to 5.6×10^8 $CD34^+$ cells for hematopoietic stem cell (HSC) transplantation for a 70-kg adult patient [47]. Production of a clinically relevant quantity of hiPSCs and/or their progenies for specific applications, sometimes considered as ~1 to 2 billion [122], in a chemically defined condition by robust, reproducible and economic methods remains a major challenge for advancing hiPSC technology from the bench to the clinic.

Conventionally, hiPSCs are induced and expanded on feeder cells as adherent colonies in media containing sera or serum replacement containing human or animal serum albumin [160, 161]. The involvement of animal products or sera impedes these culture conditions to meet the strict requirement of clinical or pre-clinical utilization because of the uncertainty of complex components and the quality variance from batch to batch. Since the first isolation of hiPSCs, significant improvements in feeder- and serum-

free chemically defined culture medium and substrates for adherent hiPSC culture have been developed [73, 85, 89, 162, 163]. However, these approaches involving adherent culture of hiPSCs in Petri dishes still raise a major hurdle of large scale and well-controlled expansion for clinical use.

Suspension culture for hiPSC expansion provides a feasible solution for its scale-up capacity. After a Rho-associated-coiled-coil kinase (ROCK) inhibitor Y27632 was reported to permit the survival of dissociated hESCs when supplemented in the medium only on the first day of seeding [123], detailed protocols were established for the single-cell inoculation and suspension culture of hPSCs as cell aggregates in a variety of vessel types [112, 113, 124]. Other studies have also reported successful suspension culture in spinner flasks in 100-ml vessels [110, 111, 114-116, 125, 164]. Despite the rapid development of hPSC suspension culture in these studies, most of the reproducible systems are based on commerciality available serum-free media, mTeSR or StemPro, which are complex and expensive. The unknown composition and high cost of these media pose a major concern for large-scale expansion.

Chen *et al.* recently reported the development of a significantly improved hiPSC culture medium, E8, which contains only seven other completely defined and xeno-free components supplementing the standard DMEM/F-12 medium [73]. We did confirm that this significantly improved medium without the need to add BSA or human albumin supported the growth of multiple hiPSC lines under feeder-free conditions in adhesion. Based on this, we sought to test whether the significantly simplified E8 medium could support a robust and economic suspension culture system in a stirred bioreactor for large-scale expansion and cryopreservation of hiPSCs. Here, we used two integration-free

hiPSC lines, BC1 and TNC1, which were derived from leukocytes of either a healthy donor or a sickle cell disease patient using plasmid-based episomal vectors [11]. We began by evaluating the capacity of E8 medium to support the expansion of hiPSCs in static suspension cultures. We then optimized the operating protocol for direct adaptation and expansion of the hiPSCs in spinner flasks using computational simulation of the hydrodynamic properties and experimental tests. Furthermore, we tested serial passaging and differentiation potential of hiPSCs expanded in spinner flasks. Finally, xeno-free cryopreservation and recovery methods were established for hiPSCs cultured in the bioreactor.

3.2 *Materials and Methods*

3.2.1 **Suspension culture of hiPSCs**

BC1 and TNC1 were cultured in feeder-free adhesion culture for at least 5 passages before transfer in suspension culture. Prior to the passage, hiPSCs were treated with Y27632 for 1 hour and dissociated with pre-warmed Accutase for 2 to 3 min in 37°C. After gently pipetting, the single cell solution was diluted 1:10 with DMEM/F-12, and centrifuged at 200g or 5 min. Cells were resuspend by adding E8 medium with 10 μM Y27632 and plated at density of 1.5×10^5 to 2.0×10^5 cells/ml in ultra-low attachment plates or seeded at 4×10^5 to 5×10^5 cells/ml. Daily medium change was performed by replacing 70% of the medium with fresh E8 medium without ROCK inhibitor. Cells were cultured in static condition or in spinner flasks (CELLSPIN system of 100 ml capacity with a single glass-ball stirring pendulum, Integra Bio-sciences) in standard 5% CO_2 incubator at 37°C and passaged every 3 to 4 days using Accutase as aforementioned.

3.2.2 **Computational fluid dynamics (CFD) analysis of glass-ball spinner flasks**

The "Chemical engineering" module in COMSOL Multiphysics® 3.5 software was used to perform the numerical calculation of the velocity field and shear stress distribution in the spinner flask. A 3-dimentional (3D) "Rotating machinery" model was established following the user guide of the software to simulate the agitating effect of the glass-ball impeller. The geometry of the spinner flask was measured from the real object, and the total volume of the fluid body in the model was set as 45.6 ml or 639.6 ml for the simulation of 100-ml or 1-L spinner flask, respectively. The gap between the moving mesh coordinates and the fixed mesh coordinates was set to 0.02 mm. An automatic generated fine mesh divided the entire fluid body into >10, 000 elements. The velocity field was calculated following Navier-Stocks equation for incompressible fluid at steady state, neglecting gravity:

$$\rho(\boldsymbol{u}\cdot\nabla)\boldsymbol{u} = \nabla\cdot[-p\boldsymbol{I} + \mu(\nabla\boldsymbol{u} + (\nabla\boldsymbol{u})^T)] \quad \text{(Eq. 1)}$$

where r and m are the density and the dynamic viscosity of the fluid, respectively; $\boldsymbol{u}$ is the vector of velocity in three directions; p is pressure, and ∇ is the gradient operator. On a certain X-Y plate, the x-y component of the shear stress tensor was defined as:

$$\tau_{xy} = \mu\left(\frac{dv_x}{dy} + \frac{dv_y}{dx}\right) \quad \text{(Eq. 2)}$$

where v_x and v_y are the velocity in x-direction and y-direction, respectively.

The element Reynolds number (local Re) was calculated as

$$Re = \frac{\rho\bar{u}}{\mu}(V)^{1/3} \quad \text{(Eq. 3)}$$

where $\bar{u}$ is the mean velocity of the flow in an element, and V is the volume of the element. The initial velocity of every element was set as orbital rotation in the

geometrically corresponding cylinder without the impeller to get a quick convergence at relative tolerance set as 0.001.

3.2.3 **Analysis for aggregates and metabolism**

Samples of cell aggregates were analyzed for cell number, viability, and metabolic products. Briefly, 0.5 to 1.5 ml of samples were taken and placed still for 5 min. Supernatants were filtered, stored in -20°C, and tested for glucose, lactate, and pH in a blood gas analyzer (Radiometer, ABL 710). Light microscopy images were captured using Axiovert phase contrast microscope (Zeiss). The total number of cell aggregates N_{agg} in a 1-ml sample was analyzed by using the "Embryoid body analysis" module in Celigo imaging cytometer (Brooks). The average equivalent diameter of aggregates d and the size of each aggregate in the sample were also measured in this analysis. For counting the cell number in a 1-ml sample N_{cell} and the cell viability, cell aggregates were dissociated by Accutase, stained with 0.4% Trypan Blue, and counted by Countess automated cell counter (Life technologies). The average cell number per aggregate $N = N_{cell}/N_{agg}$ was calculated in 8 samples containing aggregates in different average diameters d from three independent culture cycles. In the plot of N-d, the data points fit best to a 3rd-order polynomial, defined by having the smallest R^2 value comparing to other fitting functions. Dissolved oxygen (DO) level in the suspension medium was monitored real-time using a non-invasive optical fiber probe and PSt3 sensor spots via Oxy-4 mini transmitter (PreSens).

3.2.4 **Immunofluorescent staining of cell aggregates in suspension culture**

Whole aggregate staining was performed for immunofluorescence microscopy as described before [116]. Fluorescent images of whole cell aggregates were captured and analyzed by LSM 510 META confocal microscope (Zeiss).

3.2.5 **Karyotyping**

Karyotype of hiPSCs was examined by a certified cytogeneticist using G-banding (300-500 bands) method as previously described [11]. At least 20 metaphases were checked for each sample. For example, passage number of BC1 p30+21+21 means that the examined BC1 cells has been cultured for 30 passages on MEF, followed by 21 passages on VNT-N and 21 passages in bioreactor. For TNC1 p30+17+19, there have been 30 passages on MEF, 17 passages on Matrigel, and 19 passages in bioreactor.

3.2.6 ***In vitro* spontaneous differentiation of germ cells**

Single cells were seeded in ultra-low-attachment plates in ESC medium supplemented with 10% fetal bovine serum (FBS, Hyclone) at 3.3×10^5 cells/ml to initiate EB formation. For iPSCs maintained in suspension in spinner flasks, cell aggregates were washed, and the entire medium was changed from E8 to differentiation medium to induce transformation from cell aggregates to EBs on day 3 after passaging. After 8 days, EBs were transferred onto gelatin-coated plates and attached. Differentiated cells on day 12 were stained for fluorescence microscopy as described.

3.2.7 **Teratoma formation assay**

The use of immunocompromised mice for teratoma formation assay was approved by the Animal Care and Use Committee in Johns Hopkins University. The assay was

performed as we described before [11]. Approximately 5×10^6 hiPSCs were collected after Accutase digestion of the culture in spinner flask for more than 10 passages, washed with PBS and resuspended in 200 ml diluted (1:1) Matrigel solution (BD). Cells were injected intra-muscularly into NOD/SCID/IL2RG(γc)-/- immunocompromised mice with a further reduced level of natural killer cells. Teratomas were excised 6-10 weeks after injection. After sectioning, slides containing various regions of teratomas were stained by H&E and analyzed under microscope.

3.2.8 **Cryopreservation and recovery of hiPSCs in suspension culture**

Cell aggregates on day 2 or day 3 were pre-treated with 10 μM Y27632 for 1 hour and dissociated into a single cell suspension with Accutase. After washing with PBS once, cells were suspended in E8 + 10 μM Y27632 and distributed into Cryovial aliquots. The same amount of E8 + Y27632 + 20% (in volume) DMSO cryopreservation medium was added dropwise. Cells were immediately frozen cells at -80°C in isopropanol freezing containers overnight, and transferred to liquid nitrogen for storage. For recovery from frozen stock, the cells were thawed by following standard cell culture protocol. Single cells were seeded at 5×10^4 cells/cm^2 in either Matrigel- or VNT-N-coated 150-cm^2 flasks or ultra-low attachment plates, or at 5×10^5 cells/ml directly in spinner flasks at agitating speed of 60 rpm. The aforementioned culture and passaging protocols were followed afterwards.

3.3 *Results*

3.3.1 **Adaptation and robust growth in feeder-free adhesion culture**

To prevent contamination of feeder cells in suspension culture, we first acclimated hiPSCs expanded in conventional MEF culture conditions [11] into feeder-free condition. BC1 and TNC1 were transferred directly to E8 medium [73] on culture plates coated with diluted Matrigel or on purified recombinant vitronectin substrate [73]. We found that a step-by-step adaptation process, which is typically associated with other feeder-free conditions [165-167], is not required when we switched to E8 feeder-free conditions. Culture on either Matrigel or VNT-N supports robust and long-term culture of adherent, undifferentiated hiPSCs as a monolayer in adhesion (Figure 3-1). The hiPSCs were routinely passaged in single cells (using Accutase) or in small clumps (by EDTA) [73] at a split ratio of 1:8 to 1:12 every 3 to 4 days. They expressed TRA-1-60, SSEA4, OCT4, and NANOG, that are markers for undifferentiated hPSCs (Figure. 3-1, C-E). After more than 30 passages cultured in E8 medium and feeder-free conditions, hiPSCs maintained normal karyotype (Figure 3-1, F). These hiPSCs were able to form EBs *in vitro* containing cells from all three germ layers (Figure 3-2, A), confirming that the hiPSCs retained their pluripotency. We also examined directed hematopoietic differentiation of BC1 and TNC1 cultured under the E8 feeder-free conditions for at least 10 passages. Using forced aggregation method in 96-well plates [168-170] in a feeder-free and serum-free condition, we found that on day 14, ~25%-80% of the differentiating hiPSCs were $CD34^{+}CD45^{+}$ HSPCs (Figure 3-2, B). Moreover, hiPSCs expanded in E8 feeder-free condition showed comparable potential to generate multiple hematopoietic

lineages as hiPSCs expanded in MEF culture conditions in the standard CFU assay [170, 171] (Figure 3-2, C).

Figure 3-1. Long-term adhesion culture of hiPSCs in feeder-free conditions in E8 medium

Morphology (A), expansion rate (B), and expression of pluripotency markers (C-E) of hiPSCs cultured on feeder or feeder-free substrates. (F) Karyotypes of hiPSCs after long-term culture on Matrigel or xeno-free VNT-N in E8. Passage numbers represent the passages in feeder-free conditions. Scale bars represent 200 μm, except for those in images of TNC1 in (E), which represent 100 μm.

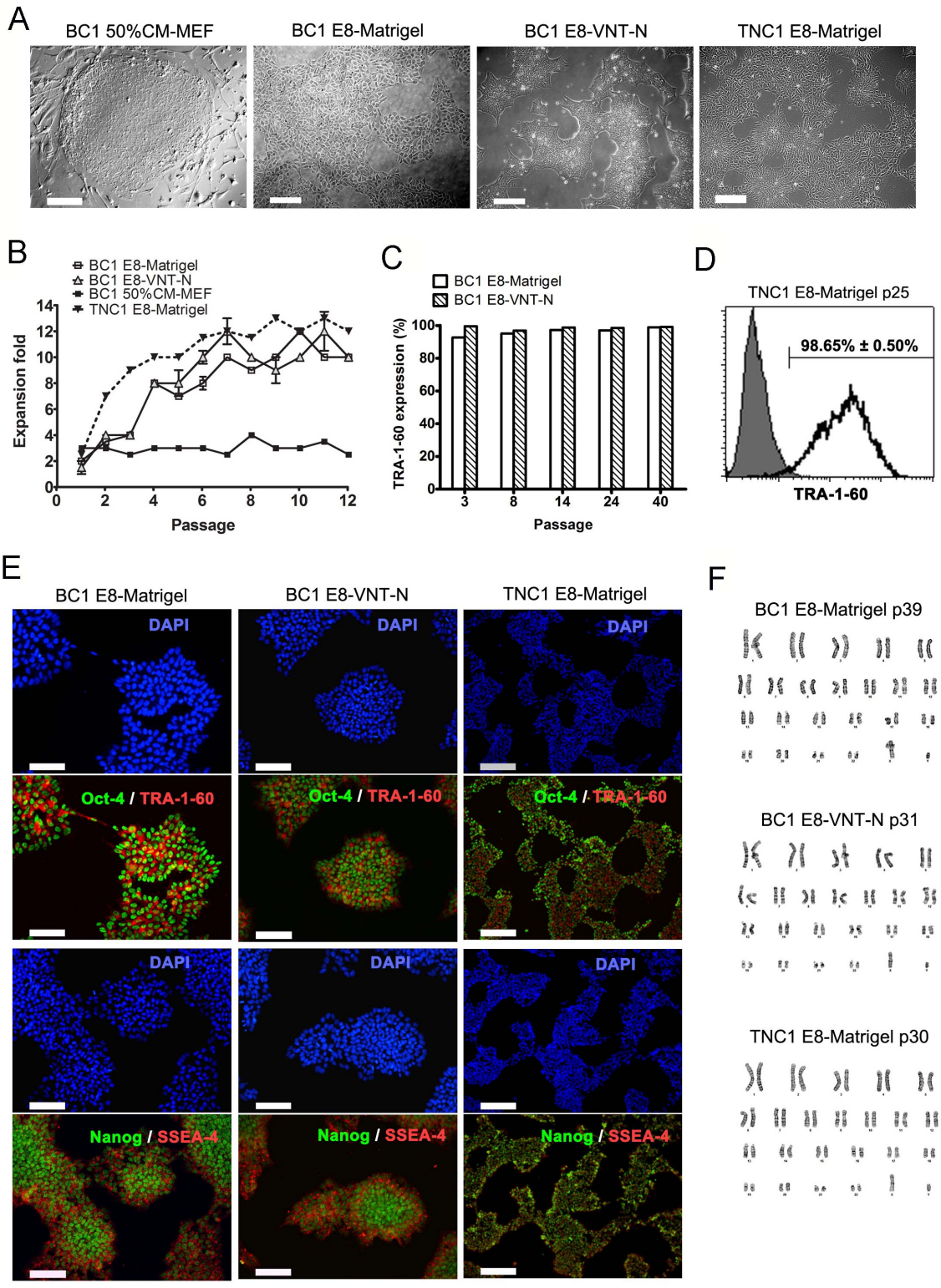
A
BC1 50%CM-MEF
BC1 E8-Matrigel
BC1 E8-VNT-N
TNC1 E8-Matrigel
B
BC1 E8-Matrigel
BC1 E8-VNT-N
BC1 50%CM-MEF
TNC1 E8-Matrigel
Expansion fold
Passage
C
BC1 E8-Matrigel
BC1 E8-VNT-N
TRA-1-60 expression (%)
Passage
D
TNC1 E8-Matrigel p25
98.65% ± 0.50%
TRA-1-60
E
BC1 E8-Matrigel
BC1 E8-VNT-N
TNC1 E8-Matrigel
DAPI
Oct-4 / TRA-1-60
Nanog / SSEA-4
F
BC1 E8-Matrigel p39
BC1 E8-VNT-N p31
TNC1 E8-Matrigel p30

Figure 3-2. Spontaneous and directed hematopoietic differentiation of hiPSCs culture in E8 medium

(A) Immunofluorescence staining for markers of germ cells (in red), including AFP (endoderm), CD31 (mesoderm), and β-3-tubulin (ectoderm). (B) Morphology and flow cytometry plots of the EBs and $CD34^{+}CD45^{+}$ HPCs derived from hiPSCs by FA-EB method after long-term expansion in E8 feeder-free conditions. (C) Representative images and colony counting of different types of colonies in CFU assay of the cells harvested from day-14 EBs in hematopoietic differentiation.

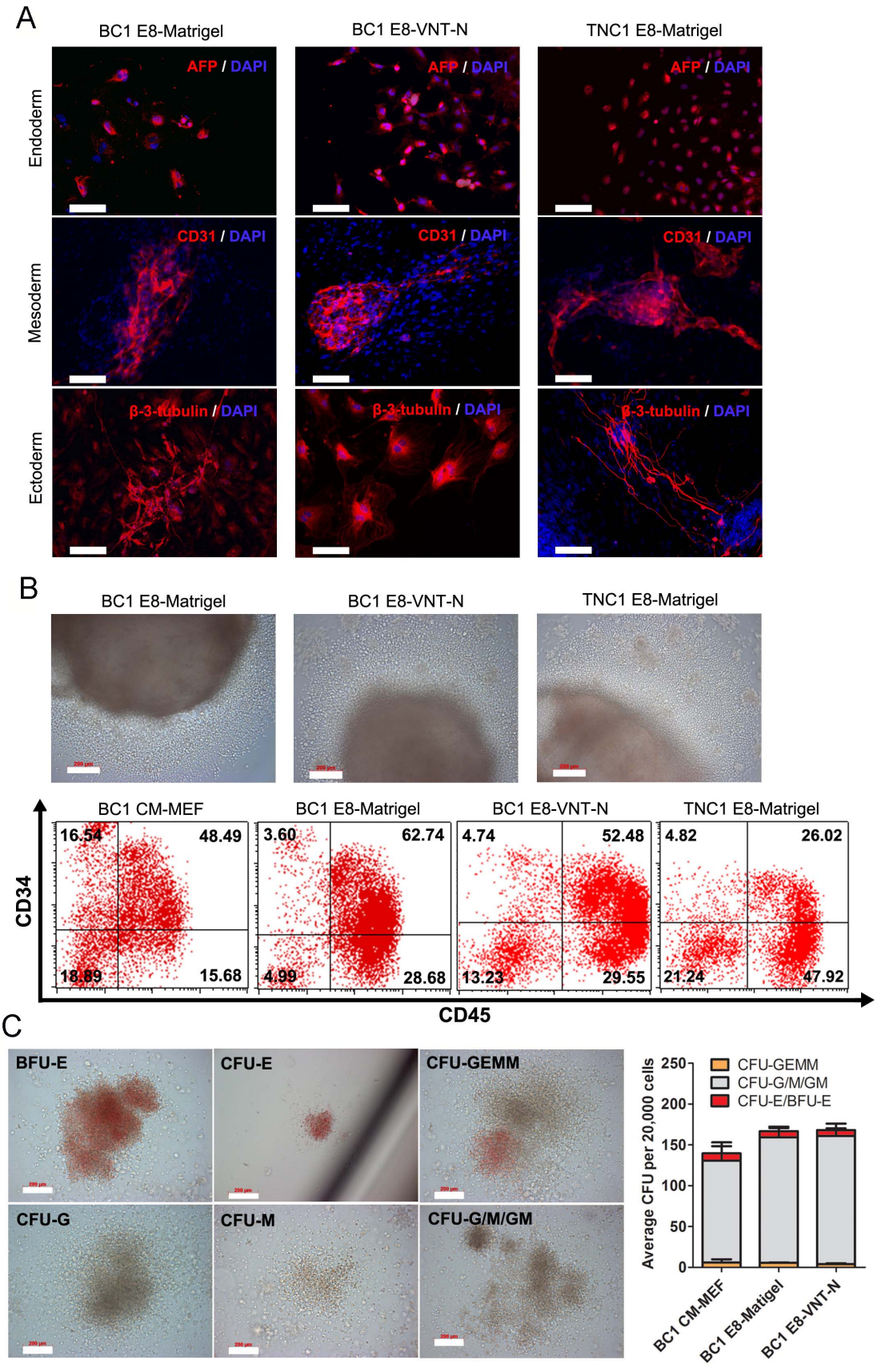
A
BC1 E8-Matrigel
BC1 E8-VNT-N
TNC1 E8-Matrigel
Endoderm
Mesoderm
Ectoderm
AFP / DAPI
CD31 / DAPI
β-3-tubulin / DAPI
B
BC1 E8-Matrigel
BC1 E8-VNT-N
TNC1 E8-Matrigel
BC1 CM-MEF
BC1 E8-Matrigel
BC1 E8-VNT-N
TNC1 E8-Matrigel
CD34
CD45
16.54
48.49
18.89
15.68
3.60
62.74
4.99
28.68
4.74
52.48
13.23
29.55
4.82
26.02
21.24
47.92
C
BFU-E
CFU-E
CFU-GEMM
CFU-G
CFU-M
CFU-G/M/GM
Average CFU per 20,000 cells
250
200
150
100
50
0
CFU-GEMM
CFU-G/M/GM
CFU-E/BFU-E
BC1 CM-MEF
BC1 E8-Matrigel
BC1 E8-VNT-N

3.3.2 **Serial passaging and expansion in static suspension culture**

It has not been reported whether the significantly simplified E8 medium is sufficient to support the survival and proliferation of undifferentiated hPSCs in suspension culture. Thus our studies began by establishing a static suspension culture condition in E8 medium for serial passaging and expansion of hiPSCs. BC1 cells cultured on E8 feeder-free conditions (E8-Matrigel or E8-VNT-N) for at least 3 passages were seeded as a single cell suspension in E8 medium supplemented with Y27632 on the first day [123]. The cells survived and formed convex dish-shaped aggregates within 24 hours due to the gravity force (Figure 3-3, A). The size of the cell aggregates gradually increased corresponding to the cell number along the culture period. BC1 cells expanded in static suspension in E8 medium with an average rate of 3.7±0.9 fold per passage, 3.7×10^6 fold increase in total with >99% of the cells being TRA-1-60$^+$ after 13 passages (Figure 3-3, B-C). We also examined the differentiation potential of expanded cells, using the spin-EB method [168-170]. We found that under the hematopoiesis-inducing condition, leukocyte-like cells emerged around day 10 (Figure 3-3, D) with 46.8% ± 1.6% of the cells becoming CD34$^+$CD45$^+$ HPCs (Figure 3-3, E). These results indicate that undifferentiated hiPSCs can be expanded in suspension in E8 medium supplemented with one-day treatment of Y27632, and retain their differentiation potential [172].

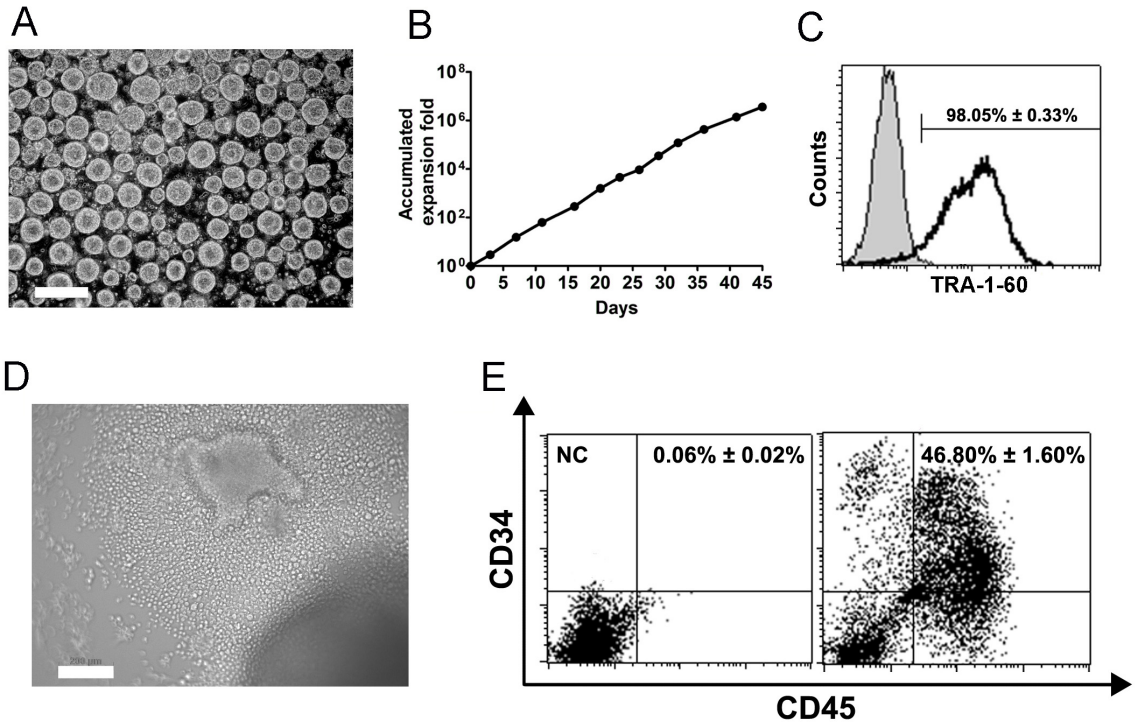

Figure 3-3. Serial passaging of hiPSCs in static suspension in E8 medium

(A) Light microscope image of aggregates after 48 hours post-inoculation of single suspension BC1 cells in ultra-low attachment plates. (B) BC1 cells cultured in E8 medium, expanded in static suspension culture for 13 passages (45 days, n = 3). (C) Flow cytometry plots (n = 3) of TRA-1-60 expression in hiPSCs after 13 passages in static suspension. (D) Light microscope image of HPC-like single suspending cells emerging around a spin-EB on day 14. (E) Flow cytometry plots (n = 2) of CD34 and CD45 expression in day-14 spin EBs. NC = negative control. Scale bars = 200 μm.

3.3.3 Computational fluid dynamics (CFD) analysis of glass-ball spinner flask

Many Previous studies suggest that an adaptation of hPSCs expanded in adherent culture to suspension culture in static conditions is needed prior to inoculation in dynamic suspension culture [112-114]. To support a robust production of hiPSCs from the bench to a clinical setting, we sought to adapt the cells directly from feeder-free adhesion

culture to dynamic suspension culture in spinner flasks. A key parameter of spinner flasks to control is the agitation forces, which should be sufficient to ensure homogeneous distribution of cell aggregates, nutrients and oxygen, but not too severe to harm the cells. Human PSCs are sensitive to high shear stress that may cause unexpected cell death [114, 122] and differentiation [126, 173]. Thus the velocity field profile and the shear stress distribution in the vessel are major considerations in the bioreactor design and setting for suspension culture of hPSCs. Spinner flasks equipped with pendulum-shaped (glass-ball) impellers were advantageous compared to other impeller types in previous studies [112, 119] that might be due to mild shear stress generated by the smooth surface. Therefore, we chose the CELLSPIN system with a 100-ml spinner flask equipped with a single glass-ball stirring pendulum as the platform for hiPSC suspension culture. To predict the hydrodynamic property, we performed CFD analysis for a 3-D model of the glass-ball spinner flask. The physical properties of 37°C pure water were applied to approximate the properties of a single cell suspension in E8 medium during the first 12 hours after inoculation when the cells are most vulnerable to high shear stress. The simulation of the steady-state CFD at agitating speeds of 40 rpm, 60 rpm and 75 rpm (maximum spinning speed available of the system) was performed. A stable flow profile was found in all agitating speeds examined without inadequate mixing or large disturbing turbulence (representatively showing 60 rpm, Figure 3-4, A). Highest local Reynolds number, *Re,* was found at the small area tracking the rotating pendulum, which increased from laminar flow regime ($Re < 1000$) to laminar-turbulent transition regime ($1000 < Re < 2000$) [174, 175] as the agitating speed increased (Figure 3-5, A). The profile of the z-direction velocity and the streamline indicated that even at the lowest agitation speed of 40 rpm,

the rotating pendulum provides appropriate convective flow in the vertical direction that enhances the mass transfer (Figure 3-4, B). At the maximum spinning speed, 75 rpm, the highest shear stress was determined as 0.152 N/m^2 (1.52 dyn/cm^2) at the point near the farthest reach of the glass ball from the spinning axis (Figure 3-4, C). This shear stress level is lower than spinner flasks equipped with other types of impellers, such as pitched-blade impeller (2-5.2 dyn/cm^2, 50-100 rpm) [176] and paddled impeller (4.5-7.8 dyn/cm^2, 80-120 rpm) [122, 177], indicating mild hydrodynamic impact on the cells.

Figure 3-4. Initiation and optimization of dynamic suspension culture in E8 medium

(A-C) 3-D CFD analysis of the velocity field at different agitating speeds in 100-ml glass-ball type spinner flasks. (A) Absolute value of velocity vectors of the fluid represented by heat map on two x-y slices at the agitating speed of 60 rpm. (B) Vertical flow in the bioreactor at 40 rpm. Heat plot on an x-z slice showed distribution of vertical flow. The sign of the value indicated directions of the vectors. Red solid lines were streamlines of the velocity field. (C) Heat map of shear stress distribution at the x-y slice. (D-G) Direct adaptation of BC1 cells in dynamic suspension culture from feeder-free adhesion culture at 40 rpm, 60 rpm, and 75 rpm. (D) Representative images of the cells aggregates on day 1, day 3, and day 5 after seeded as single cells at different agitating speeds. Scale bars = 200 μm. (E) Box-and-whisker plot of the sizes of cell aggregates. (F) Growth curves of a 5-day culture in the first passage in spinner flask at 40 rpm, 60 rpm, and 75 rpm. Means ± SD, n = 3. $*P < 0.05$; $**P < 0.01$; $***P < 0.001$. (G) Cell viability along the 5-day culture (n = 3).

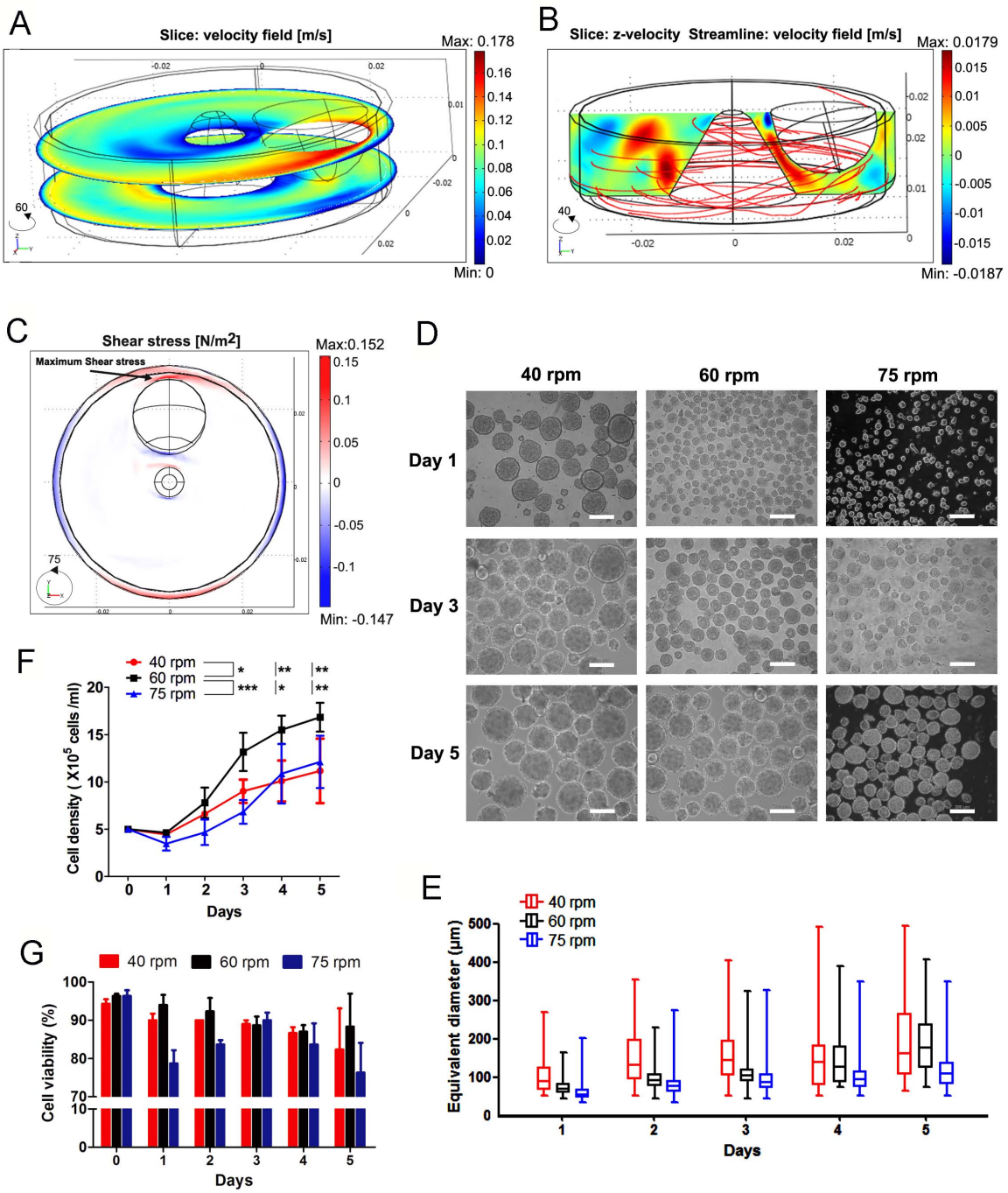
A
Slice: velocity field [m/s]
Max: 0.178
Min: 0
B
Slice: z-velocity Streamline: velocity field [m/s]
Max: 0.0179
Min: -0.0187
C
Shear stress [N/m2]
Maximum Shear stress
Max:0.152
Min: -0.147
D
40 rpm
60 rpm
75 rpm
Day 1
Day 3
Day 5
E
40 rpm
60 rpm
75 rpm
Equivalent diameter (μm)
Days
F
40 rpm
60 rpm
75 rpm
Cell density (X10^5 cells /ml)
Days
G
40 rpm
60 rpm
75 rpm
Cell viability (%)
Days

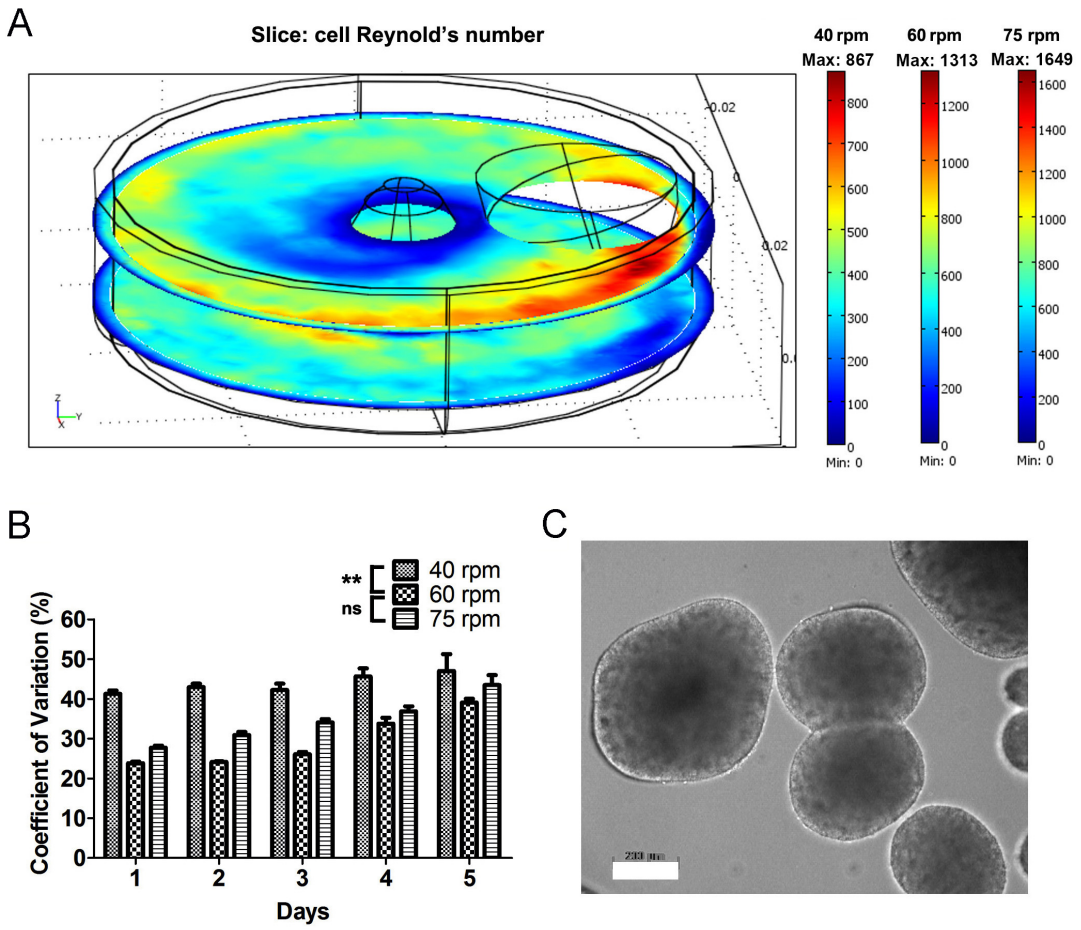

Figure 3-5. Additional information about optimization of dynamic suspension culture in spinner flask

(A) Illustration of cell Reynolds number calculated in CFD analysis of 100-ml glass-ball spinner flask. Within the performed agitating speed, the distribution of the cell Reynolds number shows the same pattern at different speed, only with variant scale of values. (B) The coefficient of variation (SD/Average×100%) in average the samples of cell aggregates from different time points during a 5-day culture at 40 rpm, 60 rpm and 75 rpm. Two-way ANOVA, $P = 0.0188$, followed by Bonferroni posttests. **P < 0.01, ns = not significant. (C) Representative image of cell aggregate agglomeration on day 4 in spinner flask at 40 rpm.

3.3.4 **Optimization of agitating speed and cell split interval**

BC1 cells cultured in E8-Matrigel condition were used for the optimization of agitating speed and cell split interval. Consistent with previous studies [111, 112], preliminary experiments using seeding density lower than 4×10^5 cells/ml showed inconsistent cell survival and proliferation (data not shown). Thus, we used 4×10^5 to 5×10^5 cells/ml as the seeding density for all following experiments. After treatment with ROCK inhibitor and dissociation, a single cell suspension of BC1 hiPSCs from feeder-free adhesion culture was directly inoculated into the spinner flask with 45 ml of E8 + Y27632. Cell growth at agitating speeds of 40 rpm, 60 rpm, and 75 rpm were compared, and three independent repeats were performed in each condition (n = 3). Within 24 hours, hiPSCs formed spherical aggregates with diameters of 104.2 ± 44.8 μm, 80.6 ± 20.3 μm, and 60.8 ± 16.5 μm on average in 40 rpm, 60 rpm and 75 rpm, respectively (Figure 3-4, D-E). The cell aggregates gradually increased in size along the culture period reaching 120-300 μm on Day 5. This is partially due to aggregate agglomeration, but mostly due to the expansion of the cells with 2-3 fold increase after 5-day culture (Figure 3-4 F-G). These results further demonstrated significantly higher cell density (Figure 3-4, F, P = 0.0188) without compromising cell viability (Figure 3-4, G) in hiPSCs cultured in agitation rate of 60 rpm. Moreover, hiPSCs formed more homogeneous aggregates at 60 rpm compared to hiPSCs cultured in 40 rpm and 75 rpm (Figure 3-4, E and Figure 3-5, A). The cell expansion rate decreased from day 3 to day 4 (Figure 3-4, F) while the cell viability varied on day 5 (Figure 3-4, G). Therefore, we decided to culture the cells at 60 rpm and split them every 3 to 4 days.

3.3.5 **Characterization of hiPSCs in dynamic suspension culture**

We continued to characterize BC1 cells cultured in the spinner flasks for pluripotency associated marker expression, apoptosis level, and metabolism. We found that >98% of the cells are positive for TRA-1-60, SSEA4, NANOG, and OCT4 after 4 days of culture by flow cytometry analysis (Figure 3-6, A). The fluorescent images by confocal microscopy showed the nuclear expression of OCT4 with membrane localization of SSEA4 in BC1 cell aggregates sampled from suspension culture on day 3 (Figure 3-6, B), indicating the maintenance of the undifferentiated state inside the cell aggregates. We further found that the cell number per aggregate increased in the order of the cubic diameter -- the volume (Figure 3-6, C). Together with the confocal z-stack images of cell aggregates, our data suggested an even distribution of cells throughout the entire aggregate without compact center or hollow cavity. The rate of apoptosis in the cell aggregates was found to be 1.56% ± 0.1% (n = 3, Figure 3-6, D), indicating no severe programmed cell death due to the aggregate formation and the dynamic culture. Cell metabolism was monitored by measuring the consumption of glucose, the accumulation of lactate, the change of pH and the oxygen partial pressure (pO_2) in the culture medium. We found that by replacing 2/3 of the medium daily with pre-warmed fresh E8, the consumption of glucose did not exceed 40%. Also, the concentration of lactate was restricted under 10 mM (Figure 3-6, E), and the pH dropped to 6.75 by day 5 (Figure 3-6, F). For real-time monitoring of pO_2 in the medium, a non-invasive O_2 sensor and optical fiber probe were equipped to the bioreactor [178]. We show that the pO_2 was kept above 15% (Figure 3-6, G), indicating a sufficient oxygen supply merely by diffusion through the gas-liquid interface and convective transport in the medium. These data are consistent

with the exponential growth on the first three days followed by a reduced expansion rate after day 4 when the cell density reached ~1.5×10^6 cells/ml (Figure 3-4, F).

Figure 3-6. Characterization of cell aggregates in spinner flasks

(A-B) Expression of the markers for undifferentiated state in BC1 cultured in spinner flasks. (A) Flow cytometry plot (n = 3) of TRA-1-60$^+$, SSEA4$^+$, NANOG$^+$, and OCT4$^+$ cells on day 5. Gray area represents isotype control. (B) Confocal microscope images of the immunofluorescence staining for OCT4 (in green) and SSEA4 (in red) at the center z-slice of a cell aggregate on day 3. DAPI stained for nuclei. Scale bar = 100 μm. (C) A fitting curve of the cell number per aggregate to the diameter of the aggregate, means ± SEM, n = 300-2000. (D) Flow cytometry plots (n = 2) of TUNEL assay on day 3 aggregates, means ± SD, n = 3, NC = negative control, PC = positive control. (E-F) Concentration of glucose and lactate (E) and pH (F) in the media samples. Note: the two data points on the same day represent the concentration before and after media change, means ± SD, n = 3. (G) The pO_2 level as percentage of the O_2 saturation in three independent experiments (three colors).

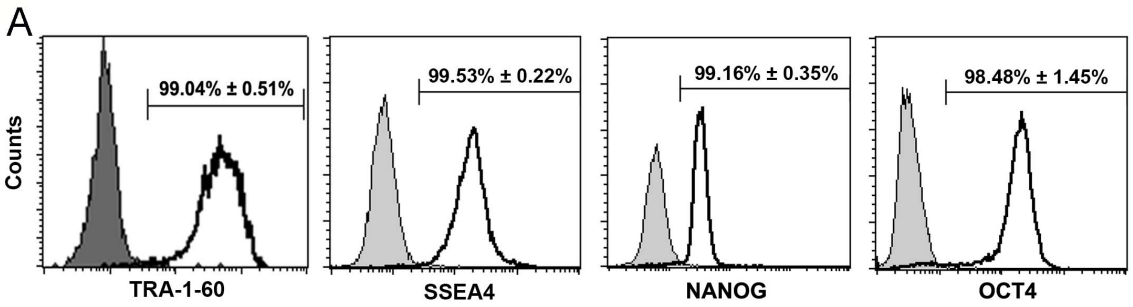
A
Counts
99.04% ± 0.51%
99.53% ± 0.22%
99.16% ± 0.35%
98.48% ± 1.45%
TRA-1-60
SSEA4
NANOG
OCT4

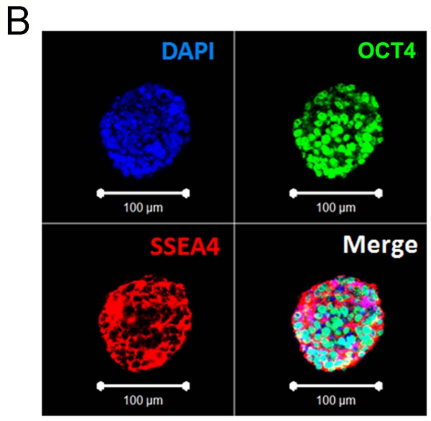
B
DAPI
OCT4
SSEA4
Merge
100 μm

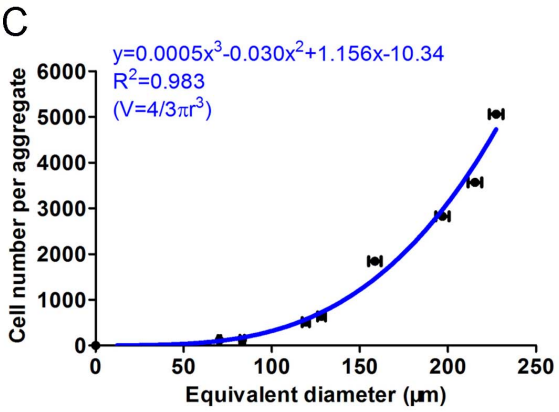
C
y=0.0005x3-0.030x2+1.156x-10.34
R2=0.983
(V=4/3πr3)
Cell number per aggregate
Equivalent diameter (μm)

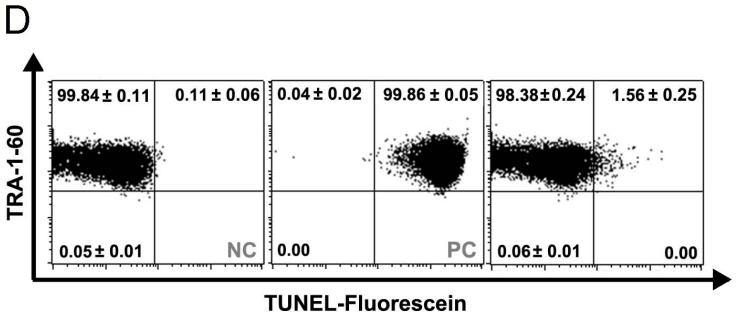
D
99.84 ± 0.11
0.11 ± 0.06
0.04 ± 0.02
99.86 ± 0.05
98.38±0.24
1.56 ± 0.25
0.05 ± 0.01
NC
0.00
PC
0.06 ± 0.01
0.00
TRA-1-60
TUNEL-Fluorescein

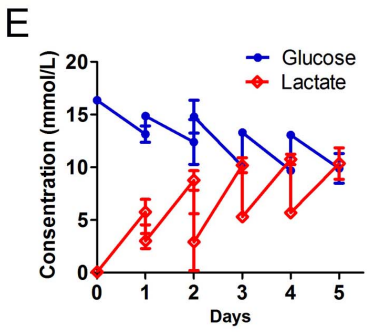
E
Glucose
Lactate
Consentration (mmol/L)
Days

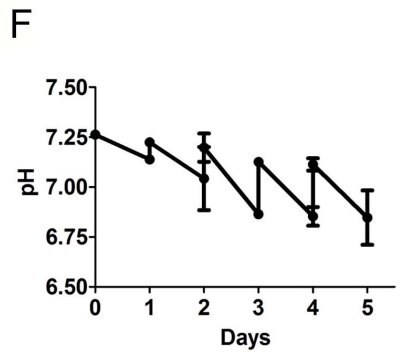
F
pH
Days

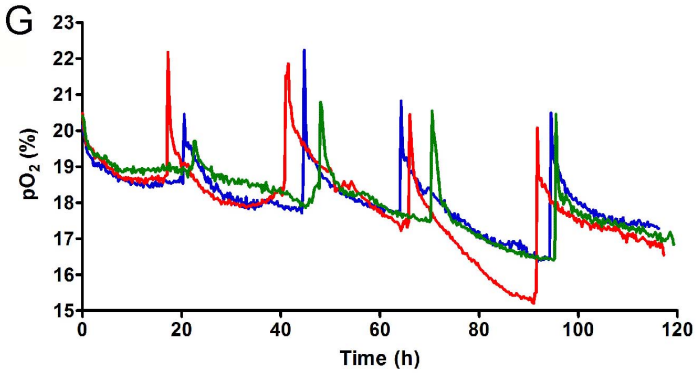
G
pO2 (%)
Time (h)

3.3.6 **Serial passaging and expansion of hiPSCs in suspension culture**

To meet the requirement of scale-up processes for hiPSC production, serial passaging and extended expansion of BC1 and TNC1 cells cultured in our bioreactor system was tested. Human iPSCs were inoculated into spinner flasks as mentioned above, cultured for 3 to 4 days, passaged as a single cell suspension, and re-inoculated at the same conditions. Both BC1 and TNC1 cells were maintained in spinner flasks for at least 2.5 months with 25 passages. During the culture period, BC1 showed an average expansion rate of 2.4±0.3 per passage, while TNC1 expanded 3.5±0.5 folds per passage on average (Figure 3-7, A), indicating variation of growth rate in suspension culture between the two different cell lines. The cells maintained high viability during the serial passaging in suspension. The overall viability was 92.9% ± 2.1% for BC1 and 95.0% ± 1.6% for TNC1 (Figure 3-7, B). Both cell lines were also maintained in their undifferentiated state, as indicated by 95-100% positive stain of TRA-1-60, SSEA4, OCT4, and NANOG during the expansion period (Figure 3-7, C). Furthermore, BC1 and TNC1 cultured for up to 20 passages in spinner flask (plus at least 20 passages in feeder-free adhesion culture before transfer to suspension culture) retained normal karyotypes (Figure 3-7, D).

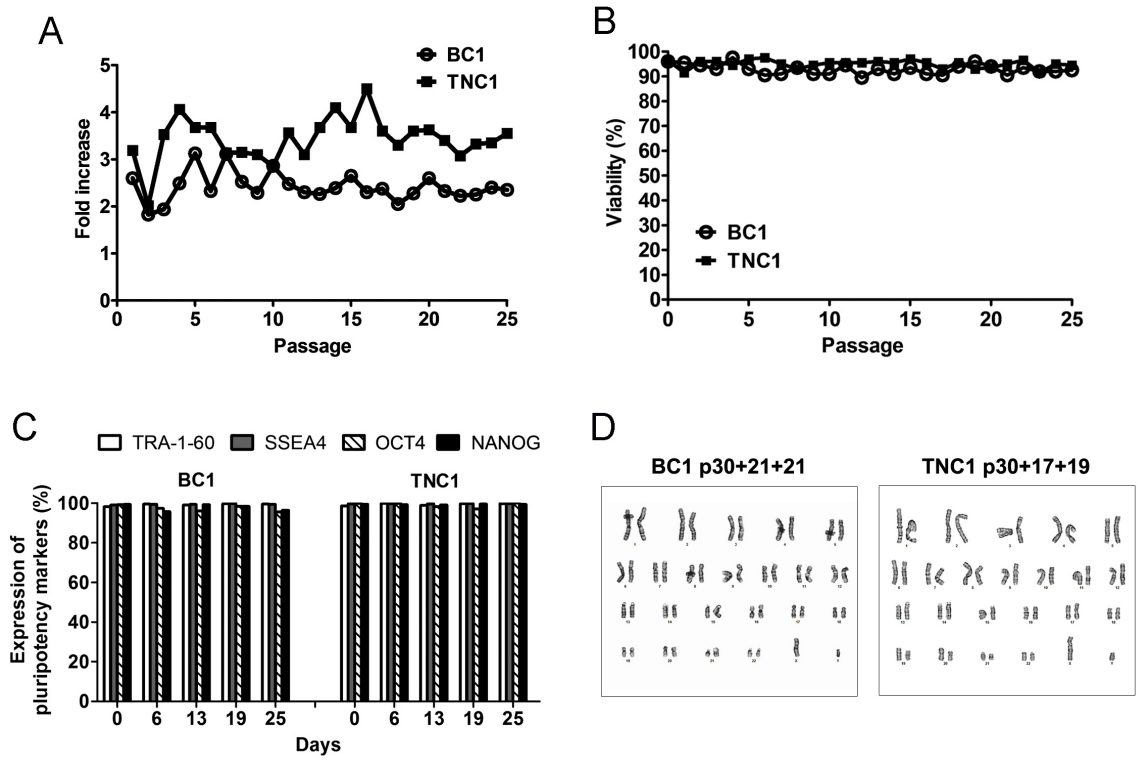

Figure 3-7. Serial passaging and expansion of hiPSCs in xeno-free condition

(A-B) The expansion fold (A) and the cell viability (B) at the end of each passage during the expansion of BC1 and TNC1. (C) The percentage of TRA-1-60$^+$, SSEA4$^+$, OCT4$^+$, and NANOG$^+$ cells in the aggregates at the beginning of the suspension culture (passage 0) and along the culture period (passage 6, 13, 19, and 25). (D) G-banding karyotyping of BC1 and TNC1 after extensive culture in spinner flask. The TNC1 cell line had been undergone 5 times of freeze-thaw cycles in suspension culture.

3.3.7 **Differentiation potential of hiPSCs in suspension culture**

BC1 and TNC1 hiPSCs cultured in spinner flasks for more than 10 passages were tested for their pluripotency by *in vitro* and *in vivo* differentiation methods. For *in vitro* assay, by simply replacing the entire E8 medium with differentiation medium of day-2 spinner flask suspension culture, BC1 and TNC1 aggregates transformed into EBs and

started spontaneous differentiation under the stimulation of 10% serum (Figure 3-8). After 8 days in spinner flask followed by 4 days on gelatin-coated tissue culture plates in differentiation medium, cells of all three germ layers could be detected by immunofluorescent staining of specific markers (Figure 3-9, A). In contrast, undifferentiated hiPSCs on day-0 showed negative staining of all germ markers (data not shown). For *in vivo* assay, BC1 and TNC1 harvested from suspension culture in spinner flasks were injected into immunocompromised mice and were able to form teratomas containing cells of all germ layers, including glandular epithelium, chondrocytes, and neural rosettes (Figure 3-9, B). Directed hematopoietic differentiation potential was also tested as previously described (Figure 3-9, C). Differentiating BC1 and TNC1 cells contained 43.57% ± 4.35% (n = 3) and 43.22% ± 7.13% (n = 3) $CD34^{+}CD45^{+}$ HPCs on day 14 of differentiation, respectively. The CFU assay measuring hematopoietic progenitors showed that hiPSCs cultured in spinner flasks were able to generate colonies of different hematopoietic cell lineages. The total number of CFUs was comparable or significantly larger ($P = 0.0307$, n = 3) than cells cultured in parallel in adhesion cultures (Figure 3-9, D).

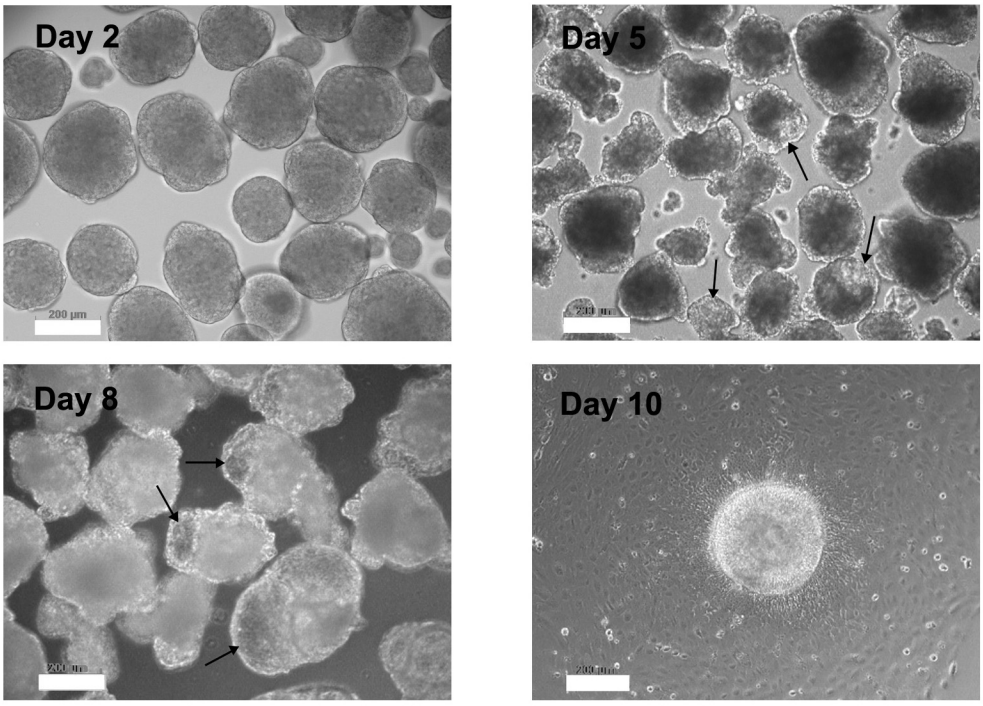

Figure 3-8. Transformation from cell aggregates to EBs during the spontaneous differentiation of hiPSCs in the bioreactor

E8 medium was replaced by differentiation medium containing serum on day 2. Cells started to differentiate and formed EB structures (arrows in images of Day 5 and Day 8). EBs were transferred on gelatin-coated plates, attached (image of Day 10), and gave rise of cells of all three germ layers.

Figure 3-9. Differentiation potential of hiPSCs after prolonged expansion in bioreactor

(A) Immunofluorescence analysis of *in vitro* spontaneous differentiation of day-3 hiPSC aggregates. Germ cell markers (red): alpha-fetoprotein (AFP, endoderm), CD31 (mesoderm), and β-3-tubulin (ectoderm). (B) H&E staining of biopsies of teratoma generated from hiPSCs in immunodeficient mice, n = 2 for each cell line. Black arrows indicate glandular epithelium. (D) Exemplary microscope images and flow cytometry results of $CD34^{+}CD45^{+}$ cells from directed *in vitro* hematopoietic differentiation. The percentage of $CD34^{+}CD45^{+}$ cells is presented as mean ± SD, n = 3. (D) CFU assay. (**i**) Representative images of different types of colonies in CFU assay. BFU-E: burst-forming unit-erythroid; CFU-E: erythroid; CFU-GEMM: granulocyte-erythroid-macrophage-megakaryocyte, CFU-GM: macrophage-granulocyte. The hiPSCs cultured in spinner flasks (SF) were compared with the parallel feeder-free culture of the same cell line in adhesion (AD). The total number of CFU was analyzed by the two-tailed Student's t-test, means ± SD, n = 3. Scale bars: 200 μm.

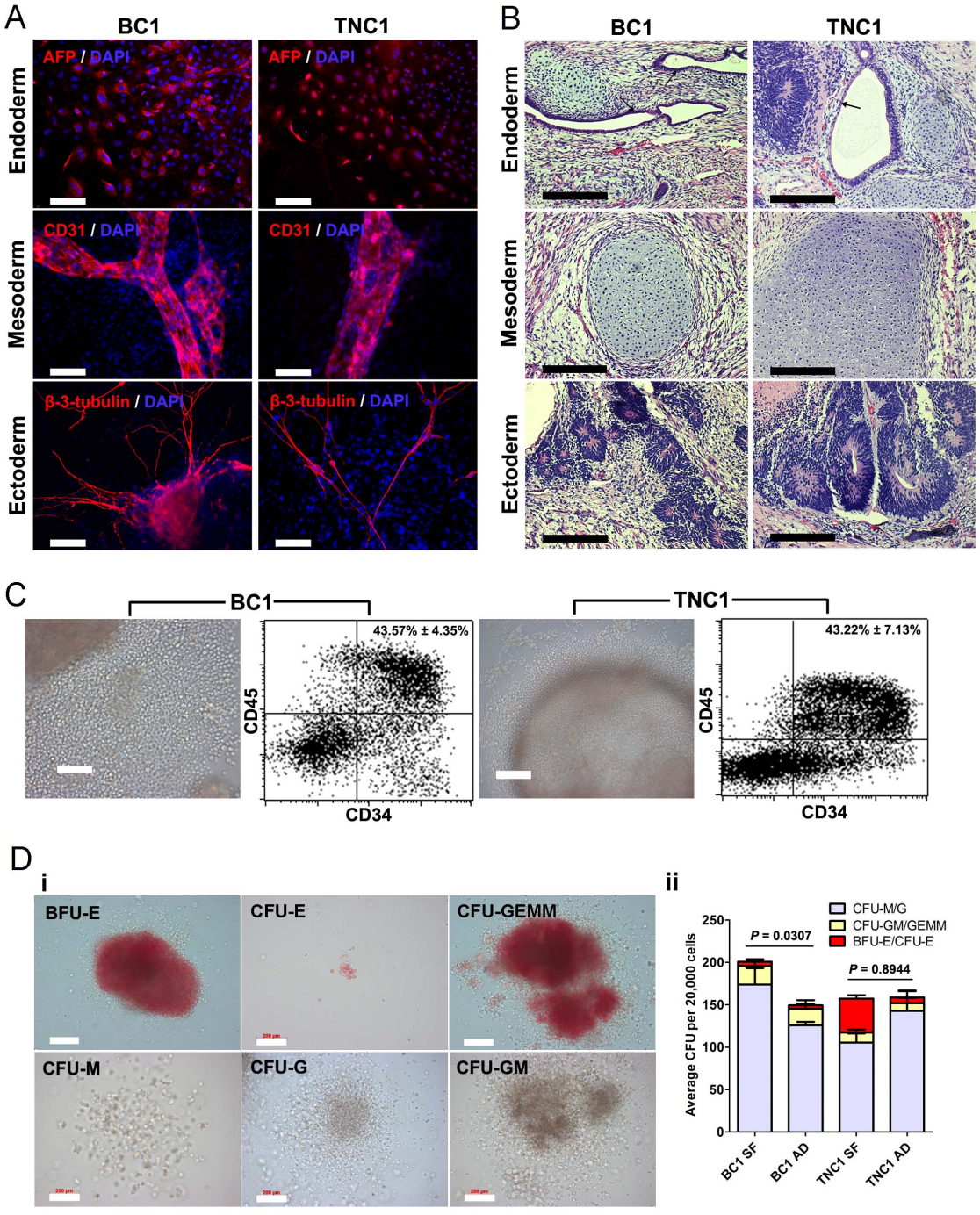
A
BC1
TNC1
Endoderm
Mesoderm
Ectoderm
AFP / DAPI
CD31 / DAPI
β-3-tubulin / DAPI
B
BC1
TNC1
Endoderm
Mesoderm
Ectoderm
C
BC1
TNC1
43.57% ± 4.35%
43.22% ± 7.13%
CD45
CD34
D
i
BFU-E
CFU-E
CFU-GEMM
CFU-M
CFU-G
CFU-GM
ii
CFU-M/G
CFU-GM/GEMM
BFU-E/CFU-E
P = 0.0307
P = 0.8944
Average CFU per 20,000 cells
250
200
150
100
50
0
BC1 SF
BC1 AD
TNC1 SF
TNC1 AD

3.3.8 **Cryopreservation and recovery of hiPSCs in suspension culture**

It has been reported that E8 medium with 10% DMSO can be used as cryopreservation medium for hPSCs frozen in small clumps [159]. However, whether E8-based freezing medium can support single-cell cryopreservation has not been reported. As the inclusion of Y27632 in freezing medium was proven to enhance single cell survival at thaw [177], we examined cryopreservation of hiPSCs harvested from expansion in bioreactors in E8 medium supplemented with 10% (in volume) DMSO and 10 μM Y27632. Following at least two weeks of storage in liquid nitrogen, we thawed the frozen cells in both adhesion and suspension culture conditions. The viability of the frozen cells upon thaw was measured as 89% ± 4% for BC1 (n = 3) and 93% ± 2% for TNC1 (n = 3). Moreover, both BC1 and TNC1 showed good attachment and typical morphology of undifferentiated hiPSCs on Matrigel or VNT-N (Figure 3-10, A). The cells reached 80% confluence after 3 to 4 days in culture and were passaged routinely hereafter, indicating a rapid recovery and good adaptation back in adhesion culture. Thawed cells were also able to survive and form aggregates in both static and dynamic suspension culture (Figure 3-10, A). Three protocols for recovery were tested for the purpose of further expansion in suspension. Cells were thawed in adhesion (AD), ultra-low attachment plate (UL), or spinner flask (SF) for the first passage, and then transferred directly to spinner flasks on the next splitting (AD-SF, UL-SF, and SF, respectively, Figure 3-10, B). We note that the first passage after thawing in static or dynamic suspension culture conditions usually required longer culture period (5 to 6 days) to allow enough cell growth for splitting (Figure 3-10, B). Cells regained typical expansion rate at the third passage after thawing (Figure 3-10, B) and contained >98% of the population

with positive staining of TRA-1-60, SSEA4, OCT4, and NANOG after 5 passages (Figure 3-10, C). Cells in AD-SF and UL-SF conditions showed 2-3 folds higher expansion rate in the first passage than hiPSCs that were directly thawed in spinner flasks (Figure 3-10, B). The spin-EB hematopoietic differentiation of hiPSCs recovered from UL-SF protocol demonstrated an efficient differentiation into hematopoietic progenitor cells (Figure 3-10, D). Furthermore, hiPSCs were tested for karyotype stability after sequential freeze-thaw cycles using single-cell cryopreservation. After more than 5 times of sequential freeze-thaw process after adapted to completely xeno-free conditions, including at least 4 times of cryopreservation following UL-SF protocol, both BC1 and TNC1 after ~70 passages maintained normal karyotype (Figure 3-10, E and Figure 3-7, D), indicating a reliable cryopreservation protocol for hiPSCs throughout their useful lifespan. This xeno-free cryopreservation and recovery protocol completed our bioreactor system, offering opportunities for large-scale cell growth and banking of hiPSC lines.

Figure 3-10. Cryopreservation and recovery of hiPSCs cultured in suspension

(A) Morphology of hiPSCs on day 3 after thawing either on Matrigel or VNT-N coated plates for adhesion culture, or in ultra-low attachment plates (UL) or in spinner flasks (SF) for dynamic suspension culture, respectively, from single-cell cryopreservation in E8-based freezing medium. Scale bars: 200 μm. (B) The expansion of hiPSCs from cryopreservation following three protocols. AD-SF or UL-SF: thawing cells in adhesion or in UL, respectively, and transferred in SF at first splitting. SF: directly thawing cells in spinner flask. The significance of difference between UL-SF and SF on the first passage after thawing was analyzed by two-tailed Student's t-test, means ± SD, n = 3. (C) Expression of TRA-1-60, SSEA4, OCT4, and NANOG at the end of passage 5 following a freeze-thaw cycle as determined by flow cytometry. (D) hiPSCs recovered from UL-SF protocol at passage 5 after thaw kept the potential to differentiate into $CD34^{+}CD45^{+}$ HPCs. (E) G-banding karyotyping of BC1 cells after total 72 passages with 30 passages on MEF, 24 passages on VNT-N, and 18 passages in suspension, and at least 5 times of freeze-thaw cycles.

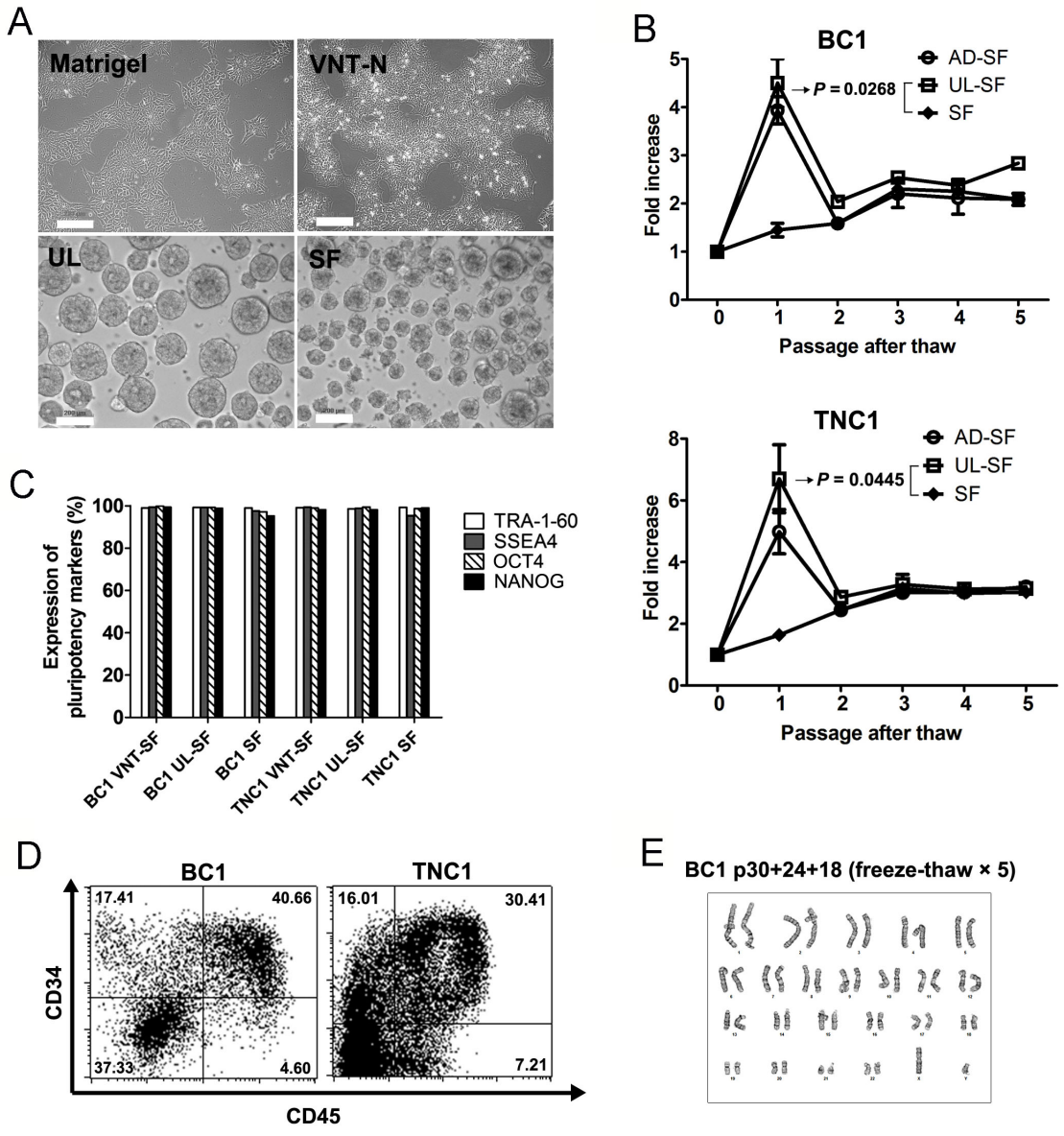

3.4 *Discussion*

Following the demonstration that a ROCK inhibitor such as Y27632 permits the survival of single-cell hESCs [123], several groups utilized it to establish suspension culture systems for the expansion of hPSCs based on single-cell inoculation [110-116,

124, 125, 164] as discussed in Chapter 1. Most of these approaches were based on serum-free media that contains BSA Faction V or human serum albumin as the major protein component. The batch-to-batch variance of this animal-source product led to compromised defined medium [73]. Towards this, we first transferred hPSCs into the newly developed E8 medium on human vitronectin substrate, to avoid BSA and have a completely xeno-free condition with low concentration of protein components. We then demonstrated that E8 medium (with Y27632 on the first day of seeding) is sufficient to support hiPSC aggregation and survival, and serial passaging in the undifferentiated state using static suspension culture.

We next aimed to optimize the protocol for dynamic suspension culture in spinner flasks. While there are many experimental and computational studies for assessing the flow dynamics in spinner flasks equipped with various types of paddle-shaped impellers [179-183], the relevant analysis for glass-ball spinner flasks has not been reported. We simulated the velocity field and shear stress of the flow in the glass-ball type spinner flask, providing reasonable prediction of the effect of flow on single cells during the first several hours after inoculation. Some rational approximations were applied to simplify the model, such as using the properties of 37°C water instead of the unknown data of the medium, omitting gravity due to its negligible effects on single cells compared to the agitating force, and ignoring the cell aggregation due to the complexity it would bring to the model. Although the model could not estimate the shear stress on the surface of cell aggregates after emergence, the method provides an efficient tool for the design and analysis of the bioreactors with complex vessel structures or non-standardized impeller designs [179, 182]. Using CFD analysis, we found a steady flow in all agitation speeds

(i.e. 40 rpm, 60 rpm and 75 rpm). Although small turbulent flow may occur at high agitating speeds according to the calculation of the local Reynolds number, the shear stress generated by the glass-ball impeller is considerably lower than by other types of impellers. Experimentally, we further found that an agitation speed of 60 rpm supports the formation of homogeneous cell aggregates, showing significantly higher expansion rates and relatively better cell viability than the other agitation speeds. As a comparison, hiPSCs formed relatively large aggregates on day 1 at 40 rpm, which reduced the potential of further proliferation due to the diffusion limitation. Moreover, occasions of undesired aggregate agglomeration, resulting in aggregates larger than 800 μm, were observed on later days due to insufficient agitating force. At 75 rpm, cell viability dropped significantly on day 1, leading to slower recovery and expansion. Based on these results, the optimal split interval at 60 rpm was next determined. We noticed a reduction in cell expansion after day 3 or day 4, which might be due to the diffusion limitation as cell aggregates grow. It is widely accepted that the diffusion limitation of oxygen in human tissue is 100 to 200 μm [184]. Therefore, we determined to split the cells on day 3 or day 4 when most of the cell aggregate diameters reached ~150-200 μm. The concentration of glucose and lactate in the culture media also suggested a reduced growth after day 3, when the pH of the media drop to ~6.75 as cell density increased, which might be harmful for the hiPSC lines that are more sensitive to changes in pH and influence the expansion. This issue may be solved by gradually increasing the culture volume or the media change frequency. The inclusion of a non-invasive O_2 probe-patch made it possible to monitor pO_2 levels in real-time without disturbing the flow and the

rotation of the impeller in the glass-ball bioreactor, which are normally difficult to equip with a standard large O_2 probe [112, 120].

Using the optimized operating conditions we demonstrate serial passaging and expansion of two integration-free hiPSC lines in completely defined xeno-free media in 100-ml bioreactors. The cells exhibited homogeneous aggregate formation, steady expansion in their pluripotent state, and normal karyotype after ~20 passages. Note that one experiment of extended expansion of TNC1 cells in spinner flask (p30+6+21) showed abnormal karyotype (47, XXY). However, there is no evidence that it should be attributed to the suspension culture. In general, recently improved iPSC culture conditions reduce selective pressure for the growth of mutated cells that acquire growth advantages. Although karyotypically abnormal cells were found occasionally after long-term cultures under both adherent and suspension conditions, the frequency is low (5% of tested batches of hiPSCs and hESCs). The standard karyotyping or other genotyping methods like what we performed here will remain necessary to manage this inherent issue of long-term cell cultures.

Undifferentiated hiPSCs expanded in bioreactors retained their potential of spontaneous and directed hematopoietic differentiation comparable to cells cultured via adherent culture. The transformation from day-2 or day-3 cell aggregates to EBs for spontaneous differentiation in the spinner flask demonstrate the possibility to use this system for a continuous bioprocess that begins with a large-scale expansion and directed differentiation in one single batch. Interestingly, although comparable amount of HPCs and CFU were derived from hiPSCs expanded in bioreactor as in adhesion, HPCs derived from TNC1 in bioreactor generated a considerably higher proportion of cells in erythroid

lineage rather than in myelocyte lineage. Further studies are needed to reveal the significance and the mechanism underlying the contribution of hydrodynamic forces to hPSCs differentiation in suspension. Studies of hematopoietic differentiation in spinner flasks are ongoing.

The development of a single-cell cryopreservation protocol concluded the establishment of our chemically defined xeno-free suspension culture system. For continuous expansion, UL-SF protocol was the preferred method for recovery with small number of hiPSCs from cryopreservation. The hiPSCs can be directly thawed in a spinner flask; cells cultured in a spinner flask can be transferred back to VNT-N-coated surface for the applications that require adhesion culture, indicating good flexibility of the system. The single-cell cryopreservation protocol and the suspension culture system can significantly reduce the workload when handling cells in the scale required for translational uses. Furthermore, this xeno-free protocol of cryopreservation and recovery was theoretically proved to be compliant to a scale-up strategy for hiPSCs in suspension and under cGMP condition, allowing a yield of ~1×10^9 cells within 20 days after thawing of 1×10^6 frozen cells (Figure 3-11). The scale-up strategy, which includes multiple xeno-free processes, employs 100-ml and 1-L spinner flasks, enabling the transition from lab scale to pilot scale of hiPSC expansion. The CFD simulation of the 1-L spinner flask (Figure 3-12) equipped with two glass-ball stirring pendulums (such as one from Integra Bio-sciences) indicated that it could be scalable using 1-L spinner flasks toward clinically relevant quantities of hiPSCs from a single batch . The simulation revealed a steady flow at the highest agitating speed of 75 rpm and an even lower maximum shear stress (0.047 N/m^2) comparing to the 100-ml spinner flask in steady state. On one hand, the distance

between the farthest points of the pendulums and the spin axis (r = 38.9 mm in Figure 3-12, equivalent to impeller radius of paddle impellers) in the 1-L spinner flask is not much longer than the 100-ml spinner flask (r = 28.2 mm); thus, the highest velocity in 1-L spinner flasks is not much higher than that in 100-ml spinner flasks ($v_{max,1L}$ = 0.309 m/s vs. $v_{max,100ml}$ = 0.224 m/s). On the other hand, there is much more space between the pendulums to the flask wall in the radial direction (l in Figure 3-12, l_{1L} = 29.1 mm vs. l_{100ml} = 3.5 mm). This causes a more moderate drop of velocity from the maximum at the far reach of the pendulums to zero at the flask wall in 1-L spinner flask compared to the 100-ml spinner flask, leading to a significant decrease of the gradient of velocity, dv_z / dx, which contributes to the majority of the shear stress. Before reaching steady state, stepping acceleration could be used to protect the cells from sudden exposure to high-speed flow. Also, the liquid level of 600-ml medium in the 1-L spinner flask is similar to that of 60-ml medium in the 100-ml spinner flask, which was proven in this study not to cause any reduced O_2 transport. While optimization of the agitation speed should be performed for different hiPSC lines to support appropriate size aggregate formation (for example, diameter of 50-80 μm after 24 hours), this direct scale-up process in 1-L spinner flasks with the same well-designed system should be attainable.

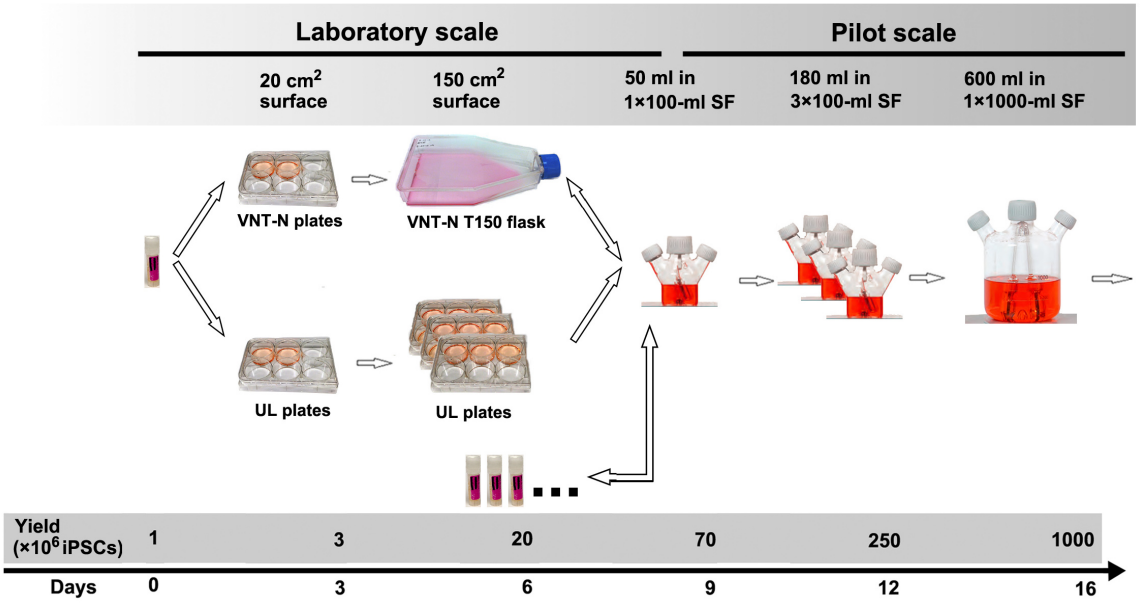

Figure 3-11. Schematic presentation of the cryopreservation and scale-up expansion of hiPSCs in xeno-free culture system

The days and the yield of hiPSCs are presented as approximate amount. Drawing not to scale.

Another practical advantage of the system is relatively low cost. The high price of current commercially available serum-free media such as StemPro and mTeSR always hinders the universal application of the scale-up technologies for hiPSC expansion, especially for xeno-free media when albumin is required in the medium [73]. The simplicity of the medium dramatically cuts down the price (~30%-60%) and makes it possible for bulk production in academic laboratories and cGMP-compliant institutions

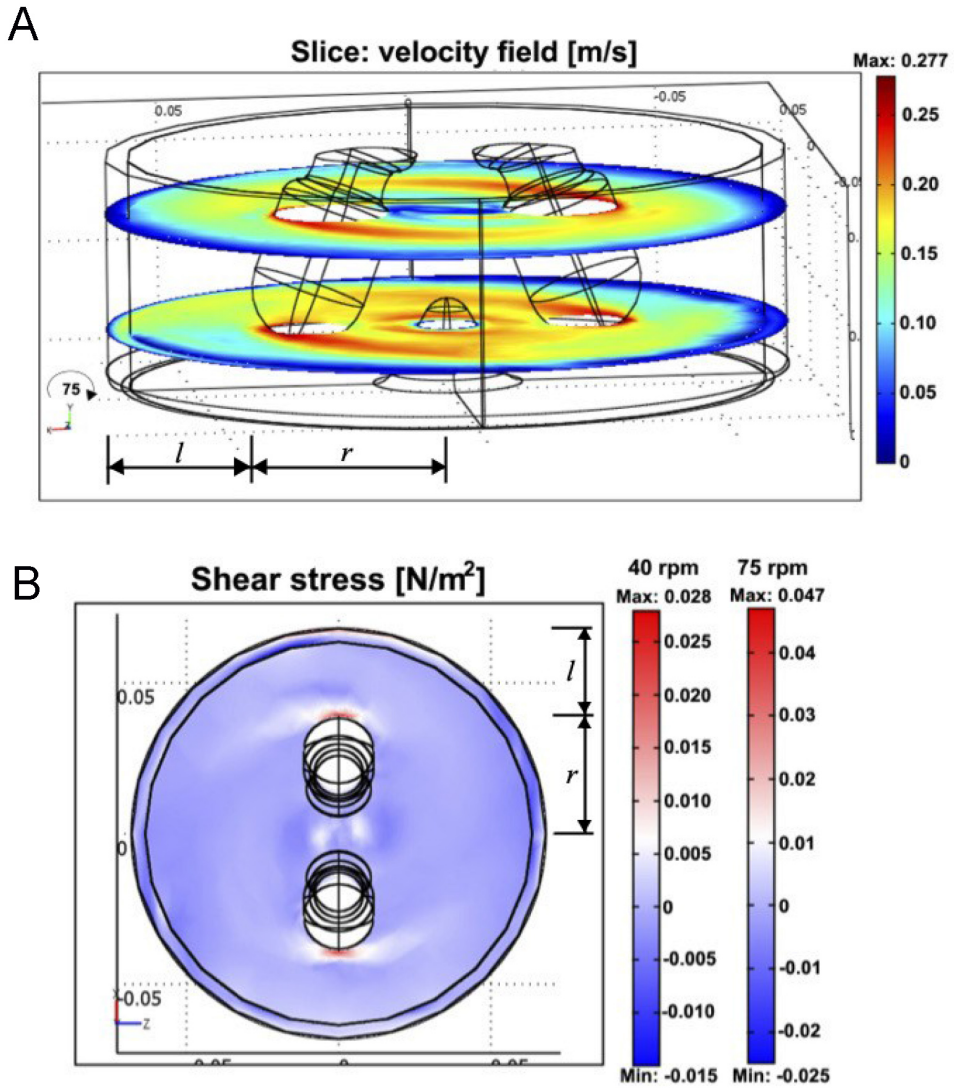

Figure 3-12. CFD simulation of ~600 ml of culture media at steady state at 40 or 75 rpm in a 1-L spinner flask

(A) The velocity field on two representative cross-sections in the spinner flask at 75 rpm. (B) The cross-section of shear stress profile on the plane that showed the highest shear stress, which located around the far reach of the pendulums (red area). r is the distance between the far reach point of the pendulum and the spinning axis. l is the distance between far reach point of the pendulum and the inner wall of the flask.

.

3.5 *Conclusion*

In this chapter, we established a reproducible approach for rapid, economic, and scalable expansion of hiPSCs in xeno-free condition to meet the demand of practical research and clinical applications. The complete elimination of components from animal sources and remarkably reduced cost of this system provide a reliable technology for scale-up of hiPSC expansion and take a significant step toward the realization of stem cell therapies. The results discussed in this chapter have been published in Ref. 213.

4 *Efficient and reproducible production of HSPCs and enucleated erythrocytes from hiPSCs*

Ex vivo generation of erythrocytes from hiPSCs would provide a renewable cell source of RBCs for treating transfusion-dependent patients, as well as a better understanding of human erythropoiesis. The key requirements in this approach include developing a robust and consistent method for the production of functional progenitor and progeny cells such as HSPCs from hiPSCs, and minimizing risk and variation due to the animal-derived products in cell cultures. In this chpater, we first developed an efficient system to generate HSPCs from hiPSCs under a feeder-free and xeno-free condition, in which all the animal-derived products were eliminated. Several crucial reagents were evaluated and replaced with FDA-approved pharmacological reagents, including Romiplostium (Nplate®, a thrombopoietin analog), and Plasbumin (human albumin). Human iPSCs generated from sickle cell disease (SCD) patients have a missense homozygous point mutation in the *HBB* gene encoding adult β-globin proteins and can be used as a model system to improve strategies of human gene therapy. Erythrocytes from either the *HBB* gene-corrected or its parental (uncorrected) iPSC lines derived from SCD patients were generated with similar efficiencies. Approximately ~6%-10% of these erythrocytes indeed lacked nuclei, characteristic of mature erythrocytes. We also detected the 16-kD β-globin protein expressed from the corrected

HBB allele in the erythrocytes differentiated from genome-edited iPSCs. Our results represent a significant step towards the clinical applications of genome editing using patient-derived iPSCs to generate disease-free cells for cell and gene therapies.

4.1 *Introduction*

Human iPSC is a promising cell source that can be easily derived from donor somatic cells and expanded indefinitely [9]. They would provide a potentially unlimited source of RBCs perfectly matching to patients or a favorable donor with any antigen types, especially the universal donor type and rare-phenotype matching RBCs [150, 185-187]. Recently, hiPSCs derived from healthy donors or patients with blood-related disorders were successfully differentiated towards erythroid lineages and completed terminal maturation, which is marked by enucleation, blood antigen display, fetal-to-adult hemoglobin switch, functional oxygen carrying ability and many other characteristic features comparable with primary blood cells or those derived from primary HSPCs [188-192].

The current methodology for the *in vitro* generation of RBCs from hiPSCs generally includes three distinguishable steps: (1) formation of definitive HSPCs that express both CD34 and CD45 markers ($CD34^+CD45^+$); (2) erythroblast specification and expansion; and (3) erythrocyte maturation. To complete step (1), various protocols were established to promote mesodermal commitment and hematopoietic specification of hiPSCs [193]. For example, co-culturing with mouse stromal cells [148, 188, 194] or human stromal cells [146, 195, 196] harbored hiPSCs or HSPCs in stromal niches that recapitulated the *in vivo* environments of hematopoiesis, and sometimes was integrated

together with the latter two steps. Efficient feeder-free differentiation of hiPSC in monolayer adhesion culture on supporting substrates has not been established until a recent study showed that tenascin C could replace confluent OP-9 mouse stromal cell line, although the erythrocyte production from the new culture system has not been demonstrated [197]. The most commonly used method for step (1) so far is by forming EBs that are self-organized to mimic early human embryonic structures and development [198]. The mesodermal commitment and hematopoietic differentiation with EBs are further enhanced by adding exogenous cytokines such as BMP4, bFGF, SCF, VEGF, IL-3, etc. [153, 191, 199-202]. There are a number of approaches to form EBs, such as hanging drop, self-aggregation in static/dynamic suspension and FA method. Among these approaches, others and we found that FA in 96-well plates and micro-patterned plates that forms individual EBs while preventing multiple EBs from fusion and agglomeration, efficiently generate $CD34^{+}CD45^{+}$ definitive HSPCs [13, 169, 189, 203-205]. However, these studies used animal-derived products such as BSA [169, 206]. These xenogeneic and undefined reagents often cause low reproducibility and conflict with the strict requirements of clinical or pre-clinical applications [207, 208]. To search for a robust and efficient culture condition to generate HSPCs, we seek to develop a serum-free and feeder-free system of hiPSC differentiation with a high level of reproducibility. Moreover, we also evaluated some FDA-approved pharmacological agents to replace TPO and BSA in culture medium, which is important for future clinical applications.

Importantly, previous studies did not show the production of the corrected HBB protein, after hematopoietic differentiation of the gene-corrected iPSCs [37, 209]. The

lack of evidence in producing HBB protein after iPSC gene correction and differentiation could be due to: 1) defects in the donor vector that is unable to express the corrected gene from the endogenous regulatory element after genome targeting; 2) defects in the iPSC lines in these earlier studies that were derived from adult fibroblasts by vectors inserting and disputing the native human genome; 3) lack of an efficient differentiation method to generate mature erythrocytes that produce the adult form of beta-globin encoded by the *HBB* gene; or 4) combinations of the above.

Using a specific guide RNA and Cas9 in CRISPR/Cas9 gene correction, we readily corrected one allele of the SCD *HBB* gene in human iPSCs by homologous recombination with a donor DNA containing the wild-type *HBB* and a selection cassette for targeted insertion. An ultimate task would be to efficiently and specifically target the SCD mutation in high quality hiPSCs (such as those free of vector insertion), differentiate them into erythrocytes expressing a high-level of *HBB* mRNA, and demonstrate the production of *HBB*-encoded protein from the corrected allele. In this chapter, we demonstrated that we achieved these objectives, and established an efficient and reproducible method that is applicable to generate enucleated and β-globin expressing erythrocytes from hiPSCs.

4.2 *Materials and Methods*

4.2.1 **HSPC generation from hiPSCs using forced aggregation (FA) method**

The forced aggregation or "spin-embryoid body" (spin-EB) method in feeder- and serum-free conditions was modified from previously described protocols [13, 210, 211]. Single hiPSCs were suspended in serum-free differentiation medium (SFM, Table 4-1).

Table 4-1. Formulation of SFM for HSPC differentiation

Components	Final concentration	Resources
Iscove's modified Dulbecco medium (IMDM)	~ 50%	Gibco
Ham's F-12	~ 50%	Gibco
Bovine serum albumin or	0.5%	Sigma
Plasbumin-25 (human albumin)		Amgen
Chemically defined lipid concentrate	1%	Gibco
GlutaMAX	2 mM	Gibco
L-ascorbic acid phosphate magnesium salt	50 mg/ml	Sigma
1-thioglycerol	437 mM	Sigma
Insulin-Transferrin-Selenium-X	1x	Gibco

In brief, the SFM contain components including ITS and BSA. We also substituted BSA in the original SFM with FDA-approved human albumin made from pooled human venous plasma. One source is Plasbumin made by Grifols (NDC13533-684-20). We added 10 mM Y27632, 10 ng/ml recombinant human FGF2 (R&D

Systems), and 10 ng/ml BMP4 (R&D Systems). Cells (3, 000) were seeded into non-treated round-bottom 96-well plates (Costar) in 50 µl per well, and centrifuged at 300×g for 5 min. From day 2 to day 14, the cells were cultured in SFM containing FGF2 (10 ng/ml), BMP4 (10 ng/ml), SCF (50 ng/ml, R&D Systems), and VEGF-A (10 ng/ml, PeproTech). TPO (20 ng/ml, PeproTech) or romiplostim (Nplate, 20 ng/ml, Amgen) was added into the medium at day 11. Nplate is an US Food and Drug Administration (FDA) approved TPO analog [212]. On day 13-14, the suspended cells were harvested, and then filtered through 40-µm cell strainers (BD Biosciences) to remove EBs.

4.2.2 **Hematopoietic and erythroblast differentiation of hiPSC-derived HSPCs**

Hematopoietic and erythroblast differentiation of BC1, TNC1 and targeted iPSCs were done as described previously [205, 213]. Briefly, 5×10^5 cells/ml of either pooled or $CD34^+$ enriched suspension cells after EB day 13-14 were cultured in SFM containing human albumin, SCF (100 ng/ml, R&D Systems), erythropoietin (EPO, 3 U/ml, R&D Systems), human holo-transferrin (100 µg/ml, R&D systems) and interleukin 3 (IL-3, 10 ng/ml, R&D Systems). Cells were cultured at 37°C in a humid atmosphere of 5% CO_2 in air for 10 days and the medium was changed once every three days.

4.2.3 **Erythroid terminal maturation of erythroblasts generated from hiPSCs**

We counted the erythroblast cell number at day 10 of erythroblast differentiation and expansion culture and washed erythroblasts twice with PBS after we confirmed the normal erythroblast phenotype by flow cytometry. We then seeded erythroblasts in erythroid terminal maturation medium (TM) at 1 million per ml at 37°C in a humid atmosphere of 5% CO_2 in air. The erythroid TM medium is made by mixing with IMDM

(Invitrogen) plus 3 U/ml Epo (R&D Systems), 500 μg/ml human holo-transferrin (R&D systems), 4 U/ml heparin (Sigma), 10 μg/ml insulin (Sigma), and 10% pooled normal adult human peripheral blood plasma (innovative-research, Cat# IPLA-N). Fresh medium with cytokines was added every 2 to 3 days. The cell density is maintained below 4 million per ml. The maturating cells were taken for analysis at different days up to ten days from the beginning of terminal maturation.

4.2.4 **RNA extraction and quantitative RT-PCR to measure gene expression**

RT-PCR analysis of globin gene expression was done as described before [214]. All experiments were performed in triplicate and a non-template control (lacking cDNA template) was included in each assay. Relative gene expression was normalized to the housekeeping gene GAPDH.

4.2.5 **Western blot of HBB protein production**

Western blot for analyzing HBB protein level in differentiated cells is carried out using a monoclonal antibody against human HBB (Santa Cruz Biotechnology, sc-21757) and GAPDH (Cell Signaling Technology, Cat. 5174), according to the manufacturer's instructions. We used the protein extract from the same number of cells at different stages of differentiation to estimate HBB content in differentiated cells.

4.2.6 **O_2 binding capacity and affinity**

O_2 equilibrium curves of day 8 erythrocytes after terminal maturation (TM8) differentiated from iPSCs or fresh human CB as a control were determined using a Hemox-Analyzer (TCS Scientific, New Hope, PA) in accordance to manufacturer's recommendations as previously described [214].

4.3 *Results*

4.3.1 **A complete xeno-free condition supplemented with human albumin for reproducible HSPC generation**

In our original medium formulation for hematopoietic differentiation, which was adapted from BPEL medium reported first by Ng et al. [210], BSA is a critical component in a serum-free medium to nourish the cells and induce efficient differentiation (Table 4-1). However, commercial sources of BSA, which are known as Cohn fraction V and enriched in bovine albumin proteins, also contain other proteins and bioactive substances including undefined amounts of fatty acids, hormones, and metal ions. We have tested several BSA preparations from different sources and selected one product that gave the best results regarding $CD45^+CD34^+$ HSPC production. However, different lots of BSA product gave inconsistent result even with the same hiPSC line such as BC1 (Figure 4-1, A). "Good" lots (such as BSA Lot #1 and #5 in Figure 4-1, B) could lead to efficient differentiation (Figure 4-1,A, left panel), while a "bad" lot (such as BSA Lot #2 to #4 in Figure 4-1, B) caused low viability on day 2, which led to the failure of EB formation, or large cystic EBs with no release of single HPCs (Figure 4-1, A**,** right panel). As a result, we had difficulties in establishing a standard culture condition for the differentiation of multiple hiPSC lines. To achieve consistent hiPSC differentiation to HSPCs, we replaced BSA in serum-free medium with Plasbumin, which is a clinic-grade agent enriched for human albumin made from serum plasma. We found that Plasbumin from several lots consistently gave significantly higher efficiency and smaller variation during HSPC differentiation to generate $CD45^+CD34^+$ cells ($1.38\pm0.17\times10^6$ cells per

plate), compared to BSA fraction preparation ($0.44\pm0.54\times10^6$ cells per plate) (Figure 4-1, B, mean ± SD, n = 15).

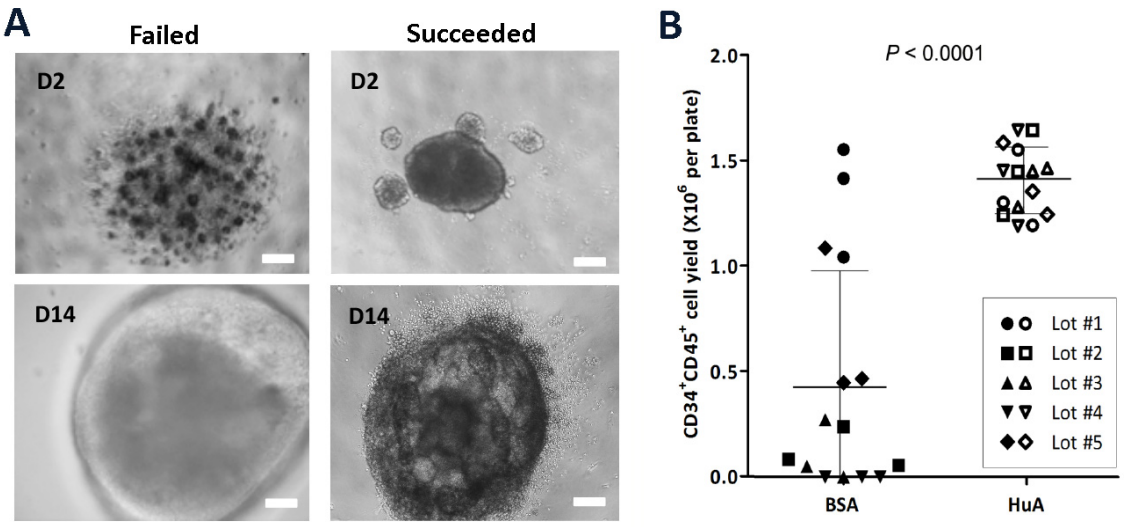

Figure 4-1. Replacing BSA with human albumin in SFM increased the efficiency and consistency of HSPC differentiation

(A) Representative images of day 2 and day 14 EBs from failed (left panel) and succeeded differentiations (right panel) using various lots of BSA and Human albumin (HuA) preparation in SFM. All scale bars represent 100 mm. (B) $CD34^+CD45^+$ HPCs generated from one 96-well plate of BC1 using SFM contained either BSA product or Human albumin of 5 different lot numbers each. Solid dots represent BSA group, and hollow dots represent Human albumin group. Mean ± SD, n = 15, $p < 0.0001$.

4.3.2 *In* vitro Microvascular Networks from Varies Cell Sources

We found that the addition of 20 ng/ml Romiplostium (TPO analog commercialized as Nplate) during the last stage of EB-mediated differentiation increased $CD34^+CD45^+$ HSPCs yield using forced aggregation method in 96-well plates (Figure 4-

2), and also enhanced subsequent megakaryocytic differentiation as a replacement of TPO [204]. Therefore, we included the Nplate treatment (one dose added at day 11) into the differentiation medium to increase HSPC yield.

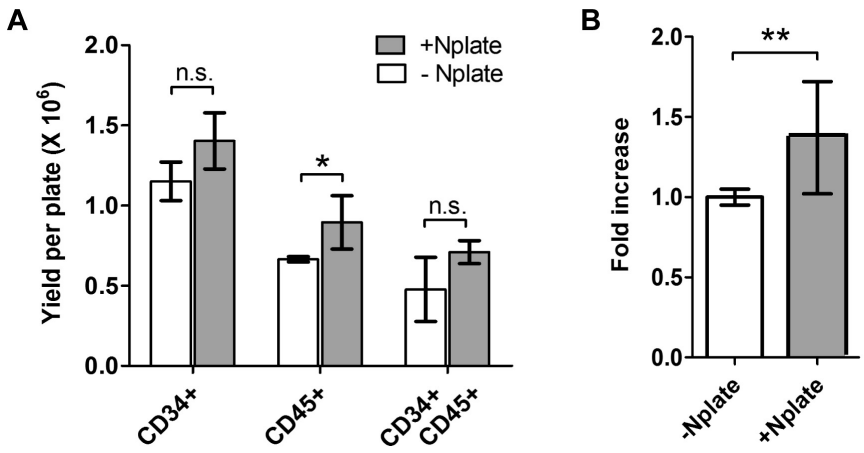

Figure 4-2. Enhancing the yield of hematopoietic progenitors on EB day 13 and erythroblasts on ED day 10 by adding Nplate during FA-EB day 11 to day 13

(A) Yield of $CD34^+$, $CD45^+$ and $CD34^+CD45^+$ per 96-well plate on FA-EB day 13. Nplate were added at the concentration of 20 ng/ml from day 11 to day 13 (n = 3, mean ± SD). (B) Fold increase of the yield of $CD36^+CD235a^+$ erythroblasts on ED day 10 between FA-EB cells with or without 3-day treatment of Nplate (n = 3, mean ± SD).

4.3.3 **Generation of enucleated erythrocytes from hiPSCs derived from blood**

We also proved that Plasbumin can be used to fully replace BSA in support of erythroblast differentiation under a serum-free culture condition, using either recombinant human proteins or human-sourced proteins. Recently we developed a method to generate human iPSC lines that are free of vector insertion in the genome from hematopoietic cells in CB, adult peripheral blood or bone marrow [11, 215]. For

example, we used peripheral blood mononuclear cells (MNCs) from an adult SCD patient and established a proliferative erythroblast culture that was reprogrammed to iPSCs by one to two plasmids [11]. One of such established iPSC lines, TNC1, contains the homozygous SCD mutation (nt. 69A>T) in the *HBB* gene [14]. After extensive expansion under a feeder-free culture condition such as one with the E8 culture medium on vitronectin as substrates, the TNC1 and BC1 iPSCs maintain pluripotency and are karyotypically stable [213]. We also analyzed the hematopoietic and erythrocytic differentiation potential of blood-derived iPSCs by first generating definitive $CD34^+CD45^+$ HSPCs followed by erythrocyte production *ex vivo*. In the first step, we used an improved method of forming individual EBs followed by hematopoietic differentiation that lasts 14 days (Figure 4-3, A), under a feeder-free and serum-free condition previously described [213]. Many hematopoietic cells released from EBs to culture medium by day 11-14 (Figure 4-3, B). We found that 55-65% of the cells harvested from culture suspension co-expressed CD45 and CD34, characteristic phenotypes of definitive HPCs (Figure 4-3, C). Compared to the input number of iPSCs, this was >3-fold expansion (Figure 4-3, D).

Next, the harvested cells from culture suspension at day 14 after EB formation or the purified $CD45^+CD34^+$ cells were expanded in erythroid differentiation (ED) culture in the presence of SCF, EPO, IL-3 and holo-transferrin (Step II in Figure 4-3, A). After 10 days, the total cells expanded ~40-fold (Figure 4-3, E), turned reddish gradually (Figure 4-3, F), expressed erythroblast markers such as CD36 and CD235a (Glycophorin A) and CD45 (not shown) at day 9-10 (Figure 4-3, G), and displayed erythroblast morphology (Figure 4-3, H).

Figure 4-3. A feeder- and xeno-free culture condition for the hematopoietic differentiation of hiPSCs

(A) A three-step differentiation strategy from iPSCs to hemoglobinized and enucleated erythrocytes, including forced aggregation mediated hematopoietic differentiation (EB), erythroid differentiation (ED), and erythroid terminal maturation (TM). (B-D) Characterization of EB day 14 cells of TNC1 iPSC cultures. (B) Phase-contrast image of an EB and surrounding hematopoietic cells. Scale bar: 200 μm. (C) Representative flow cytometric analysis of suspension cells harvested EB14 cells that co-express CD34 and CD45. The gates in all flow plots were set based on corresponding fluorescent isotype controls. (D) The yield of $CD34^+$, $CD45^+$, and $CD34^+CD45^+$ cells derived from one input hiPSC. Means ± SD, n = 4. (E-H) Erythroid differentiation (ED) step resulting in erythroid commitment, and erythroblast formation and expansion. (E) The accumulated expansion of cell numbers during the ED step. Means ± SD, n = 3. (F) Gradual color changes of cell pellets along the ED step. (G) A epresentative flow cytometric plot indicates that the majority of the ED10 cells express immature erythrocytes (erythroblasts) markers CD235a and CD36. (H) Wright-Giemsa staining of ED10 cells. Scale bar: 50 μm.

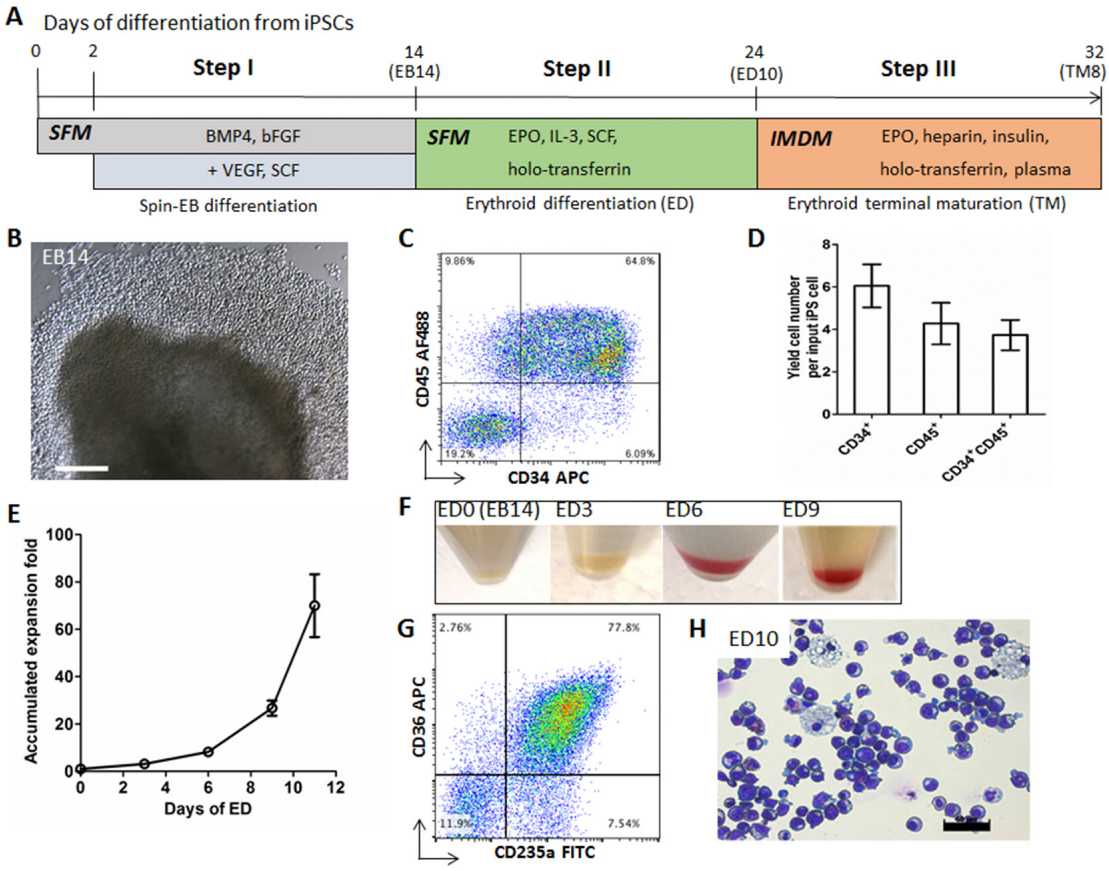

The erythroblast-like cells were allowed to terminally differentiate in culture with EPO, heparin, insulin and a high concentration of holo-transferrin (Step III in Figure 4-3, A). We also found that adding human plasma, which enhanced erythrocyte enucleation of erythroblasts derived from primary $CD34^+$ cells [216], also stimulated terminal differentiation of human iPSC-derived erythroblasts as reported recently [190, 192]. Upon terminal differentiation, the cells expanded for another 10-fold (>3 cell divisions) after 7-8 days before ceasing cell proliferation. The differentiated cells at this stage turned reddish, lost CD45 expression in the majority of cells (>98%), continued CD235a expression, and gained the expression of a maturation marker Band 3 in both nucleated

and enucleated (~10.6%) cells (Figure 4-4, A-D). In addition to Band3+ and CD235a$^+$ erythrocytes (>98%), we consistently observed a small population (0.2% to 1.6%) of nucleated cells in the harvested suspension cells after 6-8 days after terminal differentiation that express CD45, but lack CD235a and Band 3 expression (Figure 4-4, C). Morphological staining suggests that these CD45$^+$ cells resemble monocytes or macrophages (data not shown). Using quantitative RT-PCR analysis, we observed that the *HBB* gene expression in erythroblasts (ED10) and erythrocytes (TM8) from either TNC1 iPSCs or CB CD34$^+$ cells under the same improved culture condition, while the *HBG* gene expression is ~10–fold than *HBB* (Figure, 4-4, F). We further confirmed that enucleated cells expressed hemoglobin as stained by benzidine (Figure 4-4, G). Similar data were obtained using the BC1 iPSC line (Figure 4-5 and 4-6), with an enucleation rate of 4.7% ±2.8% and erythrocytes producing HBB as well as HBG proteins. Thus, we demonstrated that we can generate a population of human mature erythrocytes from blood cell-derived iPSCs using an improved xeno-free culture condition.

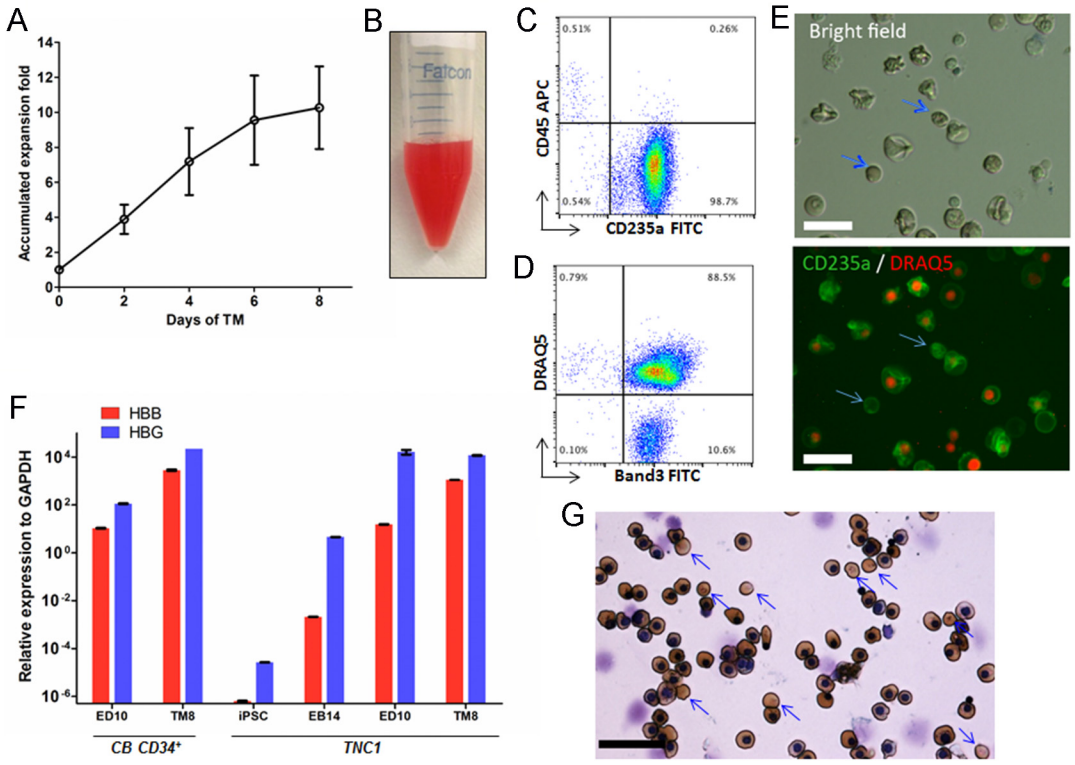

Figure 4-4. Terminal maturation of TNC1 iPSC-derived erythroblasts

(A) Cell expansion during the TM step. Means ± SD, n = 3. (B) Suspension of 90 million TM day 8 (TM8) cells in 1 ml PBS. (C, D) Representative flow cytometric plots of TM8 cells, with >98% cells co-express CD235a and Band3, and ~10% enucleation marked by negative staining of DRAQ5. (E) Phase-contrast and fluorescent images of TM8 cells. Blue arrows indicate enucleated erythrocytes. Scale bars: 30 μm. (F) Quantitative PCR analysis of gene expression of *HBB* (adult) and *HBG* (fetal) at different differentiation stages of TNC1 cells, comparing to the cultures of CB $CD34^+$ cells. Means ± SD, n = 3. (G) benzidine (brown color) for hemoglobin and Wright-Giemsa (nuclear DNA) staining of TM8 cells. 40× image. Scale bar: 50 μm. Blue arrows indicate enucleated erythrocytes lacking nucleus.

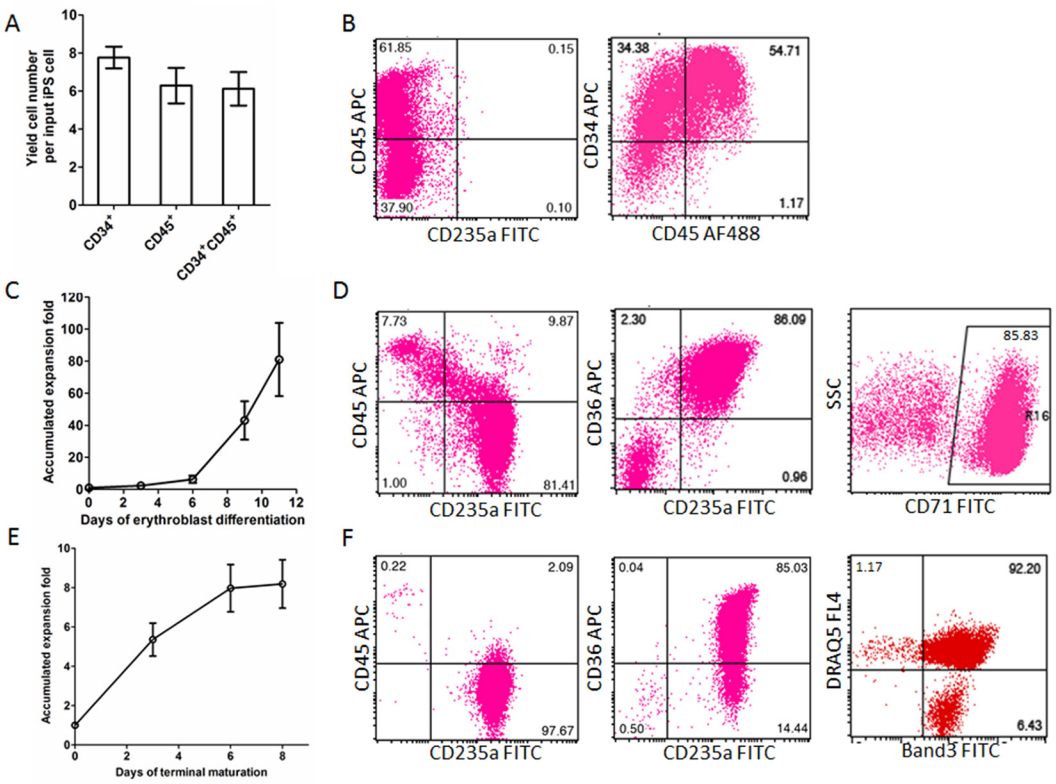

Figure 4-5. Hematopoietic differentiation and erythroid differentiation of BC1 iPSCs

The BC1 iPSCs, derived from a health adult bone marrow $CD34^+$ cells, were differentiated to erythrocytes as described in Figure 4-3 (for TNC1 iPSCs). (A) The yield of $CD34^+$, $CD45^+$, and $CD34^+CD45^+$ cells derived from one input iPSC, after EB formation and hematopoietic differentiation at day 14 (EB14). Means ± SD, n = 4. (B, D, F) Representative flow cytometry analysis of BC1 cells on EB14, erythroid differentiation at day 10 (ED10), and terminal differentiation day 8 (TM8), respectively, as described in Figure 4-3. (C, E) Cell expansion during erythroid differentiation (ED) and terminal maturation (TM). Means ± SD, n = 8.

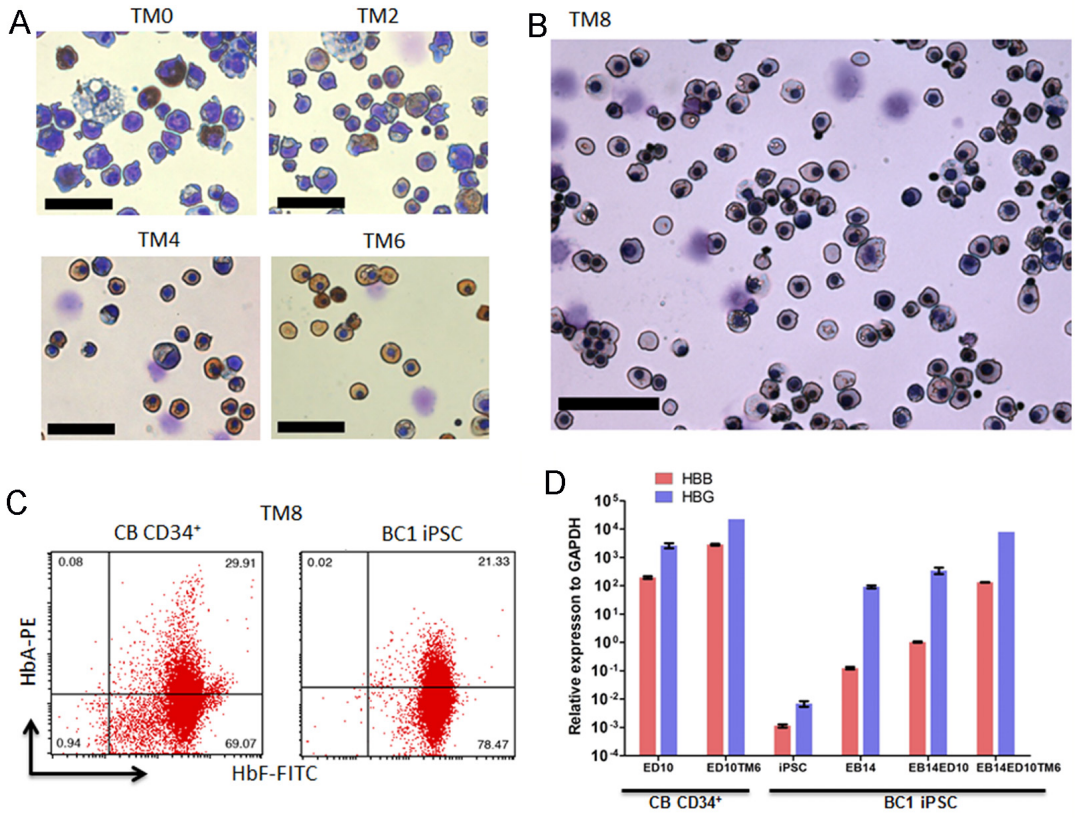

Figure 4-6. Terminal maturation of BC1 iPSC-derived erythroblasts

(A) Benzidine (gold brown color) and Wright-Giemsa staining of TM cells. (B) Wright-Giemsa staining of TM cells. 40× images. Scale bar: 50 mm. (C) Representative flow cytometry analysis of fetal (HbF) and adult (HbA) hemoglobin in TM8 BC1 cells. (D) Quantitative PCR analysis of gene expression of *HBB* (adult) and *HBG* (fetal) at different differentiation stages of BC1 cells, comparing to CB CD34$^+$ cells. Means ± SD, n = 3.

4.3.4 Production of corrected HBB proteins in erythrocytes derived from genome-edited SCD iPSCs

We specifically measured the level of corrected HBB gene expression and protein in *ex vivo* generated erythrocytes (TM8) from the gene-edited SC15-Cre2 clones, in comparison to the parental TNC1 that expressed the β^S protein (Figure 4-7). The RT-

PCR primers and the HBB antibody would not distinguish the wild-type and β^s forms, allowing us to quantitatively compare the level of HBB mRNAs or proteins in erythrocytes from the corrected SC15-Cre2 or parental TNC1 iPSCs. By RT-PCR, the level of HBB mRNA in SC15-Cre2 after terminal differentiation (TM8) increased further over those at earlier stages, but appeared >10-fold lower than those in erythrocytes from CB or TNC1 iPSCs (Figure 4-7, A). By Western blot, the HBB protein level in the erythrocyte culture from the SC15-Cre2 iPSCs is comparable to that from the parental TNC1 iPSCs (Figure 4-7, B). The HBB protein level in SC15-Cre2 derived erythrocytes appeared to be higher than that from the SC15 iPSCs, the genome-edited clones without the removal of the PGK-puromycin selection cassette located in the *HBB* intron 1.

We measured the HBB and HBG proteins in the native form of hemoglobin tetramers in individual cells by flow cytometric analysis (Figure 4-7, C). We detected >85% and >98% of cells expressed HBB and HBG proteins, respectively. The level of HBB proteins appears ~10-fold lower that that of HBG (Figure 4-7, C).

We also measured the functionality of O_2 binding by hemoglobin produced in the erythrocyte generated from hiPSCs, in comparison with primary CB erythrocytes (Figue 4-7, D). The iPSC-generated cells have an O_2-binding curve similar to that of cord blood, except that the affinity is slightly higher (p50 is 16.6 in SC15-Cre2 vs. 22.9 for CB). This may reflect the fact that HbF (containing HBG), which has a higher affinity for oxygen, are more abundant in the erythrocytes derived the hiPSCs.

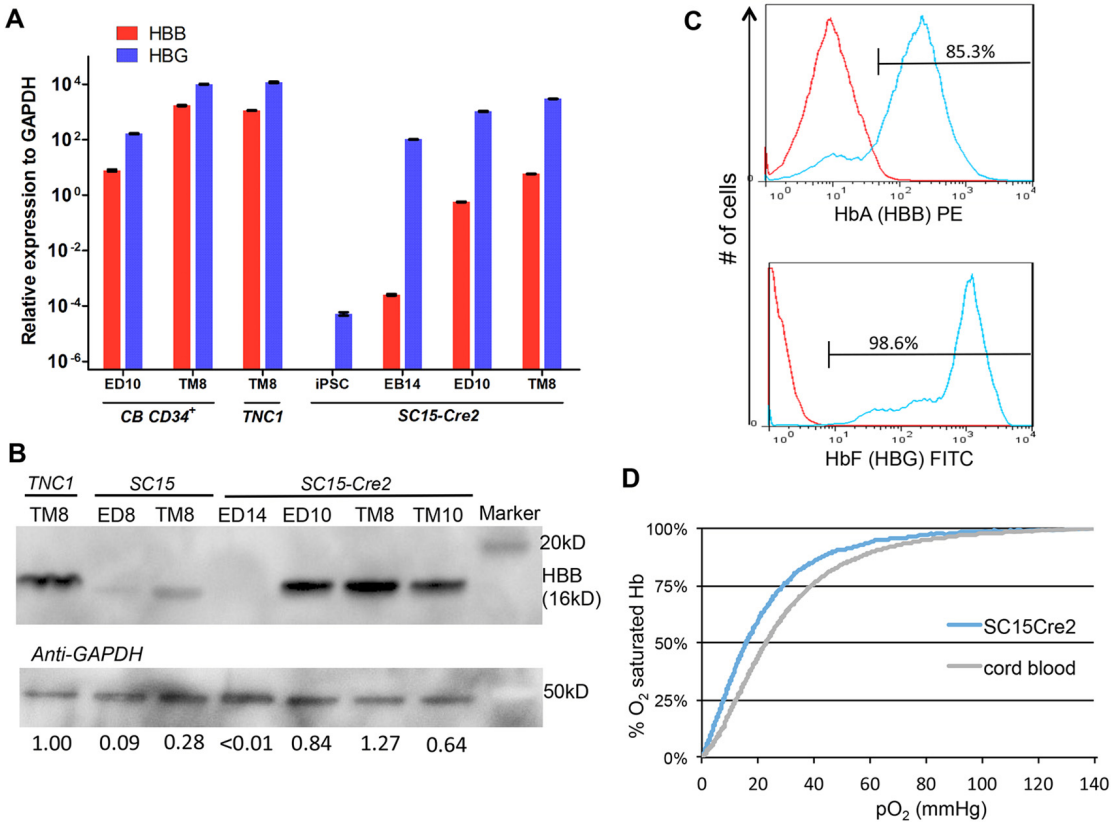

Figure 4-7. Analysis of globin gene and protein expressions of the corrected erythrocytes and their function

(A) Quantitative RT-PCR analysis of *HBB* and *HBG* gene expression in iPSCs, after hematopoietic differentiation (EB14), erythroid differentiation (ED10) and terminal maturation (TM8) from SC15-Cre2 and parental TNC1 iPSCs and a control of cord blood (CB) CD34+ cells. (B) Western blot analysis of adult hemoglobin beta (HBB) protein level during the differentiation of hiPSC clones before and after correction and excision. The relative levels of full-length HBB proteins normalized to the GAPDH control are also indicated. (C) FACS analysis of intracellular adult and fetal hemoglobin protein expression of maturated erythrocytes generated from SC15-Cre2 iPSC clone. (D) Oxygen affinity curves of erythrocytes from SC15-Cre2 after terminal maturation and a cord blood control as measured by a Hemox Analyzer.

4.4 *Discussion*

In this study, we developed a three-step differentiation system for efficient and reproducible erythrocyte production under a feeder-free and xeno-free condition. In the first step of HPC generation, we used a forced aggregation EB method to induce hiPSC differentiation, based on a pioneering study from Elefanty's group in 2005 [169]. We and others have since improved this method. To develop a clinically applicable procedure, we evaluated critical reagents in terms of reliability and cost effectiveness. More importantly, we would introduce reagents that are already approved by FDA and available in pharmacy. We replaced unreliable sources of BSA by FDA-approved human albumin Plasbumin. These improvements gave much more consistent results in generation of HSPCs. The differences observed among hiPSC lines from different individuals may be largely due to genetic variations in the human population rather than the inconsistency of differentiation conditions. This finding and our experimental system should provide a platform to study genetic influences on erythropoiesis in the future.

Using this method, we proved that the CRISPR/Cas9-mediated genome editing has little adverse effect on the integrity of targeted iPSCs, since they can differentiate into mature progeny such as enucleated erythrocytes that express the corrected *HBB* gene in SCD iPSCs. The level of HBB protein expression is similar to that of erythrocytes differentiated from untargeted iPSCs. Our study showing HBB protein expression in human erythrocytes differentiated from corrected iPSCs would not have been possible, if the HBB mRNA expression and protein synthesis had remained at low levels as previously observed [37, 147, 148, 188, 209, 217-219]. Previously, HBB protein expression was not detected in erythrocytes generated from human iPSCs or ESCs *ex*

vivo, unless transgene expression promoting erythroid formation [220-222] or co-culture with mouse stromal cell lines such as OP9 or MS5 were used [188, 192, 223]. Compared to these pioneering studies, we achieved much higher levels of HBB mRNA expression under the culture condition for producing erythrocytes generated from iPSCs such as TNC1 and their corrected progeny (Figure 4-4). In addition, we also observed the presence of enucleated erythrocytes under the feeder-free and xeno-free culture condition, although the percentage was not high (typically 5-10%) compared to that derived from CB $CD34^+$ cell cultures (30%-60%).

The much improved erythrocyte maturation and HBB protein expression from hiPSCs that we reported here could be due to at least the following two possibilities, which are not mutually exclusive. The first one is that we improved culture condition for terminal differentiation: we added human plasma that is known to promote enucleation, and omitted dexamethasone that promotes stressed erythropoiesis and fetal globin expression. The second one is that we used blood-derived iPSCs that have some residual epigenetic memory inherited from parental cells (TNC1 was derived from peripheral blood erythroblasts and BC1 was from adult bone marrow hematopoietic cells). This notion is also supported by a recent study showing that blood-derived iPSCs tend to have better erythroid differentiation potential than fibroblast-derived iPSCs [221]. Together, these studies provide additional strong evidence that residual epigenetic memory found in these blood-derived iPSCs [224-226] favors differentiation back to erythrocytes, especially when the differentiation condition is still sub-optimal. According to this notion, blood MNC-derived iPSCs are a better choice for efficient erythroid differentiation than fibroblast-derived iPSCs and human ESC lines (especially those

earlier ones on the NIH registry). This may explain the observations that in a previous study, erythrocytes generated ex vivo from fibroblast-derived iPSCs (in the presence of human plasma) did not produce sufficient levels of HBB proteins, until after they were infused to mice and matured further *in vivo* [190]. It is of note, however, that the fibroblast-derived iPSCs could generate enucleated cells and express the HBB proteins under enhanced conditions [190, 192], even though at an efficiency lower than that from blood-derived hiPSCs as we report here.

Under the current culture conditions, however, the level of HBB expression (at both mRNA and protein levels) is still >10-fold lower than that of the HBG. This may explain the fact that we and others did not observe sickling or defect in erythrocytes generated from hiPSCs derived from SCD patients [190]. The high-level of HBG protein may prevent the sickling of $\alpha_2\beta^s_2$ complexes, especially under culture conditions with a normoxic level of O_2. In the future, human differentiated erythrocytes generated *ex vivo* from hiPSCs (with or without genome editing) should be also tested *in vivo* using improved immune-deficient mice and conditioning [23], to examine *in vivo* properties of human erythrocyte in the circulation of the mouse models.

For future therapeutic uses, it is desirable to correct at least one of the β^s HBB allele in the iPSCs derived from SCD patients, before the iPSC-derived HPCs or erythrocyte can be used for autologous cell transplantation or transfusion. In addition to achieving the elusive objective to develop a robust and reproducible method for generating transplantable HSPCs [150, 193], we could also use erythrocytes generated from patient-specific iPSCs, with or without genome-editing to correct the underlying genetic defect, for transfusion medicine. The enucleated erythrocytes generated from

hiPSC lines, which could be further irradiated to block DNA replication, may have less risk than other nucleated progeny in causing cancers [186, 187, 227]. We also envision that we could generate genetically modified erythrocytes from genome-engineered iPSCs, for providing a source of functionally enhanced erythrocytes for cell therapies, not just a source of replacement in transfusion medicine [187]. Future studies are warranted to test efficacy and safety of erythrocytes from genome-edited iPSCs in preclinical models and in clinical trials.

4.5 *Conclusion*

In this chapter, we developed an efficient and reproducible differentiation system to generate HSPCs from hiPSCs under a feeder-free and xeno-free condition, in which all the animal-derived products were eliminated. By replacing BSA with human albumin in EB differentiation and using human plasma in terminal maturation, we can consistently generate hiPSC-derived HSPCs and erythrocytes, showing enucleation and adult-hemoglobin expression in gene-corrected iPSCs from SCD patients. The results discussed in this chapter have been published in Ref. 189 and Ref. 204.

5 *Scalable production of matured erythrocytes from hiPSCs*

In vitro production of erythrocytes in physiologic numbers from hiPSCs holds great promise for improved transfusion medicine and novel cell therapies. We report here, for the first time, a strategy for scalable and xeno-free differentiation of hematopoietic stem/progenitor cells from hiPSCs and subsequent erythrocytes specification, by using stepwise cell culture conditions and by integrating spinner flasks and rocker. This system supported robust and reproducible definitive hematopoietic differentiation of multiple hiPSC lines. We demonstrated an ultra-high yield of up to 4×10^9 $CD235a^+$ erythrocytes at >98% purity when using a 1-liter spinner flask for suspension culture. Erythrocytes generated from our system can reach a mature stage with RBC characteristics of enucleation, β-globin protein expression and oxygen-binding ability. The entire process is xeno-free and clinically compliant, allowing future mass production of iPSC-derived RBCs for transfusion medicine purposes.

5.1 *Introduction*

In Chapter 4, we demonstrated a FA differentiation method in 96-well plates with modified xeno-free medium to provide robust and reproducible HSPC generation from hiPSCs [204], which can be used as a baseline for further improvement. For step (2) and (3), efficient stromal-free suspension culture was established to generate enucleated and

hemoglobin-expressing erythrocytes using medium that contained EPO and human plasma [189-191]. However, the scalability of the differentiation system for erythrocyte production places a big hurdle for the large-scale manufacturing of HSPCs and enucleated erythrocytes for potential clinical applications.

In this chapter, we aim to establish a scalable system that can support large-scale EB differentiation towards hematopoietic lineages and high-yield erythrocyte production from hiPSCs *in vitro*. To achieve this goal, we first sought to combine the expansion of undifferentiated hiPSCs and the formation of EBs in suspension using spinner flasks. Then we integrated this process with static and dynamic culture on a platform rocker to enhance the efficiency of HSPC generation. HSPCs differentiated in the scalable system were directly induced to generate mature erythrocytes in suspension in scalable settings.

5.2 *Materials and Methods*

5.2.1 **EB differentiation in scalable vessels**

BC1 and TNC1 hiPSCs were expanded in 100-ml spinner flasks (CELLSPIN, Integra Biosciences) as cell aggregates in E8 medium (Essential 8, Thermo Fisher Scientific) as previously described [213] to yield a large quantity. Cell aggregates were dissociated into single cells by Accutase and inoculated at 4×10^5 cells/ml in spinner flasks at agitating speed of 35-50 rpm to initiate EB formation in 40 ml E8-based EB-formation medium (E8-EB medium), which is E8 medium supplemented with 10 ng/ml BMP4 (R&D Systems), 0.5% w/v human albumin (Plasbumin-25, Amgen), and 10 μM ROCK inhibitor Y27632 (Stemgent). This was marked as day 0 of differentiation. On day 1, stop agitation, settle the EBs at the bottom of the flask, and change ~70% of the

medium with fresh E8-EB medium to remove dead cells. All medium was replaced by SFM-based EB differentiation medium [204] on day 2. On day 3, transfer the culture into a 150-cm^2 tissue culture flask, and place in static (TS). After changing medium on day 6, put the tissue culture flask on a platform rocker at a frequency of 10-15 rpm (TR). Change ~70% of the medium on day 8, day 10, and day 13. Nplate (Amgen) were added at a final concentration of 20 ng/ml in EB differentiation medium from day 11 to day 13 to enhance HSPC expansion. Single suspension cells were harvested on day 13 and sequentially cultured in erythroid differentiation medium that was also made xeno-free by replacing BSA with human albumin, with the same concentration of cytokines and holo-transferrin for 10 days as previously described [189], followed by terminal maturation for 6-8 days [189], in either TR or SF condition with low agitating speed. FA method (so called "spin-EB") was applied as positive control as previously described [204]. When calculating yield, one batch of FA control was set as 8 plates of 96-well plates for the same 40-ml initial capacity.

5.2.2 **Erythroid differentiation and terminal maturation**

Suspension cells harvested from EB day 13 were directly transferred into erythroid liquid culture in tissue culture plates in static condition, on rocker, or in spinner flasks without the need of $CD34^+$ isolation. The medium formulations for erythroid differentiation and terminal maturation were described previously [189, 205], except that the BSA in SFM was replaced by human albumin to make it xeno-free [204].

5.2.3 **Design and control of the DO level in glass-ball type spinner flasks**

DO level was monitored by a non-invasive optical O_2 sensor probe using PreSens Oxy-4 Mini transmitter (PreSens). A sensor spot was attached to the inner wall of a spinner flask with silicon glue, and signal was detected by an optical probe from outside. We connected a gas cylinder containing 5% O_2 + 5% CO_2 + 90% N_2 to the spinner flask and constantly flush 5% O_2 at very low flow rate (~ 3 psi gauge pressure). A medium bottle was connected between the spinner flask and O_2 cylinder, serving as both a heat exchanger for the influx O_2 and the reservoir for pre-conditioned medium. Airtightness and flow was monitored by bubbling in a water bottle at the outlet of the spinner flask. A peristaltic pump was used to change medium and sampling during the operation without disclose the system to avoid re-oxidation. When changing medium, we stopped the agitation and allowed the cell aggregates or EBs to settle down to the bottom, then change approximately 70% of the medium.

5.2.4 **Morphological analysis using light microscopy and measurement of EB size**

Images were acquired using Eclipse TE2000-U microscope (Nikon). EB size was measured as previously described using Celigo imaging cytometer (Nexcelom). Data was collected from more than 450 EBs from three independent experiments.

5.2.5 **Fluorescence microscopy analysis**

After wash, images were acquired using Eclipse TE2000-U microscope (Nikon).

5.2.6 **RNA extraction and quantitative RT-PCR**

RNA extraction and RT-PCR analysis of globin genes *HBB* and *HBG* was performed as previously described [214]. For mesodermal and hemogenic endothelial

genes, the primers were listed in the Table 5-1. All experiments were performed in triplicates, and a non-template control (no cDNA template) was included in each assay. Relative gene expression was normalized to the housekeeping gene *GAPDH*.

Table 5-1. Primers for qRT-PCR

Genes	Primers	Sequence (5' – 3')
GAPDH	Forward	AGAAGACTGTGGATGGCCCCTC
	Reverse	GATGACCTTGCCCACAGCCTT
HHEX	Forward	TACTCTGGAGCCCCTTCTTG
	Reverse	TTTGACCTGTCTCTCGCTGA
KDR	Forward	CCAATAATCAGAGTGGCAGTG
	Reverse	CATAGACATAAATGACCGAGGC
MYB	Forward	TCTTCTGCTCACACCACTGG
	Reverse	GGCTGAGAATGCATTCACG
RUNX1	Forward	GATGGCACTCTGGTCACTG
	Reverse	TTTCCCTCTTCCACTTCG
GATA2	Forward	AGCAAGGCTCGTTCCTGTTC
	Reverse	TCGGTTCTGCCCATTCATCT
TIE1	Forward	TCACCCCAACATCATCAACC
	Reverse	TCTCCGACCAGCACATTCC

5.2.7 **Western blot of HBB protein**

Western blot for HBB protein detection was performed using a monoclonal antibody against human HBB (Santa Cruz Biotechnology, sc-21757) and β-actin (Cell Signaling Technology, Cat. 3700P). The concentration of the protein extract from each cell samples was quantified using Pierce BCA Protein Assay Kit (Thermo Fisher Scientific) as per manufacturer's instructions. Protein samples of iPSCs and iPSC-derived erythrocytes were loaded as 10 μg.

5.2.8 **Measurement of oxygen-hemoglobin dissociation curve**

Oxygen-hemoglobin dissociation curves of TM day 6 cells from scalable and unscalable conditions as well as primary cord blood control were measured using a Hemox Analyzer (TCS Scientific) as previously described [214].

5.3 ***Results***

5.3.1 **The initiation of scalable EB formation in spinner flasks**

Utilizing our scalable expansion of undifferentiated hiPSC in suspension, which is matrix-independent and microcarrier-free [213], we transitioned to large-scale EB differentiation. Shear stress on hiPSCs in the suspension culture in agitating vessels is known to affect cell survival [122]. Medium flow in a spinner flask (SF) and a tissue culture flask on a platform rocker (TR) generate different levels of shear stress. Thus we first tested which scalable system better support EB formation from a single cell suspension from BC1 hiPSCs [11]. We found that the serum-free medium used in the standard forced aggregation (FA) differentiation for the first 2 days [204] could not

support consistent bulk EB formation in suspension culture especially in spinner flasks, resulting in an unexpected high level of cell death with cell viability below 65% (Figure 5-1, A). In contrast, EBs formed with a modified E8-based medium supplemented with human albumin and BMP4 in addition to the ROCK inhibitor Y27632 (called E8-EB medium thereafter) showed significantly higher cell viability, 89±4 % on EB day 1 (Figure 5-1, A), demonstrating a simple but efficacious approach to enhance cell survival in spinner flasks during EB formation. We also found that EBs formed in the E8-EB medium in spinner flasks were more uniform in size, while many large EBs with irregular shapes formed on rocker likely due to insufficient and uneven agitation (Figure 5-1, B). Quantitative analysis of EB size indicated that EBs formed in spinner flasks have a homogeneous size with an average equivalent diameter of 187±36 μm, whereas a wider distribution of EB size was found on rocker (247±128 μm) with many compact EBs larger than 400 μm (Figure 5-1, C), which would cause cell death in the center due to insufficient transport of nutrient, waste and O_2. Therefore, we chose to use E8-EB medium in spinner flasks as the optimized condition to form spatially and temporally synchronized EBs. Thus, we directly combined hiPSC expansion with EB formation in scalable suspension culture.

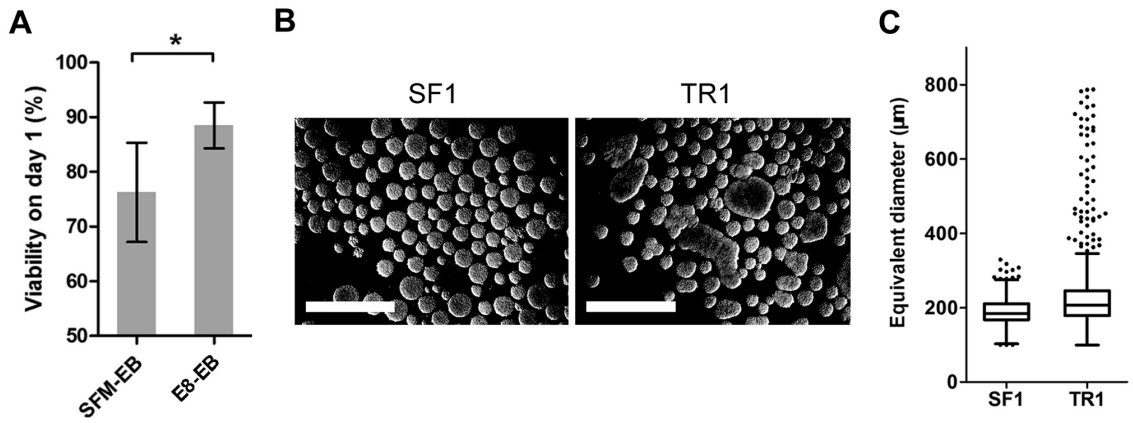

Figure 5-1. Optimization of initial EB formation in suspension cultures

(A) Levels of cell viability on day 1 using different media for EB formation in suspension cultures. All media were supplemented with 10 μM Y27632 to promote cell survival. SFM-EB: serum-free medium with BMP4 and FGF2 as the medium used in the FA control of EB formation; E8-EB: E8 medium with BMP4 and human albumin (n = 3, mean ± SD). (B) Representative images of EBs formed at day 1 in spinner flask at 35 rpm (SF1) and 150-cm^2 tissue culture flask on rocker at 10 rpm on day 1 (TR1), respectively. Irregular shape and sizes were observed in TR day 1 EBs (scale bars = 1 mm). (C) Size of EBs at day 1 generated in spinner flask (SF1) or on rocker (TR1). More than 450 EBs in each condition from three independent experiments were analyzed and illustrated in Whiskers-Tukey plot (n = 3, mean ± SEM).

5.3.2 **Scalable generation of hematopoietic cells using an optimized integration of static culture and spinner flasks**

The yield from one bioreactor run (indicated as "batch yield") is an essential parameter to measure outcomes in the scale-up process. In order to maximize the yield of the EB differentiation, we explored several strategies using SF and TR (Figure 5-2, A), based on media and timeline modified from the FA method previously established [204]. After formed in spinner flasks, EBs harvested on day 3 were cultured either in spinner flasks or on rocker. In one condition, a 3-day static culture in tissue culture flasks (TS, see illustration in Figure 5-2, A) was also applied between the spinner and the rocking condition (SF-TS-TR). We compared the yield of suspension cells released from EBs (harvested at day 13) in batches with 40-ml initial volume followed by different combinations of these module conditions (Figure 5-2, A). From four independent experiments in each condition, the conventional FA method generated $10.2\pm4.2\times10^6$ live cells from eight 96-well plates starting from 40-ml of initial single cell suspension (Figure 5-2, B). Among the strategies in scalable settings, the methods in which EBs were in free suspension throughout the culture (such as SF, TR and SF-TR, see Figure 5-2, A) showed poor reproducibility with about 50% of experiments failing to generate hematopoietic cells. Only the combinatorial SF-TS-TR strategy including a 3-day static culture in tissue culture flasks supported more consistent differentiation with higher yields. A total of $29.1\pm10.8\times10^6$ live cells were generated from SF-TS-TR suspension, 2.9-fold higher than FA control (Figure 5-2, B).

Figure 5-2. Establishment and optimization of a scalable protocol for hematopoietic cell generation in suspension

(A) Schematic presentation of strategies for scalable EB differentiation and production of hiPSC-derived erythrocytes. The differentiation was induced in three successive steps: embryoid body differentiation (EB), erythroid differentiation (ED) and terminal maturation (TM). Media and culture condition changes are illustrated according to the timeline of differentiation. (B) Yield of single suspension cells on day 13 from one batch using different EB differentiation protocols. SF and TR represent continuous EB differentiation for 13 days in spinner flasks and tissue culture flasks on rocker, respectively. SF-TS or SF-TR represent additional 8 days in static or rocking condition, respectively, after 3-day EB formation in spinner flasks (n = 4, mean ± SEM). (C) Exemplary light microscopy images of EB differentiation using SF-TS-TR on day 6 and day 13. EB attachment on day 6 and single hematopoietic suspension cells on day 13 were clearly shown (scale bars = 200 μm). (D) Batch yield of total single suspension cells from 40-ml cultures using different SF-TS-TR strategies with static culture for 1 day (TS1), 2 days (TS2) and 3 days (TS3) (n = 3, mean ± SD). (E) Expression of *KDR*, *GATA2*, *RUNX1*, *MYB* and *HHEX* genes in EB cells from continuous agitating SF or SF-TS strategies on EB day 6 (normalized to endogenous *GAPDH* as a housekeeping control; n = 2 independent experiments with 3 technical replicates each, mean ± SD).

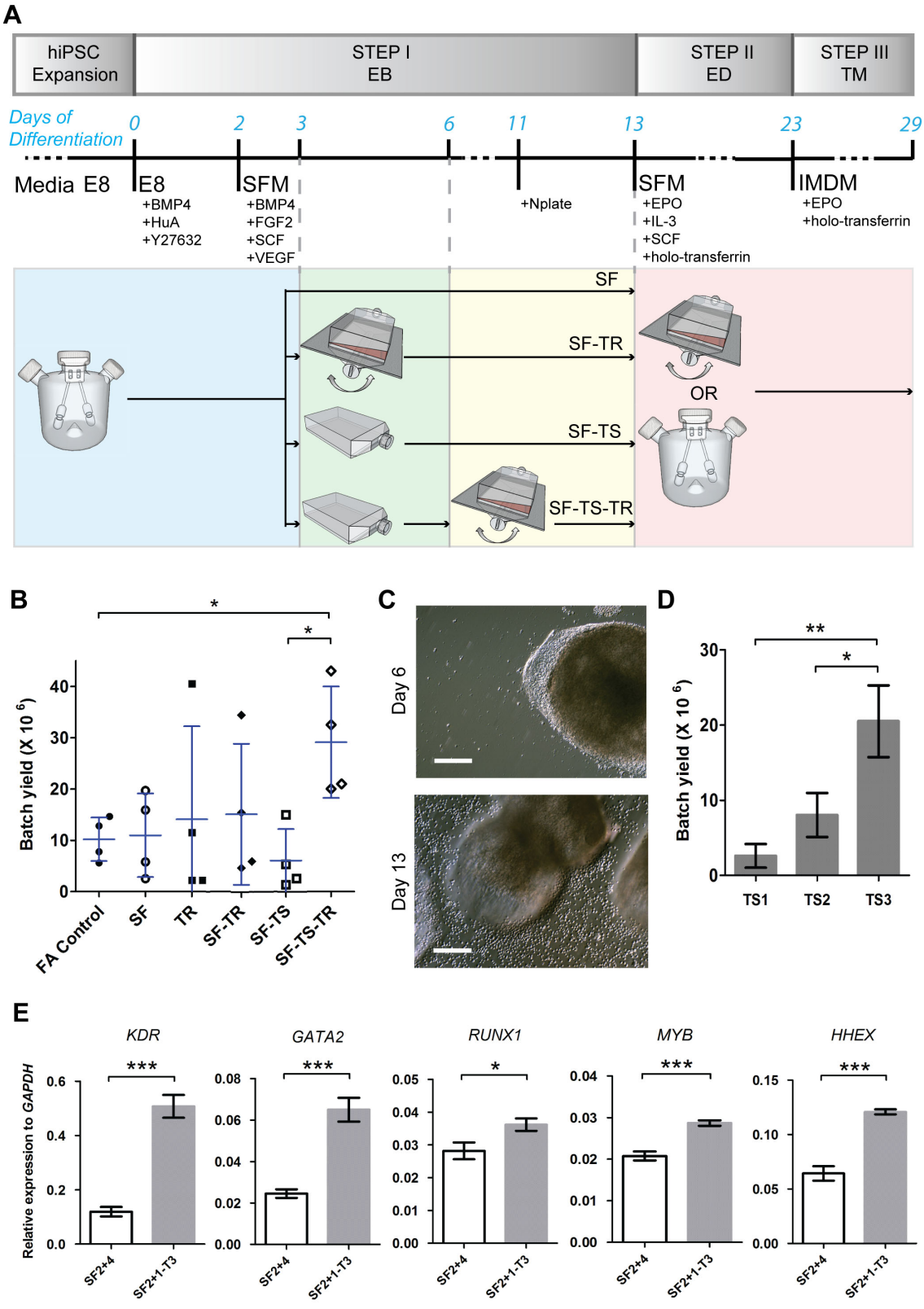
A
hiPSC Expansion
STEP I EB
STEP II ED
STEP III TM
Days of Differentiation
0
2
3
6
11
13
23
29
Media E8
E8
+BMP4
+HuA
+Y27632
SFM
+BMP4
+FGF2
+SCF
+VEGF
+Nplate
SFM
+EPO
+IL-3
+SCF
+holo-transferrin
IMDM
+EPO
+holo-transferrin
SF
SF-TR
OR
SF-TS
SF-TS-TR
B
Batch yield (X 10 6)
FA Control
SF
TR
SF-TR
SF-TS
SF-TS-TR
C
Day 6
Day 13
D
Batch yield (X 10 6)
TS1
TS2
TS3
E
Relative expression to GAPDH
KDR
GATA2
RUNX1
MYB
HHEX
SF2+4
SF2+1-T3

Next, we investigated the potential mechanisms underlying the improvement in yield when using SF-TS-TR strategy. The three days of static culture was the only difference between SF-TS-TR and SF-TR. Light microscopy images revealed distinguishable changes of EB morphology and confirmed the emergence of HSPC on day 13 (Figure 5-3 and Figure 5-2, C). Under the FA condition, EBs formed after 2-3 days of centrifugal aggregation appeared loosely attaching to the bottom of the well (even in low-attachment or untreated plates). Cystic structure inside EBs emerged on or around day 5, indicating the embryonic development and cell differentiation (Figure 5-3). In SF-TS-TR method, hiPSCs formed more homogenous EBs in size on day 2 compared to FA or SF-TR (Figure 5-3). Three days in static condition provided the environment for the EBs to loosely attach to the bottom of tissue culture flasks (Figure 5-2, C), similar to the FA method compared to completely free floating EBs in SF-TR. It was clear that the three days of static culture was beneficial for a high yield of hematopoietic cells in suspension on day 13 when compared to 2-day or 1-day static culture (Figure 5-2, D). After three days in static condition, genes associated with mesoderm commitment and hemato-vascular lineages were all elevated (Figure 5-4). As a result, cells through the 3-day static condition showed significantly higher expression of key genes related to mesoderm formation (*KDR*) [194], hemato-vascular development (*GATA2 and RUNX1*) [197, 228] and definitive hematopoiesis (*MYB* and *HHEX*) [220, 229, 230] compared to cells from suspension EB differentiation in spinner flasks (Figure 5-2, E). This is in line with the higher hematopoietic yield from cultures with 3-day in static condition in comparison to 1-day or 2-day in static condition (Figure 5-2, D).

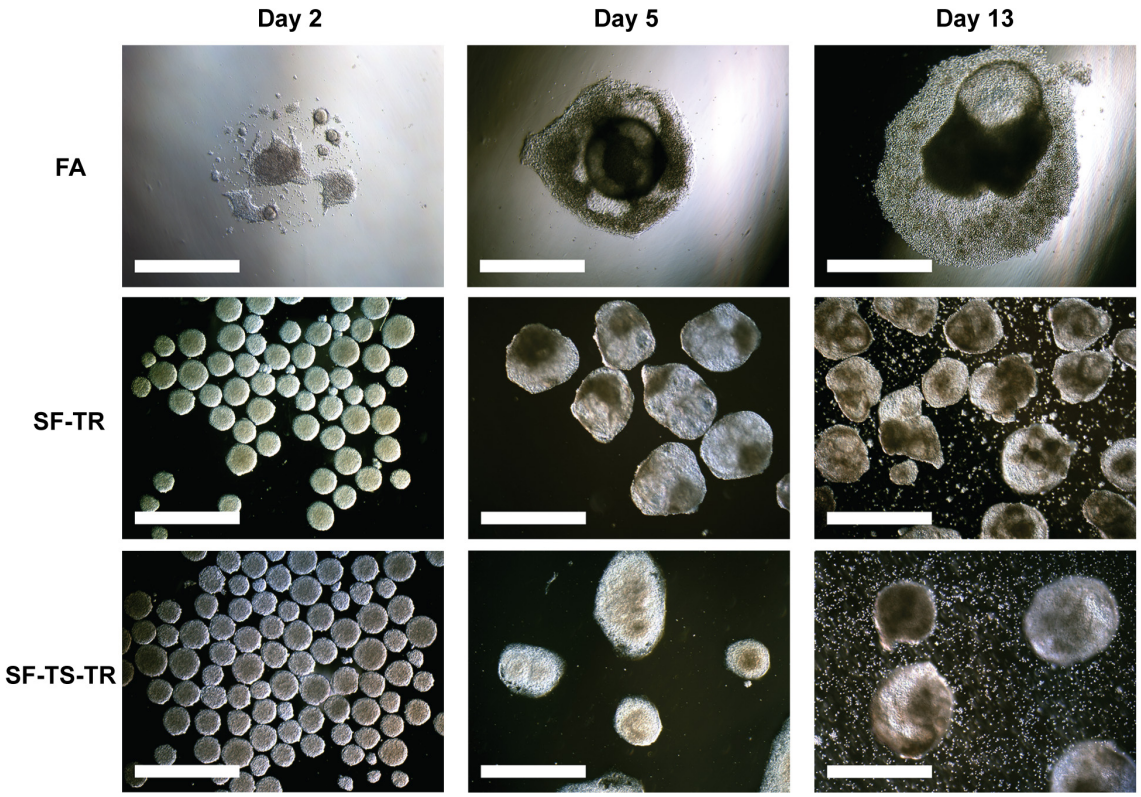

Figure 5-3. Morphology analysis of the scalable EB differentiation protocols

Low magnification images show the morphology of the whole EBs in different methods on day 2, day 5 and day 13. FA indicates forced aggregation EB control, SF-TR indicates the differentiation contains 3 days of EB formation in spinner flasks followed by 10 days of continuous suspension culture in tissue culture flasks on platform rocker. SF-TS-TR indicated 3 days in spinner flasks followed by 3 days in static condition in tissue culture flasks and 7 days of rocking culture (scale bars = 1 mm).

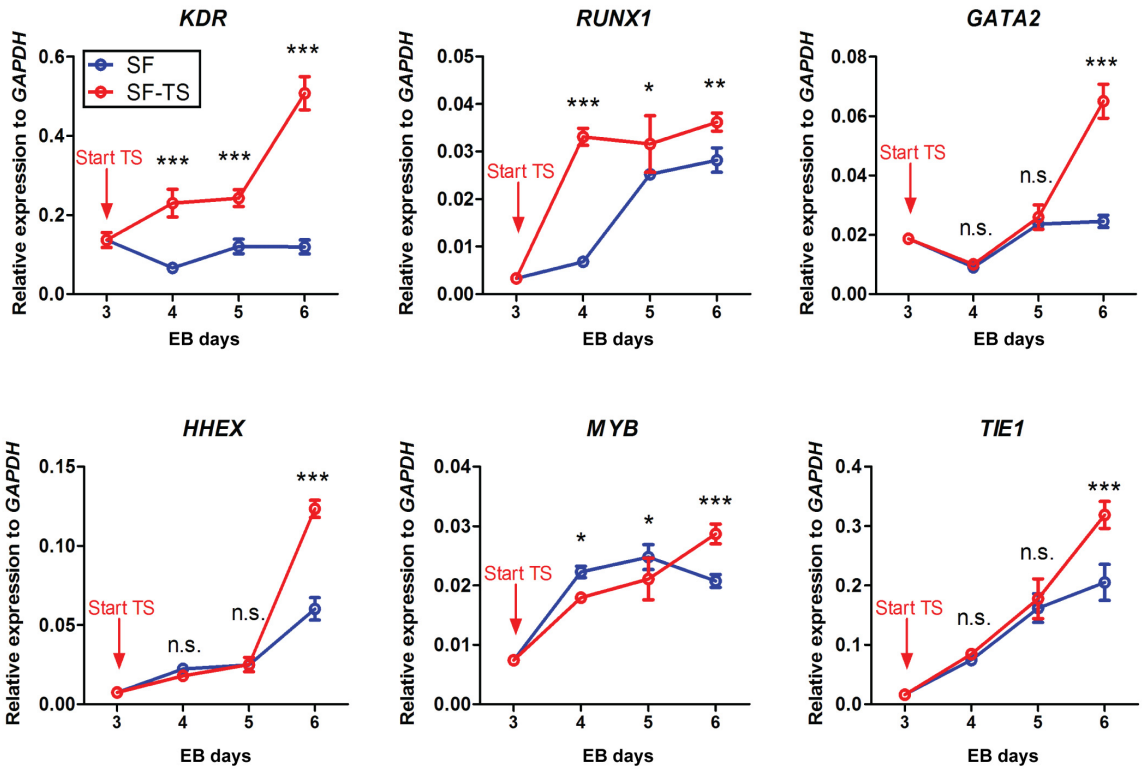

Figure 5-4. Gene expression profile of whole EB cells from continuous spinner flask and SF-TS conditions on EB day 3 to EB day 6

EBs were differentiated in spinner flasks for 2 days in E8-EB medium and 1 day in serum-free differentiation medium. TS1 means 1 day in T150 flask in static condition after 3 days in SF, and so on. Gene expression was normalized to endogenous *GAPDH* as a housekeeping control (n = 2 independent experiments with 3 technical replicates each, mean ± SD).

5.3.3 Characterization of single cells from scalable EB differentiation

Similar to the FA control, suspension cells harvested from SF-TS-TR at EB day 13 contained 75.6±12.3 % $CD34^+$ cells and 64.2±11.9 % $CD34^+CD45^+$ cells, with little erythrocytes that should express CD235a (Figure 5-6, A). The batch yield of $CD34^+CD45^+$ cells from SF-TS-TR was $14.6\pm4.5\times10^6$, which was significantly higher than the unscalable FA method (Figure 5-6, B). CFU assay was performed to test the

level of hematopoietic progenitor cells in the total and $CD34^+$ purified suspension cell populations (Figure 5-6, C). These results indicated that the $CD34^+CD45^+$ cells generated from SF-TS-TR had comparable contents of myeloid and erythroid progenitor cells as the FA method.

5.3.4 **Erythroid differentiation and terminal maturation in a scalable system**

Considering that >70% of the suspension cells were $CD34^+$ cells, we found that it was not necessary to isolate $CD34^+$ cells for downstream erythroid production under a culture condition selectively favoring erythroid cell proliferation and differentiation. After EB formation and initial hematopoietic differentiation (Figure 5-2, A), single cells were harvested at day 13 by passing the entire culture through a 40-μm cell strainer and immediately transfer to the following differentiation steps. This simple "filter-and-go" process would be highly favorable for the scale-up bioprocess. Previous studies found that even mild agitation at 15-20 rpm in stirred tank bioreactor had significant impact on the *ex vivo* erythropoiesis of peripheral blood $CD34^+$ derived cultures [231].

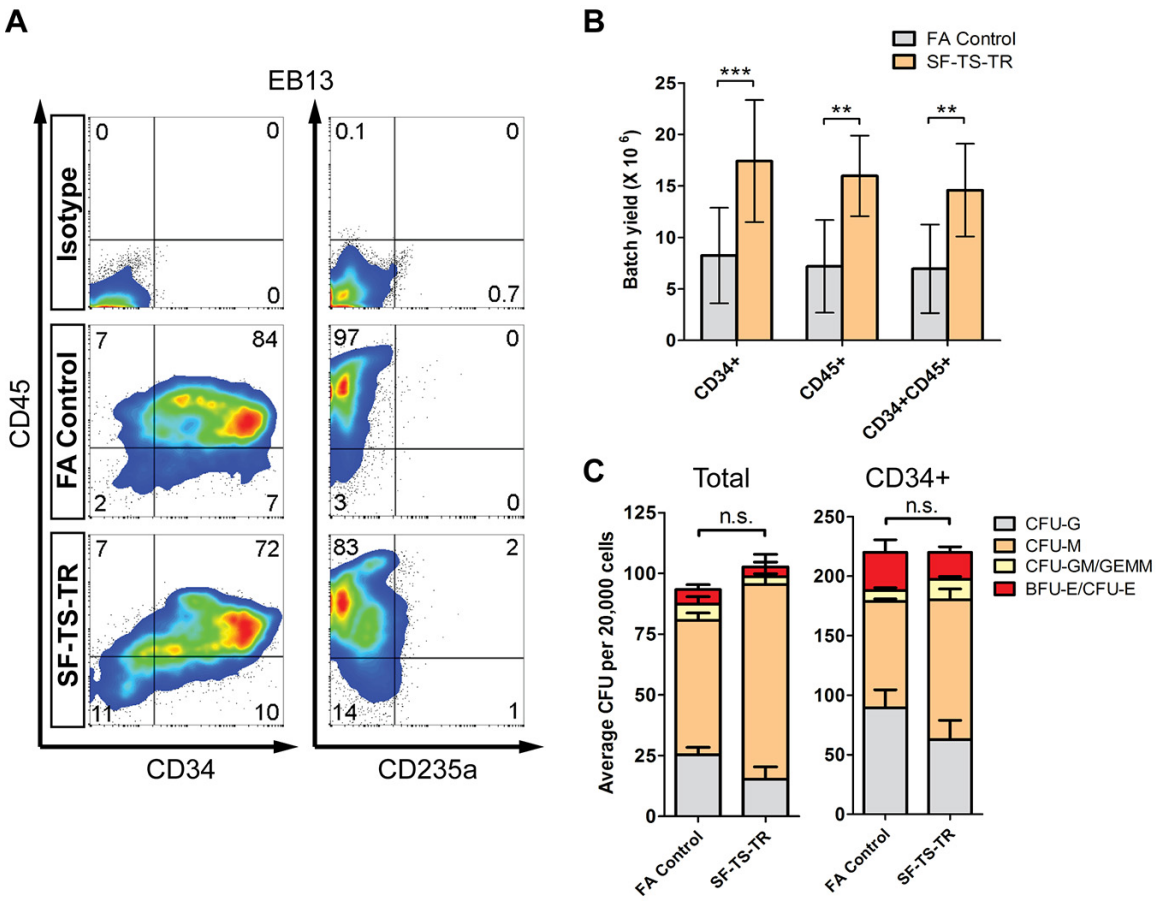

Figure 5-5. Characterizations of differentiated hematopoietic cells derived from hiPSCs using the SF-TS-TR protocol

(A) Representative flow cytometric analysis of CD34, CD45, and CD235a in the suspension cell populations harvested on EB day 13. Gates were set based on corresponding isotype controls. (B) Quantification of the batch yield of $CD34^+$, $CD45^+$, and $CD34^+CD45^+$ cells from SF-TS-TR method (n = 4, mean ± SD). (C) CFU assays of total suspension cells and anti-human CD34-bead isolated suspension single cells from SF-TS-TR method. After isolation, >95% of the cells showed $CD34^+$ by flow cytometric analysis. The total number of CFU was analyzed by the two-tailed Student's t-test (n = 2 independent experiments with 3 technical replicates each, mean ± SD).

We also confirmed that shear stress generated by agitation at medium speed range (40-50 rpm) in spinner flasks impeded the expansion rate of erythroid expansion and differentiation (Figure 5-7, A). By reducing the agitation to low speed range in SF (22.5 rpm) or TR at low rocking frequency (10-15 rpm), expansion in erythroid differentiation (ED) and terminal maturation (TM) were recovered and comparable as the static culture, calculated at 211±22 fold and 237±56 fold increase, respectively (Figure 5-7, A). The entire process in scalable system yielded $3.2\pm0.6\times10^9$ $CD235a^+$ erythrocytes, 1.5-fold higher than those from the FA control (Figure 5-7, B). After scale-up to 1-liter spinner flasks, we achieved an ultra-high yield of 4.1×10^9 hiPSC-derived erythrocytes from a 40-ml SF-TS-TR batch. Taking these steps together, we established a complete procedure for the scalable production of human erythrocytes through EB formation (Figure 5-2, A). A cell suspension containing 1×10^9 cells in 10 ml PBS showed red color like diluted blood (Figure 5-7, C).

Figure 5-6. Scalable erythroid differentiation and terminal maturation of the suspension cells from SF-TS-TR protocol

(A) Optimization of the agitating speed in scalable platforms for ED-TM using the suspension cells from SF-TS-TR by analyzing accumulated expansion fold increase (n = 3, mean ± SD). All of the other conditions were significantly higher than SF 40 rpm condition ($P < 0.05$). (B) Calculated batch yield of $CD235^+$ erythrocytes on day 6 of terminal maturation (TM6) from suspension cells generated by FA or SF-TS-TR EB and through scalable ED-TM in TR at 10 rpm and/or SF at 22.5 rpm (n = 4, mean ± SD). (C) Image of 1×10^9 TM6 cells in 10 ml PBS. Cells were from 1/3 batch of scalable production of hiPSC-derived erythrocytes. (D) Representative flow cytometry data reveals the progressive changes of phenotype during ED-TM. All gates were set based on corresponding isotype controls. (E) Representative flow cytometry analysis of enucleation rate of TM6 cells using DRAQ5 staining for nuclei. All gates were set based on corresponding isotype controls. (F) Representative fluorescent images of TM6 cells generated from SF-TS-TR EB and scalable ED-TM. Solid arrows indicate live and metabolic active enucleated erythrocytes that were double stained by CD235a and Calcein AM but lack of nuclei and DRAQ5-staining of DNA. Triangle arrowheads indicate separated nuclei after enucleation, known as pyrenocytes. White open arrows indicate pieces of broken cell membrane that were only stained by CD235a (scale bar = 20 μm). (G) Wright-Giemsa (for cytoplasm and nuclear DNA) and benzidine (for hemoglobin) staining of TM6 cells from scalable production. Most of the nucleated cells showed morphology of orthochromatic erythroblasts that contained hemoglobin (brown color by benzidine staining). Arrows indicate enucleated erythrocytes, and Triangle arrowheads indicate ejected nuclei (scale bar = 20 μm).

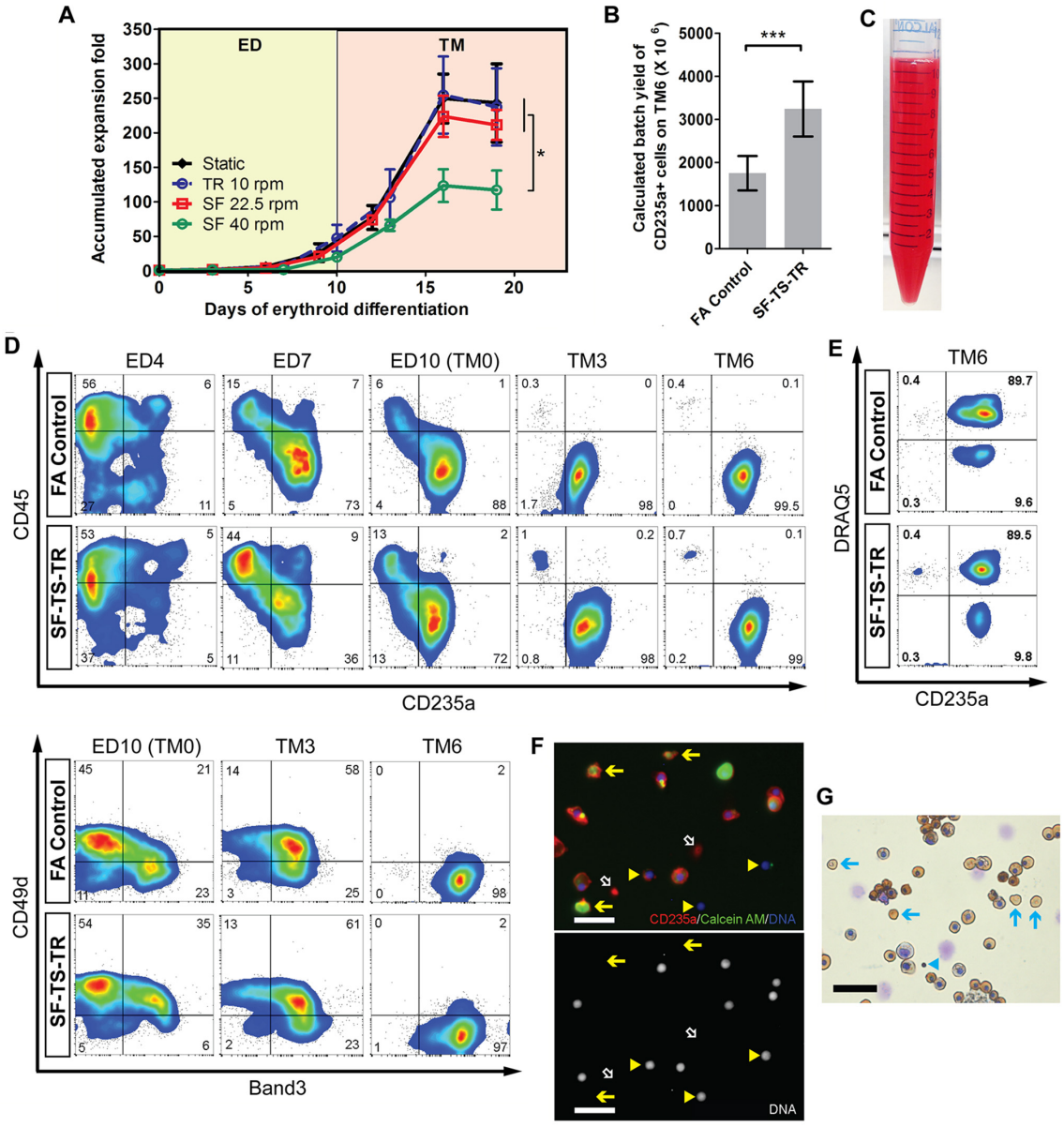
A
Accumulated expansion fold
ED
TM
Static
TR 10 rpm
SF 22.5 rpm
SF 40 rpm
Days of erythroid differentiation
B
Calculated batch yield of CD235a+ cells on TM6 (X 10 6)
***
FA Control
SF-TS-TR
C
D
ED4
ED7
ED10 (TM0)
TM3
TM6
FA Control
SF-TS-TR
CD45
CD235a
E
TM6
DRAQ5
CD235a
ED10 (TM0)
TM3
TM6
CD49d
Band3
F
CD235a/Calcein AM/DNA
DNA
G

Phenotypic changes in the suspension cells from SF-TS-TR during the scalable ED-TM steps were tracked by flow cytometry (Figure 5-7, D and 5-8). Plots of forward scatter and side scatter showed the shrinking in size of erythroblasts during the maturation period (Figure 5-8, A). The gradual loss of CD45 and gain of CD235a expression indicated the loss of multipotent HSPCs and myeloid cell populations, and enrichment of erythroid population (Figure 5-7, D). When we analyzed the expression patterns of two erythroid stage-specific markers Band3 and CD49d (alpha4 integrin), we also observed a rapid and synchronized erythroblast maturation process from $CD49d^{+}Band3^{-}$, to $CD49d^{+}Band3^{+}$, and then to $CD49d^{-}Band3^{+}$, in line of previous studies using primary $CD34^{+}$ cells or hiPSCs under the FA condition [189, 232]. After 6 days in TM culture, more than 95% of the cells were $CD45^{-}CD235a^{+}Band3^{+}CD71^{+}$. Only a few cells (0.5%-1.5%) expressed markers of myeloid lineages such as CD14, CD41, CD42a, CD15 and CD33 (Figure 5-8, B) and no cells express lymphoid markers (data not shown). These data collected a highly pure population of erythrocytes as early as day 6 of TM. Enucleation (removal of nuclei) rate was measured by staining DNA with DRAQ5, followed by flow cytometry (Figure 5-7, E). Erythrocytes from SF-TS-TR showed 2.8%-11.1% of enucleation rates from multiple experiments, similar to the same batch of FA control group and the range of variation. The enucleated cells remained metabolically active and with intact cell membrane (Figure 5-7, F) and expressed hemoglobin protein (Figure 5-7, G).

Figure 5-7. Flow cytometry analysis of ED-TM cells from scalable EB differentiation

(A) Representative flow cytometry dot plots of forward scatter (FSC) and side scatter (SSC) of cells during ED-TM from SF-TS-TR condition. Red circles indicate the mixture of pyrenocytes and cell debris. (B) Representative flow cytometry dot plots of additional markers for different types of hematopoietic cells. All gates were set based on corresponding isotype controls.

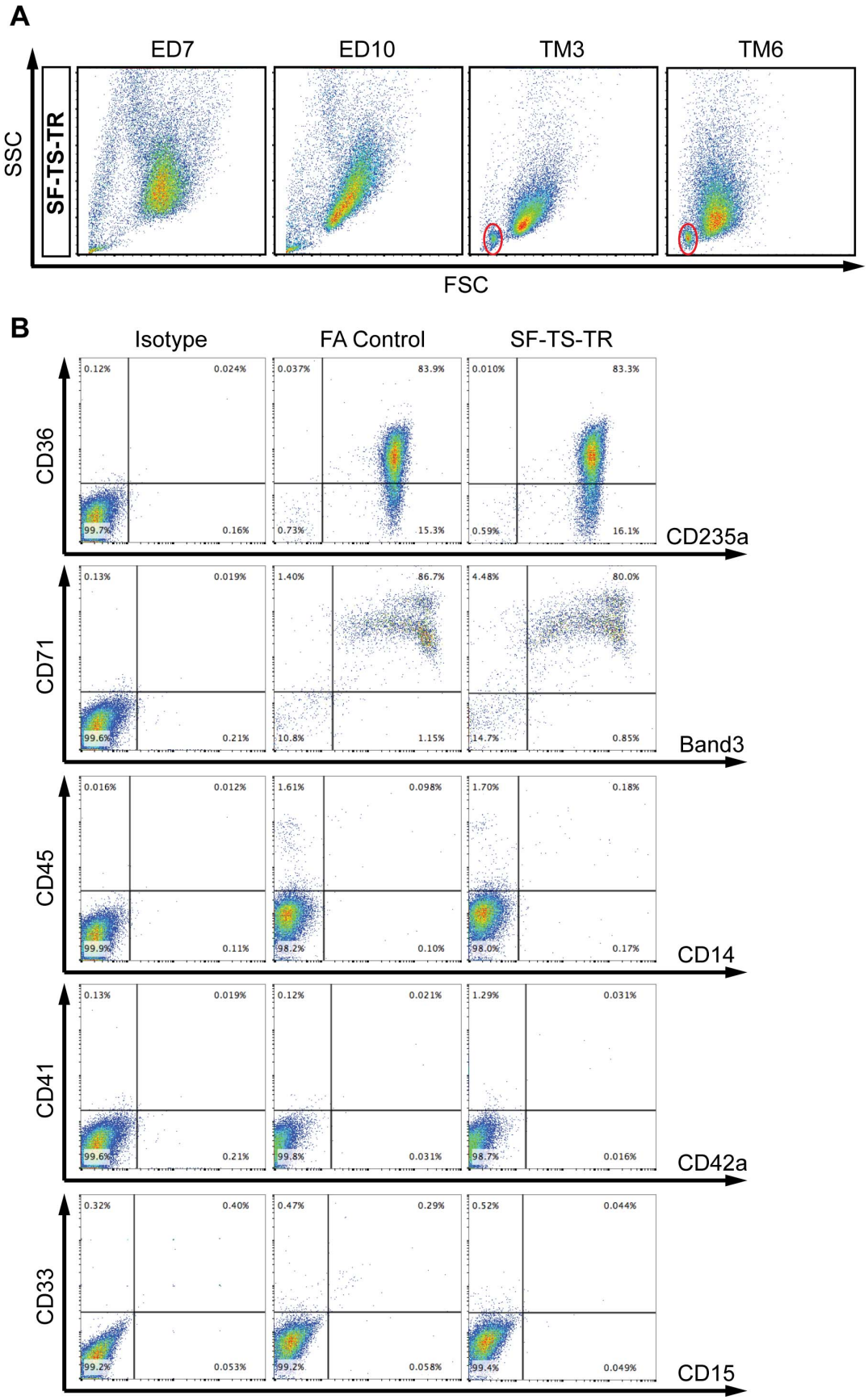
A
ED7
ED10
TM3
TM6
SSC
SF-TS-TR
FSC
B
Isotype
FA Control
SF-TS-TR
CD36
CD235a
0.12%
0.024%
99.7%
0.16%
0.037%
83.9%
0.73%
15.3%
0.010%
83.3%
0.59%
16.1%
CD71
Band3
0.13%
0.019%
99.6%
0.21%
1.40%
86.7%
10.8%
1.15%
4.48%
80.0%
14.7%
0.85%
CD45
CD14
0.016%
0.012%
99.9%
0.11%
1.61%
0.098%
98.2%
0.10%
1.70%
0.18%
98.0%
0.17%
CD41
CD42a
0.13%
0.019%
99.6%
0.21%
0.12%
0.021%
99.8%
0.031%
1.29%
0.031%
98.7%
0.016%
CD33
CD15
0.32%
0.40%
99.2%
0.053%
0.47%
0.29%
99.2%
0.058%
0.52%
0.044%
99.4%
0.049%

5.3.5 **Robust and reproducible generation of erythrocytes from hiPSC lines**

In order to test the robustness and reproducibility of the scalable differentiation system, we repeated the process in two other hiPSC lines (TNC1 and E2) using the same SF-TS-TR protocol. TNC1 was derived from human erythroblasts that were established from the peripheral blood mononuclear cells of a sickle cell disease patient, while E2 was derived from human mesenchymal stem cells that were established from the bone marrow mononuclear cells of a healthy donor. Both lines accomplished efficient and high-yield generation of HSPCs, erythroblasts and erythrocytes (Table 5-2 and Figure 5-9), confirming the robustness and adaptability of the scalable differentiation system.

Table 5-2. Summary of the yield in three hiPSC lines at the end of each differentiation steps from the scalable system

hiPSC Lines	**Yield ($\times 10^6$) from 40-ml of EB differentiation using SF-TS-TR (n = 3)**			
	EB13	**ED10**	**TM6**	
	$CD34^+CD45^+$	**$CD36^+CD235a^+$**	**$CD235a^+$**	**Enucleated**
BC1	17 ± 5	843 ± 366	3947 ± 418	385 ± 206
E2	12 ± 4	653 ± 82	3928 ± 1017	206 ± 161
TNC1	17 ± 4	1096 ± 331	5942 ± 2002	564 ± 192

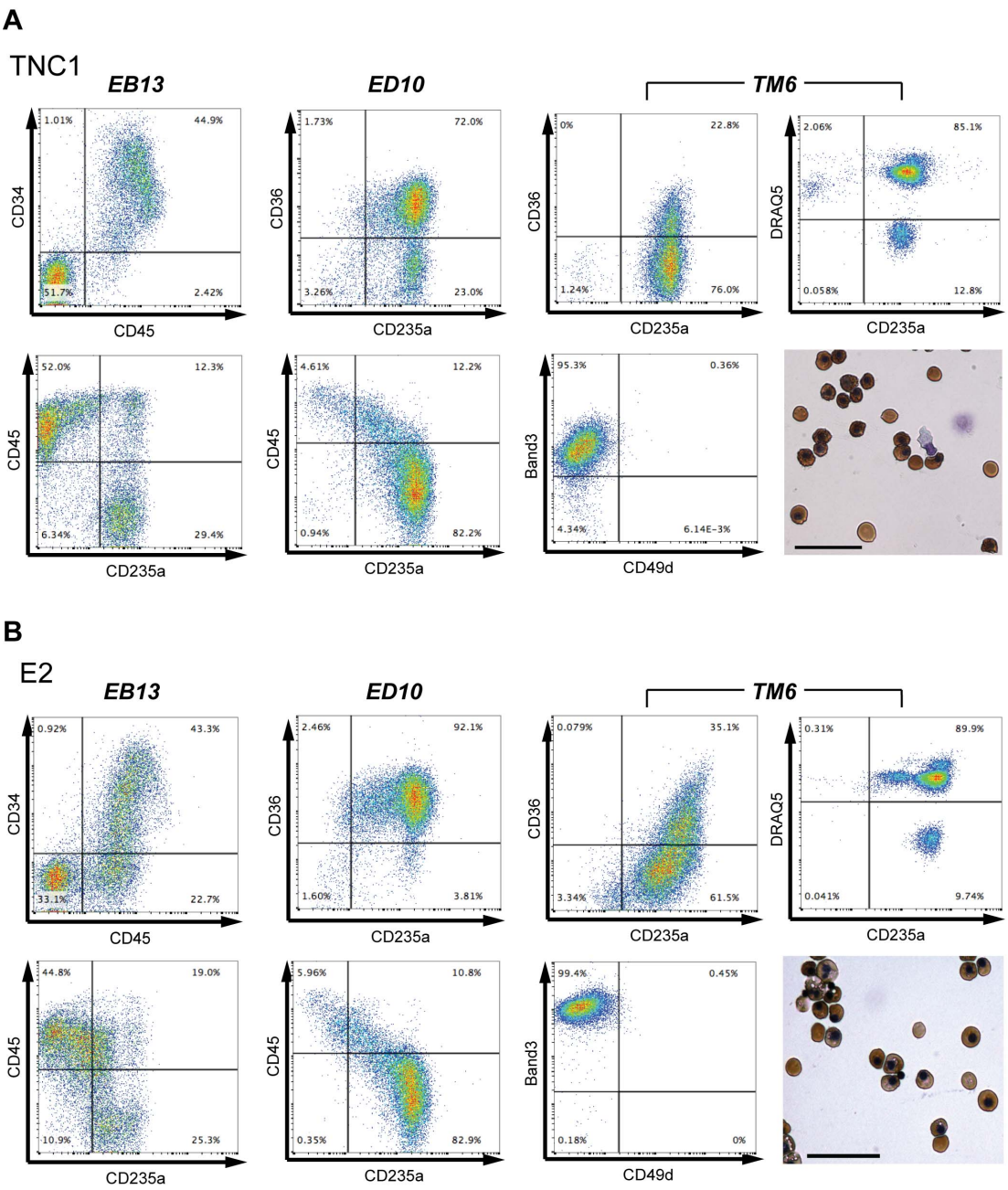

Figure 5-8. Flow cytometry analysis on TNC1 and E2 iPSC-derived HSPCs, erythroblasts and erythrocytes using the scalable strategy

Representative flow cytometry dot plots of the expression of critical markers on EB day 13, ED day 10 and TM day 6 of the differentiation of TNC1 iPSCs. An image of cytospin slide of TM6 cells stained with Benzidine and Giemsa also indicates efficient enucleation and saturation of hemoglobin in the matured erythrocytes. All gates were set by corresponding isotype controls.

5.3.6 **Hemoglobin expression and oxygen carrying function of the erythrocytes generated from the scalable system**

We analyzed the expression of hemoglobin genes particularly β-globin gene at both mRNA and protein levels. The mRNA level increased dramatically along the differentiation. On TM day 7, cells from SF-TS-TR showed similar mRNA level of *HBB* and *HBG* as erythrocytes derived from cord blood $CD34^+$ cells that were induced ED-TM in the same medium and scalable settings (Figure 5-10, A). We further found that ~64% of TM day 7 cells from SF-TS-TR contained β-globin, while nearly 100% of the cells expressed γ-globin (Figure 5-10, B). These cells produced β-globin in the similar level as those from FA (Figure 5-10, B-C).

We also determined whether the hemoglobin in the cells was functional to bind to O_2 molecules at high concentration and release them at low concentration. Oxygen-hemoglobin dissociation curve of BC1-derived erythrocytes in scalable settings were measured and found to be similar to the curve of primary cord blood RBCs (Figure 5-10, D). Interestingly, TM day 6 cells from SF-TS-TR method (P_{50} = 19.2 mmHg) showed lower O_2 binding affinity than those from FA method (P_{50} = 16.1 mmHg), and were closer to cord blood (P_{50} = 24.0 mmHg). It is known that fetal hemoglobin has a higher affinity to bind to O_2 and cord blood express both fetal and adult hemoglobin. This result is consistent with the data that the content of fetal hemoglobin in the erythrocytes from SF-TS-TR was lower than erythrocytes from FA method, but still higher than in cord blood.

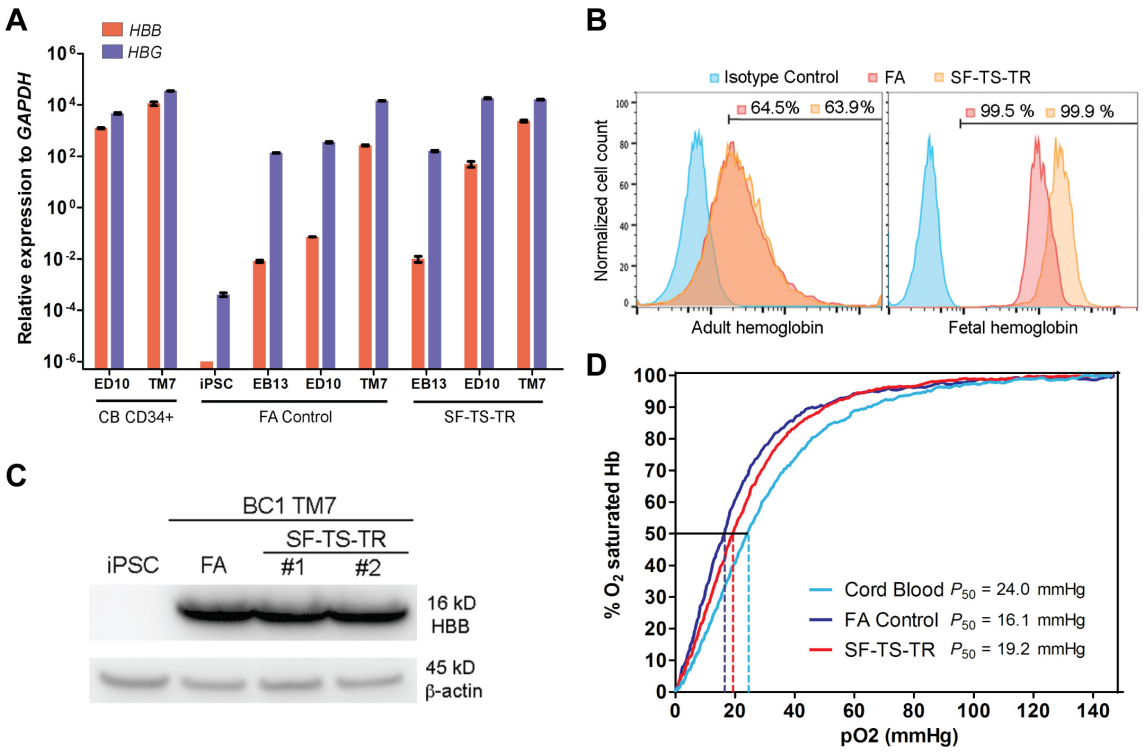

Figure 5-9. Hemoglobin expression and oxygen binding function of hiPSC-derived erythrocytes from scalable production

(A) Quantitative RT-PCR analysis of *HBB* and *HBG* gene expression in the cells generated from unscalable (FA EB to static ED-TM, marked as FA Control) and scalable strategy (SF-TS-TR EB to dynamic ED-TM, marked as SF-TS-TR) at different stages, including undifferentiated iPSCs, total suspension cells after EB differentiation day 13 (EB13), erythroid differentiation day 10 (ED10) and terminal maturation day 7 (TM7). Erythrocytes derived from cord blood $CD34^+$ cells (CB $CD34^+$) following the same ED-TM conditions were analyzed together as a control (normalized to endogenous GAPDH as a housekeeping control; n = 2 independent experiments with 3 technical replicates each, mean ± SD). (B) Representative flow cytometry plots of intracellular adult and fetal hemoglobin protein in TM7 cells. (C) Western blot analysis of human adult β−globin (HBB) protein. BC1 iPSCs and TM7 cells from FA EB and two independent runs of SF-TS-TR EB were loaded as 10 μg total protein. β-actin was stained as a housekeeping control. (D) Oxygen-hemoglobin dissociation curves of TM7 cells from scalable method (SF-TS-TR), FA control, and primary cord blood red blood cells measured by a Hemox Analyzer.

5.4 *Discussion*

Along with the flourish of transformative hiPSC technologies, cell culture conditions for scalable expansion of undifferentiated hiPSCs have been improved significantly [112, 113, 115, 122]. Chemically defined, feeder- and xeno-free culture media and substrates are able to support long-term and scalable expansion of hiPSCs while keeping a normal karyotype as we have demonstrated [233]. These improvements suggest a bypass to the elusive goal of *ex vivo* expansion of human HSPCs, especially long-term stem cell activities, which remains challenging even with primary $CD34^{+}CD45^{+}$ cells [145]. Therefore, one can expand undifferentiated hiPSCs first into a large number, followed by a large-scale and high-efficiency differentiation process of HSPC production, to achieve a high yield of a final blood cell product such as erythrocytes. During this multi-step differentiation process, the generation of HSPCs from hiPSCs that are able to generate multiple types of mature hematopoietic cells is the rate-limiting step [193]. In the current study, we demonstrated the first complete procedure for scalable production of erythrocytes from hiPSCs under a feeder-free and xeno-free culture condition, with the innovation of EB differentiation integrating spinner flask and rocker.

The current success was based on our previous study where we demonstrated that hiPSCs can form cell spheres of an average equivalent diameter of ~200 μm in spinner flask culture under an optimized speed in E8 medium [213]. Each sphere contains approximately 3,000 cells, which correspond to the optimized number of input hiPSCs to form one EB per well in the FA EB formation method. For the EB formation in suspension in differentiation medium, we found that cell viability on day 1 was a critical

checkpoint for differentiation efficiency, because apoptotic or dead cells wrapped inside the EBs would lead to break or failure of EB formation. Single cells of hiPSCs seeded on day 0 were most vulnerable to shear-induced cell death, whereas insufficient shear would also cause agglomeration and lead to transfer deficiency of O_2, nutrients and metabolic wastes. Therefore, we sought to find a balance by choosing the appropriate platform and optimizing the agitating speed and culture medium formulation for EB formation in the critical first two days. We also found that different hiPSC lines had distinct sensitivity and tolerance to shear stress in spinner flasks, indicated by cell survival and EB sizes. Some hiPSC lines such as BC1 and E2 survived poorly in spinner culture with the SFM-EB medium, even in slow agitation. In contrast, we reported here that a new EB formation medium based on the original E8 medium significantly enhanced the cell survival. Moreover, we observed that physiological O_2 tension (5%) that was known to enhance hiPSC survival also enhanced EB formation and differentiation, using an oxygen monitoring and controlling system (Figure 5-11). It was reported that the dissolved O_2 level in the media affected the rate and maturation of erythroblasts *in vitro* [234]. This oxygen monitoring and controlling system would also provide a suitable apparatus for further optimization of erythrocyte terminal differentiation by tuning O_2 tension in the culture.

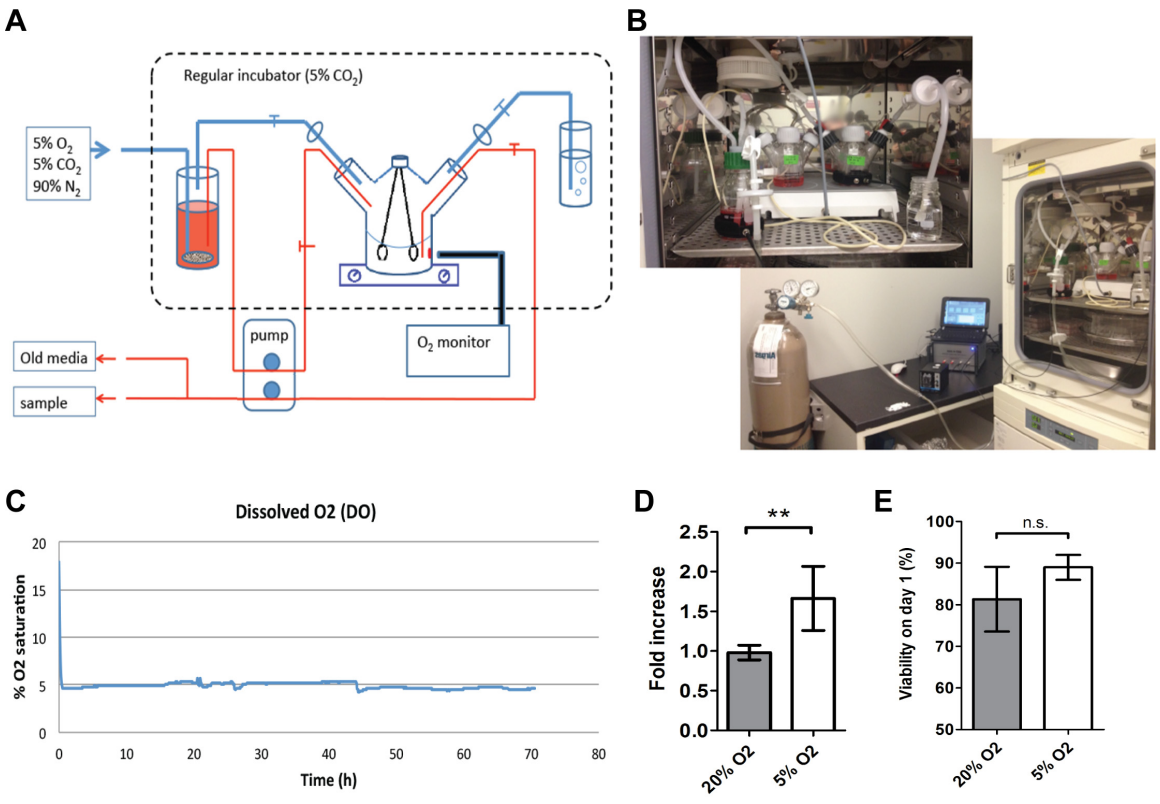

Figure 5-10. Design of an oxygen monitoring and controlling system for glass-ball type spinner flasks

(A) Schematic illustration of the design. Red lines indicate liquid channels, while blue lines indicate air flow path. (B) Pictures of system settings inside and outside the incubator. (C) Prolonged control of dissolved O_2 in the medium real-time monitored by non-invasive probe. (D) Cell density increase on day 3 of iPSC culture in E8 medium as cell aggregates in 5% O_2 compared to 20% O_2 (n = 3, mean ± SD). (E) Cell viability of BC1 cells on EB day 1 in SFM-EB differentiation medium (SFM+BMP4+bFGF) (n = 3, mean ± SD).

Shear stress induced by agitation is also known to play an important role in iPSC differentiation [235, 236]. The glass-ball type spinner flask produces laminar flow (*Re* < 1000) and mild shear rate less than 0.15 N/m^2 [213], while tissue culture flasks on a rocker mimics a wave-type bag bioreactor that generates much lower shear of

approximately 0.01 N/m^2 measured in previous studies [237]. A static condition causes no shear on EBs. Compared to the freely floating EBs in a continuous suspension condition, the stepwise SF-TS-TR procedure showed higher differentiation efficiency and reproducibility. The enhancement may be due to the static condition and the loose attachment of EBs to the surface of cell culture vessels. This semi-adhesion might provide better environment for the generation of hemogenic endothelial cells and strengthened the up-regulation of many critical genes related to mesodermal and hematopoietic development such as *KDR*, *GATA2*, *RUNX1*, *HHEX* and *MYB* [228]. The mild agitation on a rocker in the following step might be beneficial for the hematopoietic differentiation by enhancing transport and preventing complete attachment leading to loss of EB structures. The CD34$^+$CD45$^+$ cells generated from the SF-TS-TR procedure appear to be definitive hematopoietic progenitor cells because they can form multiple types of myeloid cells and erythrocytes that express HBB and mature to enucleated cells. The suspension cells harvested at EB day 13 enriched for CD34$^+$CD45$^+$ cells contained few CD235a$^+$ cells before EB day 13, the early onset of which was suggested to be an indicator of primitive hematopoiesis independent of CD34$^+$CD45$^+$ HSPC formation (Kennedy et al., 2012).

The SF-TS-TR method requires 8.3-fold more input of hiPSCs per run than the FA method to initiate EB differentiation in current settings, which causes about 3-fold decrease in the efficiency of CD235a$^+$ erythrocyte generation per input hiPSC on TM6. However, the batch yield is still about 2-fold higher. More importantly, the scalability of the SF-TS-TR system enables a volumetric scale-up process, which is more preferable in the manufacture concept other than the linear scale-out process of using the FA method.

By one batch of hiPSC differentiation, we generated 4.1×10^9 $CD235a^+$ erythrocytes using 1-liter spinner flasks at a density of approximately 4×10^6 cells/ml. Therefore, it is possible to produce sufficient erythrocytes for a clinical unit of blood (containing 2×10^{12} RBCs) from one batch of 500-liter stirred tank bioreactor or WAVE bag bioreactor. Although reducing the cost remains a challenge of *ex vivo* generation of transfusable RBCs from hiPSCs [151], the concept and improvement demonstrated in our study is an important step forward leading to a feasible solution of reducing manufacturing cost by expanding production scale.

The HSPCs generated from this scalable system were confirmed to exhibit comparable phenotype and potential for multi-lineage differentiation as the HSPCs from the FA method that were extensively evaluated in the previous studies [189]. Despite the substantially increased contents of functional hemoglobin, the enucleation rate (2%-15%) we achieved so far was still low as compared to those derived from primary $CD34^+CD45^+$ cells (≥30%), and varied between hiPSC lines and from batch-to-batch to certain degrees.

5.5 *Conclusion*

In summary, we generated erythrocytes from three hiPSC lines in a scalable differentiation system that combined spinner flask and rocker for EB differentiation, erythroid differentiation and terminal maturation. We achieved high batch yield, β-globin expression and complete terminal maturation in the hiPSC-derived erythrocytes in a scalable setting. This work provides a feasible solution for large-scale production of human RBCs from hiPSCs.

6 *Conclusion and Suggestions for future study*

6.1 *Conclusion*

Large-scale *ex vivo* generation of matured RBCs for transfusion purpose from hiPSCs holds great promise to fulfill the unmet global demand of blood transfusion. In this thesis we improved the current technologies for the expansion and hematopoietic differentiation towards erythrocytes from hiPSCs, and established scalable systems using spinner flask and rocker platform with the consideration of clinical compliance and large-scale manufacturing.

In Chapter 3, we described the establishment of a reproducible approach for rapid, economic, and scalable expansion of hiPSCs in xeno-free condition using spinner flask to meet the demand of practical research and clinical applications. The hiPSCs were maintained in dynamic suspension culture as cell aggregates for more than 20 passages with a consistent expansion rate, well-preserved pluripotency and normal karyotype. In Chapter 4, we described the development of an efficient and reproducible differentiation system to generate HSPCs from hiPSCs under a feeder-free and xeno-free condition in which all the animal-derived products were eliminated. We further generated hiPSC-derived HSPCs and erythrocytes, showing enucleation and adult-hemoglobin expression in gene-corrected iPSCs from SCD patients. In Chapter 5, we demonstrated an improved scalability of the differentiation system by applying the combination of spinner flask and rocker platform and achieved high batch yield, β-globin expression and complete

terminal maturation in the hiPSC-derived erythrocytes. Our work sheds light on the critical effects of physical conditions during *in vitro* hematopoiesis of hiPSCs. The ease of operation, the simplicity of cytokine combination and the high level of chemical definition of the components added favorable features to this system in a scale-up point of view. Furthermore, because all the components used in our system for the entire expansion and differentiation process are formulated with recombinant human proteins, FDA-approved biologics, or materials from human sources, this xeno-free and cGMP-compliant system provides the opportunity to produce clinical-grade erythrocytes from hiPSCs in a large-scale bioprocess. Therefore, this study is a significant step towards the goal of large-scale generation of RBCs for therapeutic purposes.

6.2 *Suggestions for future study*

The methods for expanding hPSCs have improved significantly in recent years, facilitating robust and scalable clinical-grade hPSC production. Current knowledge of synthetic surfaces and suspension culture systems will likely continue to progress. More ready-to-use, chemically defined and xeno-free culture systems for culturing hPSCs using cGMP will follow the development of a deeper understanding of the chemical and biological mechanisms related to hPSC self-renewal. More studies of adhesion culture systems should focus on the optimization of different combinations of synthetic surfaces and xeno-free serum-free media with only small molecule cocktails to get preferable culture systems that can widely used to support for the expansion of a broad range of hPSC lines. These culture systems should also be tested for their capability of supporting the derivation of new hPSC lines. Expansion systems specifically tailored for culturing

hPSCs at full production scales — for example, tens or hundreds of liters — will benefit from better understanding questions at scales ranging from millimeters (microcarrier engineering) to tens of meters (large bioreactor design). For MC-based culture systems, a synergetic development of synthetic surface technologies and microcarrier design (i.e. size, shape, porosity, etc.) may result in favorable microcarriers for hPSC expansion. Systematic optimization of seeding and feeding strategies could also help to overcome the hurdles of bad attachment and undesired agglomeration in large-scale bioreactors. For aggregate-based suspension culture, optimization of media composition, operation protocol, and bioreactor structure should be given the highest priority to ensure good formation and maintenance of the cell aggregates during a scale-up process. All developed systems should be tested for their capability to sustain high pluripotency, and the phenotypic, genetic, and epigenetic stability of multiple hPSC lines. More importantly, successful development of high-efficient differentiation protocols to desired cell types is really the rate-determining step. Differentiation with high efficiency in feeder-free and defined conditions should be an ultimate goal for the study on hPSC fate commitment. Using one or multiple hPSC-derived cell types to generate functional engineered tissue will take another leap to reach a whole new level of cell therapies. We can expect that, combined with other advances in derivation and differentiation technologies, more clinical trials using hPSCs and their progenies will be approved in the near future, working to reach the next generation of stem cell therapies.

The other aspect that needs to be further improved is the low enucleation rate. Although some studies suggested that the erythroblasts generated *in vitro* could eventually enucleate in circulation when being injected *in vivo* [238], it would be ideal to

reach full enucleation and eliminate all nucleated cells before being transfused into recipients. More efforts are needed to further improve the enucleation of hiPSC-derived erythrocytes. Recent reports on transcription profile of enucleating erythroblasts derived from cord blood $CD34^+$ cells [232] and hESCs [239] provide an insight in the molecular signature of the enucleation process and may lead us to find more efficacious solutions to improve enucleation in suspension culture conditions.

Furthermore, the scalability of the current differentiation system is still not ideal, largely due to the inclusion of a static culture step. Although completely suspension conditions were reported successful for the differentiation of other cell types, such as cardiomyocytes and neural progenitor cells [152, 154-156], the production of mesodermal lineages seems encountered more challenges. More work needs to be done for a better understanding of the hematopoiesis niche and the interaction between hematopoietic progenitor cells and surrounding stromal cells *in vivo* [240]. Other studies focusing on the development of novel bioactive materials and scaffolds [241-243] may also shed light on the construction of appropriate micro-environment that supports better HSPC and erythrocyte generation.

Finally, better animal models for the study of stem cell-based transfusion therapies needs to be established before more comprehensive clinical studies in human. We have been using the NSG mice to conduct *in vivo* studies. However, others and we encountered technical hurdles that remain challenging to all the investigators in the field. Current mouse models are not optimal at all to test *in vivo* functions of mature human RBCs in the circulation. Typically, a very low percentage (<1%) of circulating RBCs are human enucleated erythrocytes in mice even after transfusion with 2×10^9 human mature

RBCs in the previous studies [238]. It is widely believed that the mouse Mononuclear Phagocyte System (also called Reticuloendothelial System or Macrophage System) recognizes human RBCs as xenoantigens and destroys human RBCs, even in the NSG mice lacking functional T, B and NK cells [244]. Various approaches are in development to better demonstrate the presence and circulation of human mature RBCs in mouse models. More tests should be done focusing on the nucleated and enucleated erythrocytes (that we now can make in large quantity) in improved mouse models with various conditioning treatments, such as reducing macrophage activities by using clodronate liposome mediated macrophage-depletion.

Bibliography

1. Thomson JA, Itskovitz-Eldor J, Shapiro SS et al. Embryonic stem cell lines derived from human blastocysts. **Science**. 1998;282:1145-1147.
2. Vogel G, Holden C. Stem cells. Ethics questions add to concerns about NIH lines. **Science**. 2008;321:756-757.
3. Wilmut I, Schnieke AE, McWhir J et al. Viable offspring derived from fetal and adult mammalian cells. **Nature**. 1997;385:810-813.
4. Noggle S, Fung HL, Gore A et al. Human oocytes reprogram somatic cells to a pluripotent state. **Nature**. 2011;478:70-75.
5. Tachibana M, Amato P, Sparman M et al. Human embryonic stem cells derived by somatic cell nuclear transfer. **Cell**. 2013;153:1228-1238.
6. Takahashi K, Yamanaka S. Induction of pluripotent stem cells from mouse embryonic and adult fibroblast cultures by defined factors. **Cell**. 2006;126:663-676.
7. Takahashi K, Tanabe K, Ohnuki M et al. Induction of pluripotent stem cells from adult human fibroblasts by defined factors. **Cell**. 2007;131:861-872.
8. Yu J, Vodyanik MA, Smuga-Otto K et al. Induced pluripotent stem cell lines derived from human somatic cells. **Science**. 2007;318:1917-1920.
9. Robinton DA, Daley GQ. The promise of induced pluripotent stem cells in research and therapy. **Nature**. 2012;481:295-305.
10. Loh YH, Agarwal S, Park IH et al. Generation of induced pluripotent stem cells from human blood. **Blood**. 2009;113:5476-5479.
11. Chou BK, Mali P, Huang X et al. Efficient human iPS cell derivation by a non-integrating plasmid from blood cells with unique epigenetic and gene expression signatures. **Cell Res**. 2011;21:518-529.
12. Dowey SN, Huang XS, Chou BK et al. Generation of integration-free human induced pluripotent stem cells from postnatal blood mononuclear cells by plasmid vector expression. **Nature Protocols**. 2012;7:2013-2021.
13. Ye Z, Zhan H, Mali P et al. Human-induced pluripotent stem cells from blood cells of healthy donors and patients with acquired blood disorders. **Blood**. 2009;114:5473-5480.
14. Yamanaka S. Induced pluripotent stem cells: past, present, and future. **Cell Stem Cell**. 2012;10:678-684.
15. Drews K, Jozefczuk J, Prigione A et al. Human induced pluripotent stem cells--from mechanisms to clinical applications. **J Mol Med (Berl)**. 2012;90:735-745.
16. Bar-Nur O, Russ HA, Efrat S et al. Epigenetic memory and preferential lineage-specific differentiation in induced pluripotent stem cells derived from human pancreatic islet beta cells. **Cell Stem Cell**. 2011;9:17-23.
17. Takebe T, Sekine K, Enomura M et al. Vascularized and functional human liver from an iPSC-derived organ bud transplant. **Nature**. 2013;499:481-484.

18. Diekman BO, Christoforou N, Willard VP et al. Cartilage tissue engineering using differentiated and purified induced pluripotent stem cells. **Proc Natl Acad Sci U S A**. 2012;109:19172-19177.
19. Dimos JT, Rodolfa KT, Niakan KK et al. Induced pluripotent stem cells generated from patients with ALS can be differentiated into motor neurons. **Science**. 2008;321:1218-1221.
20. Kusuma S, Shen YI, Hanjaya-Putra D et al. Self-organized vascular networks from human pluripotent stem cells in a synthetic matrix. **Proc Natl Acad Sci U S A**. 2013;110:12601-12606.
21. Samuel R, Daheron L, Liao S et al. Generation of functionally competent and durable engineered blood vessels from human induced pluripotent stem cells. **Proc Natl Acad Sci U S A**. 2013;110:12774-12779.
22. Zhang J, Wilson GF, Soerens AG et al. Functional cardiomyocytes derived from human induced pluripotent stem cells. **Circ Res**. 2009;104:e30-41.
23. Phillips MJ, Wallace KA, Dickerson SJ et al. Blood-derived human iPS cells generate optic vesicle-like structures with the capacity to form retinal laminae and develop synapses. **Invest Ophthalmol Vis Sci**. 2012;53:2007-2019.
24. Keirstead HS, Nistor G, Bernal G et al. Human embryonic stem cell-derived oligodendrocyte progenitor cell transplants remyelinate and restore locomotion after spinal cord injury. **J Neurosci**. 2005;25:4694-4705.
25. Chen AK, Reuveny S, Oh SK. Application of human mesenchymal and pluripotent stem cell microcarrier cultures in cellular therapy: Achievements and future direction. **Biotechnol Adv**. 2013.
26. da Cruz L, Chen FK, Ahmado A et al. RPE transplantation and its role in retinal disease. **Prog Retin Eye Res**. 2007;26:598-635.
27. Schwartz SD, Hubschman JP, Heilwell G et al. Embryonic stem cell trials for macular degeneration: a preliminary report. **Lancet**. 2012;379:713-720.
28. Dionigi B, Fauza DO. Autologous Approaches to Tissue Engineering. StemBook. Cambridge (MA); 2008.
29. Lee MH, Arcidiacono JA, Bilek AM et al. Considerations for tissue-engineered and regenerative medicine product development prior to clinical trials in the United States. **Tissue Eng Part B Rev**. 2010;16:41-54.
30. Garber K. Inducing translation. **Nat Biotechnol**. 2013;31:483-486.
31. Engle SJ, Puppala D. Integrating human pluripotent stem cells into drug development. **Cell Stem Cell**. 2013;12:669-677.
32. Trounson A, Shepard KA, DeWitt ND. Human disease modeling with induced pluripotent stem cells. **Curr Opin Genet Dev**. 2012;22:509-516.
33. Pomp O, Colman A. Disease modelling using induced pluripotent stem cells: status and prospects. **Bioessays**. 2013;35:271-280.
34. Mercola M, Colas A, Willems E. Induced pluripotent stem cells in cardiovascular drug discovery. **Circ Res**. 2013;112:534-548.
35. Mali P, Cheng L. Concise review: Human cell engineering: cellular reprogramming and genome editing. **Stem Cells**. 2012;30:75-81.
36. Ye Z, Chou BK, Cheng L. Promise and challenges of human iPSC-based hematologic disease modeling and treatment. **Int J Hematol**. 2012;95:601-609.

37. Zou J, Mali P, Huang X et al. Site-specific gene correction of a point mutation in human iPS cells derived from an adult patient with sickle cell disease. **Blood**. 2011;118:4599-4608.
38. Hockemeyer D, Wang H, Kiani S et al. Genetic engineering of human pluripotent cells using TALE nucleases. **Nat Biotechnol**. 2011;29:731-734.
39. Mali P, Yang LH, Esvelt KM et al. RNA-Guided Human Genome Engineering via Cas9. **Science**. 2013;339:823-826.
40. Merkle FT, Eggan K. Modeling human disease with pluripotent stem cells: from genome association to function. **Cell Stem Cell**. 2013;12:656-668.
41. Hyun I, Lindvall O, Ahrlund-Richter L et al. New ISSCR guidelines underscore major principles for responsible translational stem cell research. **Cell Stem Cell**. 2008;3:607-609.
42. Stacey GN, Cobo F, Nieto A et al. The development of 'feeder' cells for the preparation of clinical grade hES cell lines: challenges and solutions. **J Biotechnol**. 2006;125:583-588.
43. Carlson Scholz JA, Garg R, Compton SR et al. Poliomyelitis in MuLV-infected ICR-SCID mice after injection of basement membrane matrix contaminated with lactate dehydrogenase-elevating virus. **Comp Med**. 2011;61:404-411.
44. Valamehr B, Tsutsui H, Ho CM et al. Developing defined culture systems for human pluripotent stem cells. **Regen Med**. 2011;6:623-634.
45. Ausubel LJ, Lopez PM, Couture LA. GMP scale-up and banking of pluripotent stem cells for cellular therapy applications. **Methods Mol Biol**. 2011;767:147-159.
46. Seissler J, Schott M. Generation of insulin-producing beta cells from stem cells--perspectives for cell therapy in type 1 diabetes. **Horm Metab Res**. 2008;40:155-161.
47. Mehta J, Mehta J, Frankfurt O et al. Optimizing the CD34 + cell dose for reduced-intensity allogeneic hematopoietic stem cell transplantation. **Leuk Lymphoma**. 2009;50:1434-1441.
48. Jing D, Parikh A, Canty JM, Jr. et al. Stem cells for heart cell therapies. **Tissue Eng Part B Rev**. 2008;14:393-406.
49. Hagell P, Brundin P. Cell survival and clinical outcome following intrastriatal transplantation in Parkinson disease. **J Neuropathol Exp Neurol**. 2001;60:741-752.
50. Morizane A, Li JY, Brundin P. From bench to bed: the potential of stem cells for the treatment of Parkinson's disease. **Cell Tissue Res**. 2008;331:323-336.
51. Harb N, Archer TK, Sato N. The Rho-Rock-Myosin Signaling Axis Determines Cell-Cell Integrity of Self-Renewing Pluripotent Stem Cells. **Plos One**. 2008;3.
52. Chen T, Yuan D, Wei B et al. E-cadherin-mediated cell-cell contact is critical for induced pluripotent stem cell generation. **Stem Cells**. 2010;28:1315-1325.
53. Richards M, Fong CY, Chan WK et al. Human feeders support prolonged undifferentiated growth of human inner cell masses and embryonic stem cells. **Nature Biotechnology**. 2002;20:933-936.

54. Zou C, Chou BK, Dowey SN et al. Efficient derivation and genetic modifications of human pluripotent stem cells on engineered human feeder cell lines. **Stem Cells Dev**. 2012;21:2298-2311.
55. Hovatta O, Mikkola M, Gertow K et al. A culture system using human foreskin fibroblasts as feeder cells allows production of human embryonic stem cells. **Hum Reprod**. 2003;18:1404-1409.
56. Cheng L, Hammond H, Ye Z et al. Human adult marrow cells support prolonged expansion of human embryonic stem cells in culture. **Stem Cells**. 2003;21:131-142.
57. Stojkovic P, Lako M, Stewart R et al. An autogeneic feeder cell system that efficiently supports growth of undifferentiated human embryonic stem cells. **Stem Cells**. 2005;23:306-314.
58. Wang Q, Fang ZF, Jin F et al. Derivation and growing human embryonic stem cells on feeders derived from themselves. **Stem Cells**. 2005;23:1221-1227.
59. Xu C, Inokuma MS, Denham J et al. Feeder-free growth of undifferentiated human embryonic stem cells. **Nat Biotechnol**. 2001;19:971-974.
60. Kleinman HK, McGarvey ML, Hassell JR et al. Basement membrane complexes with biological activity. **Biochemistry**. 1986;25:312-318.
61. Kleinman HK, Martin GR. Matrigel: basement membrane matrix with biological activity. **Semin Cancer Biol**. 2005;15:378-386.
62. Ludwig TE, Levenstein ME, Jones JM et al. Derivation of human embryonic stem cells in defined conditions. **Nat Biotechnol**. 2006;24:185-187.
63. Beattie GM, Lopez AD, Bucay N et al. Activin A maintains pluripotency of human embryonic stem cells in the absence of feeder layers. **Stem Cells**. 2005;23:489-495.
64. Miyazaki T, Futaki S, Hasegawa K et al. Recombinant human laminin isoforms can support the undifferentiated growth of human embryonic stem cells. **Biochem Biophys Res Commun**. 2008;375:27-32.
65. Miyazaki T, Futaki S, Suemori H et al. Laminin E8 fragments support efficient adhesion and expansion of dissociated human pluripotent stem cells. **Nat Commun**. 2012;3:1236.
66. Rodin S, Domogatskaya A, Strom S et al. Long-term self-renewal of human pluripotent stem cells on human recombinant laminin-511. **Nat Biotechnol**. 2010;28:611-615.
67. Higgins JM, Mandlebrot DA, Shaw SK et al. Direct and regulated interaction of integrin alphaEbeta7 with E-cadherin. **J Cell Biol**. 1998;140:197-210.
68. Whittard JD, Craig SE, Mould AP et al. E-cadherin is a ligand for integrin alpha2beta1. **Matrix Biol**. 2002;21:525-532.
69. Nagaoka M, Si-Tayeb K, Akaike T et al. Culture of human pluripotent stem cells using completely defined conditions on a recombinant E-cadherin substratum. **BMC Dev Biol**. 2010;10:60.
70. Danen EH, Sonneveld P, Brakebusch C et al. The fibronectin-binding integrins alpha5beta1 and alphavbeta3 differentially modulate RhoA-GTP loading, organization of cell matrix adhesions, and fibronectin fibrillogenesis. **J Cell Biol**. 2002;159:1071-1086.

71. Amit M, Shariki C, Margulets V et al. Feeder layer- and serum-free culture of human embryonic stem cells. **Biol Reprod**. 2004;70:837-845.
72. Braam SR, Zeinstra L, Litjens S et al. Recombinant vitronectin is a functionally defined substrate that supports human embryonic stem cell self-renewal via alphavbeta5 integrin. **Stem Cells**. 2008;26:2257-2265.
73. Chen GK, Gulbranson DR, Hou ZG et al. Chemically defined conditions for human iPSC derivation and culture. **Nature Methods**. 2011;8:424-U476.
74. Melkoumian Z, Weber JL, Weber DM et al. Synthetic peptide-acrylate surfaces for long-term self-renewal and cardiomyocyte differentiation of human embryonic stem cells. **Nat Biotechnol**. 2010;28:606-610.
75. Klim JR, Li L, Wrighton PJ et al. A defined glycosaminoglycan-binding substratum for human pluripotent stem cells. **Nat Methods**. 2010;7:989-994.
76. Derda R, Li L, Orner BP et al. Defined substrates for human embryonic stem cell growth identified from surface arrays. **ACS Chem Biol**. 2007;2:347-355.
77. Villa-Diaz LG, Nandivada H, Ding J et al. Synthetic polymer coatings for long-term growth of human embryonic stem cells. **Nat Biotechnol**. 2010;28:581-583.
78. Nandivada H, Villa-Diaz LG, O'Shea KS et al. Fabrication of synthetic polymer coatings and their use in feeder-free culture of human embryonic stem cells. **Nat Protoc**. 2011;6:1037-1043.
79. Villa-Diaz LG, Brown SE, Liu Y et al. Derivation of mesenchymal stem cells from human induced pluripotent stem cells cultured on synthetic substrates. **Stem Cells**. 2012;30:1174-1181.
80. Mei Y, Saha K, Bogatyrev SR et al. Combinatorial development of biomaterials for clonal growth of human pluripotent stem cells. **Nat Mater**. 2010;9:768-778.
81. Irwin EF, Gupta R, Dashti DC et al. Engineered polymer-media interfaces for the long-term self-renewal of human embryonic stem cells. **Biomaterials**. 2011;32:6912-6919.
82. Villa-Diaz LG, Ross AM, Lahann J et al. Concise review: The evolution of human pluripotent stem cell culture: from feeder cells to synthetic coatings. **Stem Cells**. 2013;31:1-7.
83. Saha K, Mei Y, Reisterer CM et al. Surface-engineered substrates for improved human pluripotent stem cell culture under fully defined conditions. **Proc Natl Acad Sci U S A**. 2011;108:18714-18719.
84. Ross AM, Nandivada H, Ryan AL et al. Synthetic substrates for long-term stem cell culture. **Polymer**. 2012;53:2533-2539.
85. Li Y, Powell S, Brunette E et al. Expansion of human embryonic stem cells in defined serum-free medium devoid of animal-derived products. **Biotechnol Bioeng**. 2005;91:688-698.
86. Liu Y, Song Z, Zhao Y et al. A novel chemical-defined medium with bFGF and N2B27 supplements supports undifferentiated growth in human embryonic stem cells. **Biochem Biophys Res Commun**. 2006;346:131-139.
87. Yao S, Chen S, Clark J et al. Long-term self-renewal and directed differentiation of human embryonic stem cells in chemically defined conditions. **Proc Natl Acad Sci U S A**. 2006;103:6907-6912.

88. Lu J, Hou R, Booth CJ et al. Defined culture conditions of human embryonic stem cells. **Proc Natl Acad Sci U S A**. 2006;103:5688-5693.
89. Wang L, Schulz TC, Sherrer ES et al. Self-renewal of human embryonic stem cells requires insulin-like growth factor-1 receptor and ERBB2 receptor signaling. **Blood**. 2007;110:4111-4119.
90. Furue MK, Na J, Jackson JP et al. Heparin promotes the growth of human embryonic stem cells in a defined serum-free medium. **Proc Natl Acad Sci U S A**. 2008;105:13409-13414.
91. Manton KJ, Richards S, Van Lonkhuyzen D et al. A chimeric vitronectin: IGF-I protein supports feeder-cell-free and serum-free culture of human embryonic stem cells. **Stem Cells Dev**. 2010;19:1297-1305.
92. Rajala K, Lindroos B, Hussein SM et al. A defined and xeno-free culture method enabling the establishment of clinical-grade human embryonic, induced pluripotent and adipose stem cells. **PLoS One**. 2010;5:e10246.
93. Tsutsui H, Valamehr B, Hindoyan A et al. An optimized small molecule inhibitor cocktail supports long-term maintenance of human embryonic stem cells. **Nat Commun**. 2011;2:167.
94. Oh SK. Human embryonic stem cells in serum-free media: growth and metabolism. In: Hayat MA, ed. Stem Cells and Cancer Stem Cells, Volume 3, 1 ed. Online: Springer Netherlands; 2012:103-112.
95. International Stem Cell Initiative C, Akopian V, Andrews PW et al. Comparison of defined culture systems for feeder cell free propagation of human embryonic stem cells. **In Vitro Cell Dev Biol Anim**. 2010;46:247-258.
96. Yoon TM, Chang B, Kim HT et al. Human embryonic stem cells (hESCs) cultured under distinctive feeder-free culture conditions display global gene expression patterns similar to hESCs from feeder-dependent culture conditions. **Stem Cell Rev**. 2010;6:425-437.
97. Merling RK, Sweeney CL, Choi U et al. Transgene-free iPSCs generated from small volume peripheral blood nonmobilized CD34+ cells. **Blood**. 2013;121:e98-107.
98. Nishishita N, Shikamura M, Takenaka C et al. Generation of virus-free induced pluripotent stem cell clones on a synthetic matrix via a single cell subcloning in the naive state. **PLoS One**. 2012;7:e38389.
99. Want AJ, Nienow AW, Hewitt CJ et al. Large-scale expansion and exploitation of pluripotent stem cells for regenerative medicine purposes: beyond the T flask. **Regen Med**. 2012;7:71-84.
100. Phillips BW, Horne R, Lay TS et al. Attachment and growth of human embryonic stem cells on microcarriers. **J Biotechnol**. 2008;138:24-32.
101. Fernandes AM, Marinho PA, Sartore RC et al. Successful scale-up of human embryonic stem cell production in a stirred microcarrier culture system. **Braz J Med Biol Res**. 2009;42:515-522.
102. Lock LT, Tzanakakis ES. Expansion and differentiation of human embryonic stem cells to endoderm progeny in a microcarrier stirred-suspension culture. **Tissue Eng Part A**. 2009;15:2051-2063.

103. Nie Y, Bergendahl V, Hei DJ et al. Scalable culture and cryopreservation of human embryonic stem cells on microcarriers. **Biotechnol Prog**. 2009;25:20-31.
104. Oh SK, Chen AK, Mok Y et al. Long-term microcarrier suspension cultures of human embryonic stem cells. **Stem Cell Res**. 2009;2:219-230.
105. Bardy J, Chen AK, Lim YM et al. Microcarrier suspension cultures for high-density expansion and differentiation of human pluripotent stem cells to neural progenitor cells. **Tissue Eng Part C Methods**. 2013;19:166-180.
106. Chen AK, Chen X, Choo AB et al. Critical microcarrier properties affecting the expansion of undifferentiated human embryonic stem cells. **Stem Cell Res**. 2011;7:97-111.
107. Marinho PA, Vareschini DT, Gomes IC et al. Xeno-free production of human embryonic stem cells in stirred microcarrier systems using a novel animal/human-component-free medium. **Tissue Eng Part C Methods**. 2013;19:146-155.
108. Serra M, Brito C, Costa EM et al. Integrating human stem cell expansion and neuronal differentiation in bioreactors. **BMC Biotechnol**. 2009;9:82.
109. Heng BC, Li J, Chen AK et al. Translating human embryonic stem cells from 2-dimensional to 3-dimensional cultures in a defined medium on laminin- and vitronectin-coated surfaces. **Stem Cells Dev**. 2012;21:1701-1715.
110. Krawetz R, Taiani JT, Liu S et al. Large-scale expansion of pluripotent human embryonic stem cells in stirred-suspension bioreactors. **Tissue Eng Part C Methods**. 2010;16:573-582.
111. Singh H, Mok P, Balakrishnan T et al. Up-scaling single cell-inoculated suspension culture of human embryonic stem cells. **Stem Cell Res**. 2010;4:165-179.
112. Zweigerdt R, Olmer R, Singh H et al. Scalable expansion of human pluripotent stem cells in suspension culture. **Nat Protoc**. 2011;6:689-700.
113. Amit M, Laevsky I, Miropolsky Y et al. Dynamic suspension culture for scalable expansion of undifferentiated human pluripotent stem cells. **Nat Protoc**. 2011;6:572-579.
114. Abbasalizadeh S, Larijani MR, Samadian A et al. Bioprocess development for mass production of size-controlled human pluripotent stem cell aggregates in stirred suspension bioreactor. **Tissue Eng Part C Methods**. 2012;18:831-851.
115. Olmer R, Lange A, Selzer S et al. Suspension culture of human pluripotent stem cells in controlled, stirred bioreactors. **Tissue Eng Part C Methods**. 2012;18:772-784.
116. Chen VC, Couture SM, Ye J et al. Scalable GMP compliant suspension culture system for human ES cells. **Stem Cell Res**. 2012;8:388-402.
117. Gerecht-Nir S, Cohen S, Itskovitz-Eldor J. Bioreactor cultivation enhances the efficiency of human embryoid body (hEB) formation and differentiation. **Biotechnol Bioeng**. 2004;86:493-502.
118. Cameron CM, Hu WS, Kaufman DS. Improved development of human embryonic stem cell-derived embryoid bodies by stirred vessel cultivation. **Biotechnol Bioeng**. 2006;94:938-948.

119. Yirme G, Amit M, Laevsky I et al. Establishing a dynamic process for the formation, propagation, and differentiation of human embryoid bodies. **Stem Cells Dev**. 2008;17:1227-1241.
120. Niebruegge S, Bauwens CL, Peerani R et al. Generation of human embryonic stem cell-derived mesoderm and cardiac cells using size-specified aggregates in an oxygen-controlled bioreactor. **Biotechnol Bioeng**. 2009;102:493-507.
121. Serra M, Leite SB, Brito C et al. Novel culture strategy for human stem cell proliferation and neuronal differentiation. **J Neurosci Res**. 2007;85:3557-3566.
122. Kehoe DE, Jing D, Lock LT et al. Scalable stirred-suspension bioreactor culture of human pluripotent stem cells. **Tissue Eng Part A**. 2010;16:405-421.
123. Watanabe K, Ueno M, Kamiya D et al. A ROCK inhibitor permits survival of dissociated human embryonic stem cells. **Nat Biotechnol**. 2007;25:681-686.
124. Olmer R, Haase A, Merkert S et al. Long term expansion of undifferentiated human iPS and ES cells in suspension culture using a defined medium. **Stem Cell Res**. 2010;5:51-64.
125. Steiner D, Khaner H, Cohen M et al. Derivation, propagation and controlled differentiation of human embryonic stem cells in suspension. **Nat Biotechnol**. 2010;28:361-364.
126. Adamo L, Naveiras O, Wenzel PL et al. Biomechanical forces promote embryonic haematopoiesis. **Nature**. 2009;459:1131-1135.
127. Ahsan T, Nerem RM. Fluid shear stress promotes an endothelial-like phenotype during the early differentiation of embryonic stem cells. **Tissue Eng Part A**. 2010;16:3547-3553.
128. Davies NL, Brindley DA, Culme-Seymour EJ et al. Streamlining cell therapy manufacture - from clinical to commercial scale. **BioProcess Int**. 2012;10:24-29.
129. Rowley J, Arbraham E, Campbell A et al. Meeting lot-size challenges of manufacturing adherent cells for therapy. **BioProcess Int**. 2012;10:16-22.
130. Terstegge S, Laufenberg I, Pochert J et al. Automated maintenance of embryonic stem cell cultures. **Biotechnol Bioeng**. 2007;96:195-201.
131. Thomas RJ, Anderson D, Chandra A et al. Automated, scalable culture of human embryonic stem cells in feeder-free conditions. **Biotechnol Bioeng**. 2009;102:1636-1644.
132. Dos Santos FF, Andrade PZ, da Silva CL et al. Bioreactor design for clinical-grade expansion of stem cells. **Biotechnol J**. 2013;8:644-654.
133. Anstee DJ. The relationship between blood groups and disease. **Blood**. 2010;115:4635-4643.
134. Migliaccio G, Di Pietro R, di Giacomo V et al. In vitro mass production of human erythroid cells from the blood of normal donors and of thalassemic patients. **Blood Cells Mol Dis**. 2002;28:169-180.
135. Fernandez-Becerra C, Lelievre J, Ferrer M et al. Red blood cells derived from peripheral blood and bone marrow CD34(+) human haematopoietic stem cells are permissive to Plasmodium parasites infection. **Mem Inst Oswaldo Cruz**. 2013;108:801-803.
136. Malik P, Fisher TC, Barsky LL et al. An in vitro model of human red blood cell production from hematopoietic progenitor cells. **Blood**. 1998;91:2664-2671.

137. Pourcher G, Mazurier C, King YY et al. Human fetal liver: an in vitro model of erythropoiesis. **Stem Cells Int**. 2011;2011:405429.
138. Baek EJ, Kim HS, Kim S et al. In vitro clinical-grade generation of red blood cells from human umbilical cord blood CD34+ cells. **Transfusion**. 2008;48:2235-2245.
139. Miharada K, Hiroyama T, Sudo K et al. Efficient enucleation of erythroblasts differentiated in vitro from hematopoietic stem and progenitor cells. **Nat Biotechnol**. 2006;24:1255-1256.
140. Fujimi A, Matsunaga T, Kobune M et al. Ex vivo large-scale generation of human red blood cells from cord blood CD34+ cells by co-culturing with macrophages. **Int J Hematol**. 2008;87:339-350.
141. Giarratana MC, Kobari L, Lapillonne H et al. Ex vivo generation of fully mature human red blood cells from hematopoietic stem cells. **Nat Biotechnol**. 2005;23:69-74.
142. Timmins NE, Athanasas S, Gunther M et al. Ultra-high-yield manufacture of red blood cells from hematopoietic stem cells. **Tissue Eng Part C Methods**. 2011;17:1131-1137.
143. Giarratana MC, Rouard H, Dumont A et al. Proof of principle for transfusion of in vitro-generated red blood cells. **Blood**. 2011;118:5071-5079.
144. Leberbauer C, Boulme F, Unfried G et al. Different steroids co-regulate long-term expansion versus terminal differentiation in primary human erythroid progenitors. **Blood**. 2005;105:85-94.
145. Dahlberg A, Delaney C, Bernstein ID. Ex vivo expansion of human hematopoietic stem and progenitor cells. **Blood**. 2011;117:6083-6090.
146. Qiu C, Olivier EN, Velho M et al. Globin switches in yolk sac-like primitive and fetal-like definitive red blood cells produced from human embryonic stem cells. **Blood**. 2008;111:2400-2408.
147. Ma F, Ebihara Y, Umeda K et al. Generation of functional erythrocytes from human embryonic stem cell-derived definitive hematopoiesis. **Proc Natl Acad Sci U S A**. 2008;105:13087-13092.
148. Lu SJ, Feng Q, Park JS et al. Biologic properties and enucleation of red blood cells from human embryonic stem cells. **Blood**. 2008;112:4475-4484.
149. Raab S, Klingenstein M, Liebau S et al. A Comparative View on Human Somatic Cell Sources for iPSC Generation. **Stem Cells Int**. 2014;2014:768391.
150. Kaufman DS. Toward clinical therapies using hematopoietic cells derived from human pluripotent stem cells. **Blood**. 2009;114:3513-3523.
151. Zeuner A, Martelli F, Vaglio S et al. Concise review: stem cell-derived erythrocytes as upcoming players in blood transfusion. **Stem Cells**. 2012;30:1587-1596.
152. Kempf H, Olmer R, Kropp C et al. Controlling expansion and cardiomyogenic differentiation of human pluripotent stem cells in scalable suspension culture. **Stem Cell Reports**. 2014;3:1132-1146.
153. Lachmann N, Ackermann M, Frenzel E et al. Large-scale hematopoietic differentiation of human induced pluripotent stem cells provides granulocytes or macrophages for cell replacement therapies. **Stem Cell Reports**. 2015;4:282-296.

154. Correia C, Serra M, Espinha N et al. Combining hypoxia and bioreactor hydrodynamics boosts induced pluripotent stem cell differentiation towards cardiomyocytes. **Stem Cell Rev**. 2014;10:786-801.
155. Ting S, Chen A, Reuveny S et al. An intermittent rocking platform for integrated expansion and differentiation of human pluripotent stem cells to cardiomyocytes in suspended microcarrier cultures. **Stem Cell Res**. 2014;13:202-213.
156. Vosough M, Omidinia E, Kadivar M et al. Generation of functional hepatocyte-like cells from human pluripotent stem cells in a scalable suspension culture. **Stem Cells Dev**. 2013;22:2693-2705.
157. Hunt CJ. Cryopreservation of Human Stem Cells for Clinical Application: A Review. **Transfus Med Hemother**. 2011;38:107-123.
158. Li Y, Ma T. Bioprocessing of cryopreservation for large-scale banking of human pluripotent stem cells. **Biores Open Access**. 2012;1:205-214.
159. Beers J, Gulbranson DR, George N et al. Passaging and colony expansion of human pluripotent stem cells by enzyme-free dissociation in chemically defined culture conditions. **Nat Protoc**. 2012;7:2029-2040.
160. Okita K, Ichisaka T, Yamanaka S. Generation of germline-competent induced pluripotent stem cells. **Nature**. 2007;448:313-U311.
161. Yu JY, Vodyanik MA, Smuga-Otto K et al. Induced pluripotent stem cell lines derived from human somatic cells. **Science**. 2007;318:1917-1920.
162. Ludwig TE, Levenstein ME, Jones JM et al. Derivation of human embryonic stem cells in defined conditions. **Nature Biotechnology**. 2006;24:185-187.
163. Vallier L, Alexander M, Pedersen RA. Activin/Nodal and FGF pathways cooperate to maintain pluripotency of human embryonic stem cells. **J Cell Sci**. 2005;118:4495-4509.
164. Fluri DA, Tonge PD, Song H et al. Derivation, expansion and differentiation of induced pluripotent stem cells in continuous suspension cultures. **Nat Methods**. 2012;9:509-516.
165. Bigdeli N, Andersson M, Strehl R et al. Adaptation of human embryonic stem cells to feeder-free and matrix-free culture conditions directly on plastic surfaces. **J Biotechnol**. 2008;133:146-153.
166. Desbordes SC, Studer L. Adapting human pluripotent stem cells to high-throughput and high-content screening. **Nat Protoc**. 2013;8:111-130.
167. Stover AE, Schwartz PH. Adaptation of human pluripotent stem cells to feeder-free conditions in chemically defined medium with enzymatic single-cell passaging. **Methods Mol Biol**. 2011;767:137-146.
168. Ng ES, Davis R, Stanley EG et al. A protocol describing the use of a recombinant protein-based, animal product-free medium (APEL) for human embryonic stem cell differentiation as spin embryoid bodies. **Nat Protoc**. 2008;3:768-776.
169. Ng ES, Davis RP, Azzola L et al. Forced aggregation of defined numbers of human embryonic stem cells into embryoid bodies fosters robust, reproducible hematopoietic differentiation. **Blood**. 2005;106:1601-1603.
170. Yu X, Zou J, Ye Z et al. Notch signaling activation in human embryonic stem cells is required for embryonic, but not trophoblastic, lineage commitment. **Cell Stem Cell**. 2008;2:461-471.

171. Zhan X, Dravid G, Ye Z et al. Functional antigen-presenting leucocytes derived from human embryonic stem cells in vitro. **Lancet**. 2004;364:163-171.
172. Joyce JA, Pollard JW. Microenvironmental regulation of metastasis. **Nat Rev Cancer**. 2009;9:239-252.
173. Yamamoto K, Sokabe T, Watabe T et al. Fluid shear stress induces differentiation of Flk-1-positive embryonic stem cells into vascular endothelial cells in vitro. **Am J Physiol Heart Circ Physiol**. 2005;288:H1915-1924.
174. O'Connor KCP, E. T. Agitation effects on microcarrier and suspension CHO cells. **Biotechnol Tech**. 1992;6:323-328.
175. Sucosky P, Osorio DF, Brown JB et al. Fluid mechanics of a spinner-flask bioreactor. **Biotechnol Bioeng**. 2004;85:34-46.
176. Cormier JT, zur Nieden NI, Rancourt DE et al. Expansion of undifferentiated murine embryonic stem cells as aggregates in suspension culture bioreactors. **Tissue Eng**. 2006;12:3233-3245.
177. Li X, Krawetz R, Liu S et al. ROCK inhibitor improves survival of cryopreserved serum/feeder-free single human embryonic stem cells. **Hum Reprod**. 2009;24:580-589.
178. Abaci HE, Devendra R, Soman R et al. Microbioreactors to manipulate oxygen tension and shear stress in the microenvironment of vascular stem and progenitor cells. **Biotechnology and Applied Biochemistry**. 2012;59:97-105.
179. Bilgen B, Barabino GA. Location of scaffolds in bioreactors modulates the hydrodynamic environment experienced by engineered tissues. **Biotechnol Bioeng**. 2007;98:282-294.
180. Collignon ML, Delafosse A, Crine M et al. Axial impeller selection for anchorage dependent animal cell culture in stirred bioreactors: Methodology based on the impeller comparison at just-suspended speed of rotation. **Chemical Engineering Science**. 2010;65:5929-5941.
181. Papoutsakis ET. Fluid-mechanical damage of animal cells in bioreactors. **Trends Biotechnol**. 1991;9:427-437.
182. Venkat RV, Stock LR, Chalmers JJ. Study of hydrodynamics in microcarrier culture spinner vessels: A particle tracking velocimetry approach. **Biotechnol Bioeng**. 1996;49:456-466.
183. Youn BS, Sen A, Behie LA et al. Scale-up of breast cancer stem cell aggregate cultures to suspension bioreactors. **Biotechnol Prog**. 2006;22:801-810.
184. Hoeben A, Landuyt B, Highley MS et al. Vascular endothelial growth factor and angiogenesis. **Pharmacol Rev**. 2004;56:549-580.
185. Peyrard T, Bardiaux L, Krause C et al. Banking of pluripotent adult stem cells as an unlimited source for red blood cell production: potential applications for alloimmunized patients and rare blood challenges. **Transfus Med Rev**. 2011;25:206-216.
186. Migliaccio AR, Whitsett C, Papayannopoulou T et al. The potential of stem cells as an in vitro source of red blood cells for transfusion. **Cell Stem Cell**. 2012;10:115-119.
187. Shah S, Huang X, Cheng L. Concise review: stem cell-based approaches to red blood cell production for transfusion. **Stem Cells Transl Med**. 2014;3:346-355.

188. Dias J, Gumenyuk M, Kang H et al. Generation of red blood cells from human induced pluripotent stem cells. **Stem Cells Dev**. 2011;20:1639-1647.
189. Huang X, Wang Y, Yan W et al. Production of Gene-Corrected Adult Beta Globin Protein in Human Erythrocytes Differentiated from Patient iPSCs After Genome Editing of the Sickle Point Mutation. **Stem Cells**. 2015;33:1470-1479.
190. Kobari L, Yates F, Oudrhiri N et al. Human induced pluripotent stem cells can reach complete terminal maturation: in vivo and in vitro evidence in the erythropoietic differentiation model. **Haematologica**. 2012;97:1795-1803.
191. Lapillonne H, Kobari L, Mazurier C et al. Red blood cell generation from human induced pluripotent stem cells: perspectives for transfusion medicine. **Haematologica**. 2010;95:1651-1659.
192. Yang CT, French A, Goh PA et al. Human induced pluripotent stem cell derived erythroblasts can undergo definitive erythropoiesis and co-express gamma and beta globins. **Br J Haematol**. 2014;166:435-448.
193. Slukvin, II. Hematopoietic specification from human pluripotent stem cells: current advances and challenges toward de novo generation of hematopoietic stem cells. **Blood**. 2013;122:4035-4046.
194. Choi KD, Vodyanik M, Slukvin, II. Hematopoietic differentiation and production of mature myeloid cells from human pluripotent stem cells. **Nat Protoc**. 2011;6:296-313.
195. Ledran MH, Krassowska A, Armstrong L et al. Efficient hematopoietic differentiation of human embryonic stem cells on stromal cells derived from hematopoietic niches. **Cell Stem Cell**. 2008;3:85-98.
196. Rafii S, Kloss CC, Butler JM et al. Human ESC-derived hemogenic endothelial cells undergo distinct waves of endothelial to hematopoietic transition. **Blood**. 2013;121:770-780.
197. Uenishi G, Theisen D, Lee JH et al. Tenascin C promotes hematoendothelial development and T lymphoid commitment from human pluripotent stem cells in chemically defined conditions. **Stem Cell Reports**. 2014;3:1073-1084.
198. Itskovitz-Eldor J, Schuldiner M, Karsenti D et al. Differentiation of human embryonic stem cells into embryoid bodies compromising the three embryonic germ layers. **Mol Med**. 2000;6:88-95.
199. Kennedy M, D'Souza SL, Lynch-Kattman M et al. Development of the hemangioblast defines the onset of hematopoiesis in human ES cell differentiation cultures. **Blood**. 2007;109:2679-2687.
200. Zambidis ET, Peault B, Park TS et al. Hematopoietic differentiation of human embryonic stem cells progresses through sequential hematoendothelial, primitive, and definitive stages resembling human yolk sac development. **Blood**. 2005;106:860-870.
201. Cerdan C, Rouleau A, Bhatia M. VEGF-A165 augments erythropoietic development from human embryonic stem cells. **Blood**. 2004;103:2504-2512.
202. Chang KH, Nelson AM, Cao H et al. Definitive-like erythroid cells derived from human embryonic stem cells coexpress high levels of embryonic and fetal globins with little or no adult globin. **Blood**. 2006;108:1515-1523.

203. Ungrin MD, Joshi C, Nica A et al. Reproducible, ultra high-throughput formation of multicellular organization from single cell suspension-derived human embryonic stem cell aggregates. **PLoS One**. 2008;3:e1565.
204. Liu Y, Wang Y, Gao Y et al. Efficient generation of megakaryocytes from human induced pluripotent stem cells using food and drug administration-approved pharmacological reagents. **Stem Cells Transl Med**. 2015;4:309-319.
205. Ye Z, Liu CF, Lanikova L et al. Differential sensitivity to JAK inhibitory drugs by isogenic human erythroblasts and hematopoietic progenitors generated from patient-specific induced pluripotent stem cells. **Stem Cells**. 2014;32:269-278.
206. Pick M, Azzola L, Osborne E et al. Generation of megakaryocytic progenitors from human embryonic stem cells in a feeder- and serum-free medium. **PLoS One**. 2013;8:e55530.
207. Chen G, Gulbranson DR, Hou Z et al. Chemically defined conditions for human iPSC derivation and culture. **Nat Methods**. 2011;8:424-429.
208. Hulse WL, Gray J, Forbes RT. Evaluating the inter and intra batch variability of protein aggregation behaviour using Taylor dispersion analysis and dynamic light scattering. **Int J Pharm**. 2013;453:351-357.
209. Sebastiano V, Maeder ML, Angstman JF et al. In situ genetic correction of the sickle cell anemia mutation in human induced pluripotent stem cells using engineered zinc finger nucleases. **Stem Cells**. 2011;29:1717-1726.
210. Yahata T, Ando K, Nakamura Y et al. Functional human T lymphocyte development from cord blood CD34+ cells in nonobese diabetic/Shi-scid, IL-2 receptor gamma null mice. **J Immunol**. 2002;169:204-209.
211. Civin CI, Almeida-Porada G, Lee MJ et al. Sustained, retransplantable, multilineage engraftment of highly purified adult human bone marrow stem cells in vivo. **Blood**. 1996;88:4102-4109.
212. Himburg HA, Harris JR, Ito T et al. Pleiotrophin regulates the retention and self-renewal of hematopoietic stem cells in the bone marrow vascular niche. **Cell Rep**. 2012;2:964-975.
213. Wang Y, Chou BK, Dowey S et al. Scalable expansion of human induced pluripotent stem cells in the defined xeno-free E8 medium under adherent and suspension culture conditions. **Stem Cell Res**. 2013;11:1103-1116.
214. Huang X, Shah S, Wang J et al. Extensive ex vivo expansion of functional human erythroid precursors established from umbilical cord blood cells by defined factors. **Mol Ther**. 2014;22:451-463.
215. Dowey SN, Huang X, Chou BK et al. Generation of integration-free human induced pluripotent stem cells from postnatal blood mononuclear cells by plasmid vector expression. **Nat Protoc**. 2012;7:2013-2021.
216. Hu J, Liu J, Xue F et al. Isolation and functional characterization of human erythroblasts at distinct stages: implications for understanding of normal and disordered erythropoiesis in vivo. **Blood**. 2013;121:3246-3253.
217. Qiu C, Hanson E, Olivier E et al. Differentiation of human embryonic stem cells into hematopoietic cells by coculture with human fetal liver cells recapitulates the globin switch that occurs early in development. **Exp Hematol**. 2005;33:1450-1458.

218. Chang KH, Huang A, Hirata RK et al. Globin phenotype of erythroid cells derived from human induced pluripotent stem cells. **Blood**. 2010;115:2553-2554.
219. Xie F, Ye L, Chang JC et al. Seamless gene correction of beta-thalassemia mutations in patient-specific iPSCs using CRISPR/Cas9 and piggyBac. **Genome Res**. 2014;24:1526-1533.
220. Ran D, Shia WJ, Lo MC et al. RUNX1a enhances hematopoietic lineage commitment from human embryonic stem cells and inducible pluripotent stem cells. **Blood**. 2013;121:2882-2890.
221. Ochi K, Takayama N, Hirose S et al. Multicolor staining of globin subtypes reveals impaired globin switching during erythropoiesis in human pluripotent stem cells. **Stem Cells Transl Med**. 2014;3:792-800.
222. Trakarnsanga K, Wilson MC, Lau W et al. Induction of adult levels of beta-globin in human erythroid cells that intrinsically express embryonic or fetal globin by transduction with KLF1 and BCL11A-XL. **Haematologica**. 2014;99:1677-1685.
223. Choi KD, Vodyanik MA, Togarrati PP et al. Identification of the hemogenic endothelial progenitor and its direct precursor in human pluripotent stem cell differentiation cultures. **Cell Rep**. 2012;2:553-567.
224. Kim K, Doi A, Wen B et al. Epigenetic memory in induced pluripotent stem cells. **Nature**. 2010;467:285-290.
225. Kim K, Zhao R, Doi A et al. Donor cell type can influence the epigenome and differentiation potential of human induced pluripotent stem cells. **Nat Biotechnol**. 2011;29:1117-1119.
226. Liang G, Zhang Y. Genetic and epigenetic variations in iPSCs: potential causes and implications for application. **Cell Stem Cell**. 2013;13:149-159.
227. Bouhassira EE. Concise review: production of cultured red blood cells from stem cells. **Stem Cells Transl Med**. 2012;1:927-933.
228. Elcheva I, Brok-Volchanskaya V, Kumar A et al. Direct induction of haematoendothelial programs in human pluripotent stem cells by transcriptional regulators. **Nat Commun**. 2014;5:4372.
229. Paz H, Lynch MR, Bogue CW et al. The homeobox gene Hhex regulates the earliest stages of definitive hematopoiesis. **Blood**. 2010;116:1254-1262.
230. Dai G, Sakamoto H, Shimoda Y et al. Over-expression of c-Myb increases the frequency of hemogenic precursors in the endothelial cell population. **Genes Cells**. 2006;11:859-870.
231. Boehm D, Murphy WG, Al-Rubeai M. The effect of mild agitation on in vitro erythroid development. **J Immunol Methods**. 2010;360:20-29.
232. An X, Schulz VP, Li J et al. Global transcriptome analyses of human and murine terminal erythroid differentiation. **Blood**. 2014;123:3466-3477.
233. Wang Y, Cheng L, Gerecht S. Efficient and scalable expansion of human pluripotent stem cells under clinically compliant settings: a view in 2013. **Ann Biomed Eng**. 2014;42:1357-1372.
234. Rogers HM, Yu X, Wen J et al. Hypoxia alters progression of the erythroid program. **Exp Hematol**. 2008;36:17-27.
235. Earls JK, Jin S, Ye K. Mechanobiology of human pluripotent stem cells. **Tissue Eng Part B Rev**. 2013;19:420-430.

236. Fridley KM, Kinney MA, McDevitt TC. Hydrodynamic modulation of pluripotent stem cells. **Stem Cell Res Ther**. 2012;3:45.
237. Oncul AA, Kalmbach A, Genzel Y et al. Characterization of flow conditions in 2 L and 20 L wave bioreactors using computational fluid dynamics. **Biotechnol Prog**. 2010;26:101-110.
238. Hirose S, Takayama N, Nakamura S et al. Immortalization of erythroblasts by c-MYC and BCL-XL enables large-scale erythrocyte production from human pluripotent stem cells. **Stem Cell Reports**. 2013;1:499-508.
239. Rouzbeh S, Kobari L, Cambot M et al. Molecular Signature of Erythroblast Enucleation in Human Embryonic Stem Cells. **Stem Cells**. 2015.
240. Mendelson A, Frenette PS. Hematopoietic stem cell niche maintenance during homeostasis and regeneration. **Nat Med**. 2014;20:833-846.
241. Di Maggio N, Piccinini E, Jaworski M et al. Toward modeling the bone marrow niche using scaffold-based 3D culture systems. **Biomaterials**. 2011;32:321-329.
242. Torisawa YS, Spina CS, Mammoto T et al. Bone marrow-on-a-chip replicates hematopoietic niche physiology in vitro. **Nat Methods**. 2014;11:663-669.
243. Raic A, Rodling L, Kalbacher H et al. Biomimetic macroporous PEG hydrogels as 3D scaffolds for the multiplication of human hematopoietic stem and progenitor cells. **Biomaterials**. 2014;35:929-940.
244. Hu Z, Van Rooijen N, Yang YG. Macrophages prevent human red blood cell reconstitution in immunodeficient mice. **Blood**. 2011;118:5938-5946.

Curriculum Vitae

Ying Wang

Date of Birth: Nov. 07, 1985 Place of Birth: Zhangjiakou, Hebei, China

Education

August, 2015 Ph.D. in Chemical and Biomolecular Engineering
Johns Hopkins University, Baltimore, MD

July, 2010 Master of Engineering in Chemical Engineering
Tsinghua University, Beijing, China

June, 2008 Bachelor of Engineering in Chemical Engineering
Tsinghua University, Beijing, China

Research Experience

2010 – 2015 **Research assistant, Sharon Gerecht Lab and Linzhao Cheng Lab, Johns Hopkins University, MD**

- Developed a novel bioreactor system for scalable expansion of human induced pluripotent stem cells (hiPSCs).
- Built 3D models using computational fluid dynamics to study the hydrodynamic properties in spinner flasks.
- Established a robust, reproducible and scalable differentiation system for the generation of erythrocytes from hiPSCs.

2007-2010 **Research assistant, Lab of Biocatalysis & Bio-nano Technology, Tsinghua University, Beijing, China**

- Lab-scale process development for cephalosporin C acylase production in *E. coli.,* including gene knockout, protein engineering and high density fermentation.

Publications

1. **Wang Y**, He C, Gao Y, Mendelsohn L, Ye Z, Gerecht S†, Cheng L†. Scalable production of human erythrocytes from induced pluripotent stem cells. In preparation. (2015)
2. Huang X*, **Wang Y***, Yan W, Smith C, Ye Z, Wang J, Gao Y, Mendelsohn L, Cheng L. Production of gene-corrected adult beta globin protein in human erythrocytes differentiated from patient iPSCs after genome editing of the sickle point mutation. *Stem Cells*. 33(5): 1470-1479. (2015)
3. Liu Y*, **Wang Y***, Gao Y, Forbes J, Qayyum R, Becker L, Cheng L†, Wang Z†.

Efficient generation of megakaryocytes from human induced pluripotent stem cells using FDA-approved pharmacological reagents. *Stem Cells Translational Medicine*. 4(4): 309-319. (2015)

4. Chou BK*, Gu H*, Gao Y*, Dowey S, **Wang Y**, Shi J, Li Y, Ye Z, Cheng T, Cheng L. A Facile Method to Establish Human iPS Cells from Adult Blood Cells under Feeder-Free and Xeno-Free Culture Conditions: a Clinically Compliant Approach. *Stem Cells Translational Medicine*. 4(4): 320-332. (2015)
5. Smith C, Gore A, Yan W, Abalde-Atristain L, Li Z, He C, **Wang Y**, Brodsky R, Zhang K, Cheng L†, Ye Z†. Whole-Genome Sequencing Analysis Reveals High Specificity of CRISPR/Cas9 and TALEN-Based Genome Editing in Human iPSCs. *Cell Stem Cell*, 15(1): 12-13. (2014)
6. **Wang Y**, Cheng L, Gerecht S. Efficient and scalable expansion of human pluripotent stem cells under clinically compliant settings: a view in 2013. *Annals of Biomedical Engineering*. 42(7): 1357-1372. (2014)
7. Zhang J, Yu H, **Wang Y**, Luo H, Shen Z. Determination of the second autoproteolytic cleavage site of cephalosporin C acylase and the effect of deleting its flanking residues in the a-C-terminal region. *Journal of Biotechnology*, 184: 138-145 (2014)
8. **Wang Y**, Chou BK, Dowey SN, He C, Gerecht S†, Cheng L†. Scalable expansion of human induced pluripotent stem cells in the defined xeno-free E8 medium under adherent and suspension culture conditions. *Stem Cell Research*, 11(3): 1103-1116 (2013)
9. **Wang Y**, Yu H, Zhang J, Luo H, Shen Z. Double knockout of β-lactamase and cephalosporin acetyl esterase genes from Escherichia coli reduces cephalosporin C decomposition. *Journal of Bioscience and Bioengineering*. 113(6): 737-41 (2012)
10. **Wang Y**, Yu H, Song W, An M, Zhang J, Luo H, Shen Z. Overexpression of synthesized cephalosporin C acylase containing mutations in the substrate transport tunnel. *Journal of Bioscience and Bioengineering*. 113(1): 36-41 (2012).
11. Wen C, Yu H, Sun Y, **Wang Y**, Shen Z. Efficient quantification of hyaluronic acid in fermentation broth by modified CTAB method. *China Biotechnology*. 30(2): 89-93 (2010).

Patents

1. Yu H, Zhang J, **Wang Y**, Luo H, Shen Z. Mutated cephalosporin C acylase. CN102925423. (2012)
2. Yu H, **Wang Y**, Zhang J, Luo H, Shen Z. Method for reducing decomposition of cephalosporin C. CN102533920. (2011)

Selected Presentations

1. "Scalable expansion and red blood cell production of human iPSCs". The 6th Annual Maryland Stem Cell Research Symposium. Baltimore, MD. Oral presentation (2013)

2. “Rapid and scalable expansion of human iPS cells in chemically defined and xeno-free suspension culture system using E8 medium”. Seattle, WA. Biomedical Engineering Society Annual Meeting. Oral presentation (2013)
3. “Scalable expansion of human iPS cells in stirred bioreactors or adherent cultures with the optimized E8 medium”. The 11th Annual Meeting of International Society of Stem Cell Research. Boston, MA. Poster (2013)
4. “Artificial synthesis, overexpression and structure-function investigation of cephalosporin C acylase”. The International Symposium on Exploring the Frontiers of Chemical and Biomedical Engineering. Beijing. Oral presentation (2010)